Published by CERN in the Proceedings of the 2012 School of High-Energy Physics, La Pommeraye, Anjou, France, 6 – 19 June 2012, edited by C. Grojean and M. Mulders, CERN–2014–008 (CERN, Geneva, 2014)

Is (Low-Energy) SUSY still Alive?

A. V. Gladyshev [a] *and D. I. Kazakov* [b]
[a] Bogoliubov Laboratory of Theoretical Physics, JINR, Dubna, Russia
[b] Institute for Theoretical and Experimental Physics, Moscow, Russia

Abstract
Supersymmetry, a new symmetry that relates bosons and fermions in particle physics, still escapes observation. Search for supersymmetry is one of the main aims of the Large Hadron Collider. The other possible manifestation of supersymmetry is the Dark Matter in the Universe. The present lectures contain a brief introduction to supersymmetry in particle physics. The main notions of supersymmetry are introduced. The supersymmetric extension of the Standard Model – the Minimal Supersymmetric Standard Model – is considered in more detail. Phenomenological features of the Minimal Supersymmetric Standard Model as well as possible experimental signatures of supersymmetry at the Large Hadron Collider are described. The present limits on supersymmetric particles are presented and the allowed region of parameter space of the MSSM is shown.

1 Introduction: what is supersymmetry

Supersymmetry is a *boson-fermion* symmetry that is aimed to unify all forces in Nature including gravity within a singe framework [1–5]. Modern views on supersymmetry in particle physics are based on a string paradigm, though low energy manifestations of supersymmetry (SUSY) can be possibly found at modern colliders and in non-accelerator experiments.

Supersymmetry emerged from attempts to generalize the Poincaré algebra to mix representations with different spin [1]. It happened to be a problematic task due to "no-go" theorems preventing such generalizations [6]. The way out was found by introducing so-called graded Lie algebras, i. e. adding anti-commutators to usual commutators of the Lorentz algebra. Such a generalization, described below, appeared to be the only possible one within the relativistic field theory.

If Q is a generator of the SUSY algebra, then acting on a boson state it produces a fermion one and vice versa

$$\bar{Q}\,|\text{boson}\rangle = |\text{fermion}\rangle, \quad Q\,|\text{fermion}\rangle = |\text{boson}\rangle.$$

Since the bosons commute with each other and the fermions anticommute, one immediately finds that the SUSY generators should also anticommute, they must be *fermionic*, i. e. they must change the spin by a half-odd amount and change the statistics. The key element of the SUSY algebra is

$$\{Q_\alpha, \bar{Q}_{\dot{\alpha}}\} = 2\,\sigma^\mu_{\alpha\dot{\alpha}} P_\mu \tag{1}$$

where Q and $\bar{Q}$ are the generators of the supersymmetry transformation and P_μ is the generator of translation, the four-momentum.

In what follows we describe the SUSY algebra in more detail and construct its representations which are needed to build the SUSY generalization of the Standard Model (SM) of fundamental interactions. Such a generalization is based on a softly broken SUSY quantum filed theory and contains the SM as the low energy theory.

Supersymmetry promises to solve some problems of the Standard Model and of Grand Unified Theories. In what follows we describe supersymmetry as the nearest option for the new physics on the TeV scale.

978–92–9083–410-6; 0531-4283 –
http://dx.doi.org/10.5170/CERN-2014-008.107

2 Motivation for SUSY in particle physics

2.1 Unification with gravity

The *general idea* is a unification of all forces of Nature including quantum gravity. However, the graviton has the spin 2, while other gauge bosons (the photon, gluons, W and Z weak bosons) have the spin 1. Therefore, they correspond to different representations of the Poincaré algebra. To mix them one can use supersymmetry transformations. Starting with the graviton state of the spin 2 and acting by the SUSY generators we get the following chain of states:

$$\text{spin } 2 \ \rightarrow \ \text{spin } \frac{3}{2} \ \rightarrow \ \text{spin } 1 \ \rightarrow \ \text{spin } \frac{1}{2} \ \rightarrow \ \text{spin } 0.$$

Thus, the partial unification of matter (the fermions) with forces (the bosons) naturally arises from an attempt to unify gravity with the other interactions.

Taking infinitesimal transformations $\delta_\epsilon = \epsilon^\alpha Q_\alpha,\ \bar{\delta}_{\bar{\epsilon}} = \bar{Q}_{\dot{\alpha}} \bar{\epsilon}^{\dot{\alpha}}$, and using Eq. (1) one gets

$$\{\delta_\epsilon, \bar{\delta}_{\bar{\epsilon}}\} = 2\,(\epsilon \sigma^\mu \bar{\epsilon}) P_\mu, \tag{2}$$

where $\epsilon, \bar{\epsilon}$ are transformation parameters. Choosing ϵ to be local, i. e. the function of the space-time point $\epsilon = \epsilon(x)$, one finds from Eq. (2) that the anticommutator of two SUSY transformations is a local coordinate translation, and the theory which is invariant under the local coordinate transformation is the General Relativity. Thus, making SUSY local, one naturally obtains the General Relativity, or the theory of gravity, or supergravity [2].

2.2 Unification of gauge couplings

According to the Grand Unification *hypothesis*, the gauge symmetry increases with the energy [7]. All known interactions are different branches of the unique interaction associated with a simple gauge group. The unification (or splitting) occurs at the high energy. To reach this goal one has to consider how the couplings change with the energy. It is described by renormalization group equations. In the SM the strong and weak couplings associated with the non-Abelian gauge groups decrease with the energy, while the electromagnetic one associated with the Abelian group on the contrary increases. Thus, it is possible that at some energy scale they are equal.

After the precise measurement of the $SU(3) \times SU(2) \times U(1)$ coupling constants, it has become possible to check the unification numerically. The three coupling constants to be compared are

$$\begin{aligned} \alpha_1 &= (5/3) g'^2/(4\pi) = 5\alpha/(3\cos^2\theta_W), \\ \alpha_2 &= g^2/(4\pi) = \alpha/\sin^2\theta_W, \\ \alpha_3 &= g_s^2/(4\pi) \end{aligned} \tag{3}$$

where $g',\ g$ and g_s are the usual $U(1)$, $SU(2)$ and $SU(3)$ couplings and α is the fine structure constant. The factor of 5/3 in α_1 has been included for proper normalization of the generators.

In the modified minimal subtraction ($\overline{MS}$) scheme, the world averaged values of the couplings at the Z^0 energy are obtained from the fit to the LEP and Tevatron data [8]:

$$\begin{aligned} \alpha^{-1}(M_Z) &= 128.978 \pm 0.027 \\ \sin^2\theta_{\overline{MS}} &= 0.23146 \pm 0.00017 \\ \alpha_s &= 0.1184 \pm 0.0031, \end{aligned} \tag{4}$$

that gives

$$\begin{aligned} \alpha_1(M_Z) &= 0.017, \\ \alpha_2(M_Z) &= 0.034, \\ \alpha_3(M_Z) &= 0.118 \pm 0.003. \end{aligned} \tag{5}$$

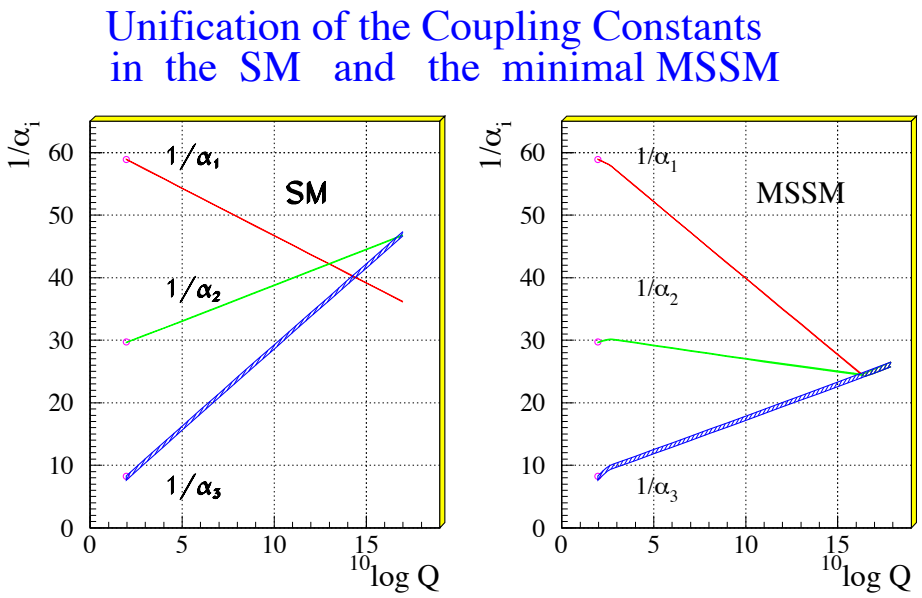

Fig. 1: The evolution of the inverse of the three coupling constants in the Standard Model (left) and in the supersymmetric extension of the SM (MSSM) (right).

Assuming that the SM is valid up to the unification scale, one can then use the known RG equations for the three couplings. In the leading order they are:

$$\frac{d\tilde{\alpha}_i}{dt} = b_i \tilde{\alpha}_i^2, \quad \tilde{\alpha}_i = \frac{\alpha_i}{4\pi}, \quad t = \log\left(\frac{Q^2}{\mu^2}\right), \tag{6}$$

where the coefficients for the SM are $b_i = (41/10, -19/6, -7)$.

The solution to Eqn. (6) is very simple

$$\frac{1}{\tilde{\alpha}_i(Q^2)} = \frac{1}{\tilde{\alpha}_i(\mu^2)} - b_i \log\left(\frac{Q^2}{\mu^2}\right). \tag{7}$$

The result is demonstrated in Fig. 1 showing the evolution of the inverse of the couplings as a function of the logarithm of energy. In this presentation, the evolution becomes a straight line in the first order. The second order corrections are small and do not cause any visible deviation from the straight line. Fig. 1 clearly demonstrates that within the SM the coupling constant unification at a single point is impossible. It is excluded by more than 8 standard deviations. This result means that the unification can only be obtained if the new physics enters between the electroweak and the Planck scales.

In the SUSY case, the slopes of the RG evolution curves are modified. The coefficients b_i in Eq. (6) now are $b_i = (33/5, 1, -3)$. The SUSY particles are assumed to contribute effectively to the running of the coupling constants only for the energies above the typical SUSY mass scale. It turns out that within the SUSY model the perfect unification can be obtained as it is shown in Fig. 1. From the fit requiring the unification one finds for the break point M_{SUSY} and the unification point M_{GUT} [9]

$$\begin{aligned} M_{SUSY} &= 10^{3.4\pm0.9\pm0.4}\ \text{GeV}, \\ M_{GUT} &= 10^{15.8\pm0.3\pm0.1}\ \text{GeV}, \\ \alpha_{GUT}^{-1} &= 26.3 \pm 1.9 \pm 1.0. \end{aligned} \tag{8}$$

The first error originates from the uncertainty in the coupling constant, while the second one is due to the uncertainty in the mass splitting between the SUSY particles.

This observation was considered as the first "evidence" for supersymmetry, especially since M_{SUSY} was found in the range preferred by the fine-tuning arguments.

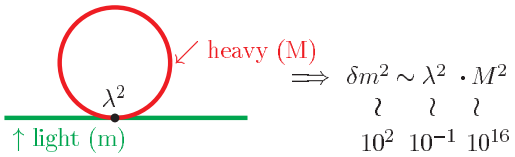

Fig. 2: Radiative correction to the light Higgs boson mass

2.3 Solution to the hierarchy problem

The appearance of two different scales $V \gg v$ in the GUT theory, namely, M_{GUT} and M_W, leads to a very serious problem which is called the *hierarchy problem*. There are two aspects of this problem.

The first one is the very existence of the hierarchy. To get the desired spontaneous symmetry breaking pattern, one needs

$$\begin{aligned} &m_H \sim v \sim 10^2 \text{ GeV} \\ &m_\Sigma \sim V \sim 10^{16} \text{ GeV} \end{aligned} \qquad \frac{m_H}{m_\Sigma} \sim 10^{-14} \ll 1, \tag{9}$$

where H and Σ are the Higgs fields responsible for the spontaneous breaking of the $SU(2)$ and GUT group, respectively. The question arises of how to get so small number in a natural way.

The second aspect of the hierarchy problem is connected with the preservation of the given hierarchy. Even if we choose the hierarchy like in Eq. (9) the radiative corrections will destroy it! To see this, let us consider the radiative correction to the light Higgs mass given by the Feynman diagram shown in Fig. 2.

This correction which is proportional to the mass squared of the heavy particle, obviously, spoils the hierarchy if it is not cancelled. This very accurate cancelation with a precision $\sim 10^{-14}$ needs a fine-tuning of the coupling constants.

The only known way of achieving this kind of cancelation of quadratic terms (also known as the cancelation of the quadratic divergencies) is supersymmetry. Moreover, SUSY automatically cancels the quadratic corrections in all orders of the perturbation theory. This is due to the contributions of superpartners of ordinary particles. The contribution from boson loops cancels those from the fermion ones because of an additional factor (-1) coming from the Fermi statistics, as shown in Fig. 3.

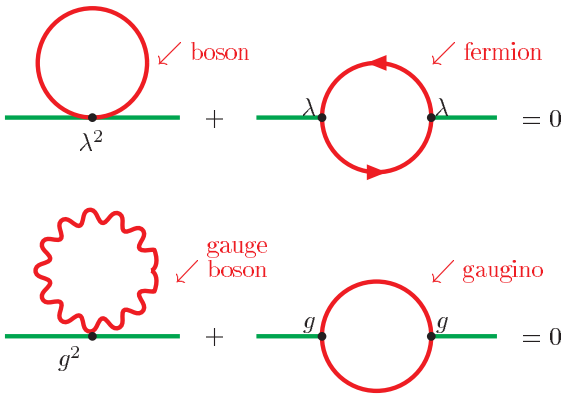

Fig. 3: Cancellation of the quadratic terms (divergencies)

One can see here two types of contribution. The first line is the contribution of the heavy Higgs boson and its superpartner (higgsino). The strength of the interaction is given by the Yukawa coupling constant λ. The second line represents the gauge interaction proportional to the gauge coupling constant g with the contribution from the heavy gauge boson and its heavy superpartner (gaugino).

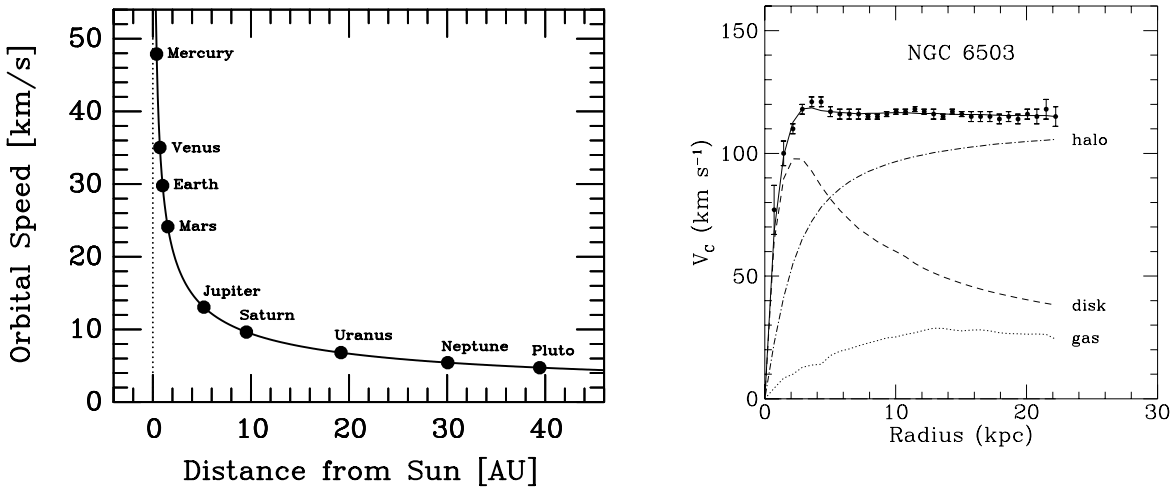

Fig. 4: Rotation curves for the solar system and the spiral galaxy

In both cases the cancelation of the quadratic terms takes place. This cancelation is true up to the SUSY breaking scale, M_{SUSY}, which should not be very large ($\leq$ 1 TeV) to make the fine-tuning natural. Indeed, let us take the Higgs boson mass. Requiring for consistency of the perturbation theory that the radiative corrections to the Higgs boson mass do not exceed the mass itself gives

$$\delta M_h^2 \sim g^2 M_{SUSY}^2 \sim M_h^2. \tag{10}$$

So, if $M_h \sim 10^2$ GeV and $g \sim 10^{-1}$, one needs $M_{SUSY} \sim 10^3$ GeV in order that the relation (10) is valid. Thus, we again get the same rough estimate of $M_{SUSY} \sim 1$ TeV as from the gauge coupling unification above.

That is why it is usually said that supersymmetry solves the hierarchy problem. We show below how SUSY can also explain the origin of the hierarchy.

2.4 Astrophysics and cosmology

The shining matter is not the only one in the Universe. Considerable amount of the energy budget consists of the so-called dark matter. The direct evidence for the presence of the dark matter are flat rotation curves of spiral galaxies [10] (see Fig. 4). To explain these curves one has to assume the existence of a galactic halo made of non-shining matter which takes part in the gravitational interaction. The halo has a size more than twice bigger than a visible galaxy. The other manifestation of existence of the dark matter is the so-called gravitational lensing caused by invisible gravitating matter in the sky [11], which leads to the appearance of circular images of distant stars when the light from them passes through the dark matter.

There are two possible types of the dark matter: the hot one, consisting of light relativistic particles and the cold one, consisting of massive weakly interacting particles (WIMPs) [12]. The hot dark matter might consist of neutrinos, however, this has problems with the galaxy formation. As for the cold dark matter, it has no candidates within the SM. At the same time, SUSY provides an excellent candidate for the cold dark matter, namely, the neutralino, the lightest superparticle [13]. It is neutral, heavy, stable and takes part in weak interactions, precisely what is needed for a WIMP.

2.5 Integrability and superstrings

Considerable progress in the SUSY field theories in recent years has shown that they possess some remarkable and attractive properties. For instance, the $N = 4$ maximally supersymmetric Yang-Mills

theory has all the features and seems to provide the first integrable model in 4 space-time dimensions. This model, though being unphysical, attracts much attention nowadays. It has no ultraviolet divergences, keeps conformal invariance at the quantum level and seems to provide exact solutions for the amplitudes. Duality of this theory to the string theory in higher dimensions (AdS/CFT correspondence) allows to go beyond the perturbation theory thus revealing the strong coupling regime. This properties distinguish the SYSY theories by their mathematical nature.

Another motivation for supersymmetry follows from even more radical changes of the basic ideas related to the ultimate goal of the construction of the consistent unified theory of everything. At the moment the only viable conception is the superstring theory [14]. In the superstring theory, the strings are considered as the fundamental objects, closed or open, and are nonlocal in their nature. The ordinary particles are considered as string excitation modes. The interactions of the strings, which are local, generate proper interactions of the usual particles, including the gravitational ones.

To be consistent, the string theory should be conformally invariant in a D-dimensional target space and have a stable vacuum. The first requirement is valid in the classical theory but may be violated by quantum anomalies. The cancelation of the quantum anomalies takes place when the space-time dimension of the target space equals to the critical one which is $D_c = 26$ for the bosonic string and $D_c = 10$ for the fermionic one.

The second requirement is that the massless string excitations (the particles of the SM) are stable. This assumes the absence of tachyons, the states with the imaginary mass, which can be guaranteed only in the supersymmetric string theories!

The low energy limit of string theories is a kind of supergravity theory which is a local supersymmetric theory. Besides Einstein gravity it contains new interactions and particles, among them the superpartner of a graviton – gravitino, a fermion with spin 3/2. Supergravity itself is not a consistent quantum field theory and is usually treated as an effective theory. It is used in supersymmetric models of particle physics to provide the soft supersymmetry breaking terms.

2.6 Where is SUSY?

After many years of unsuccessful hunt for supersymmetry in particle physics experiments the natural question arises: where is supersymmetry? We try to answer this question describing searches for SUSY at accelerators, in the deep sky with the help of telescopes, and with the help of the underground facilities. It is obvious, that only direct detection of superpartners can convince people in discovery of supersymmetry, however combined information from the sky might give hints to the mass spectra and confirm the SUSY interpretation of the data.

It seems that despite the absence of confirmation supersymmetry stays an unbeatable candidate for physics beyond the Standard Model. The beauty of SUSY lies in the paradigm of unification of all forces of Nature, the ultimate theory of everything. Therefore search for supersymmetry will continue at LHC and perhaps after it.

3 Basics of supersymmetry

3.1 Algebra of SUSY

Combined with the usual Poincaré and internal symmetry algebra the Super-Poincaré Lie algebra contains additional SUSY generators Q^i_α and $\bar{Q}^i_{\dot{\alpha}}$ [3]

$$
\begin{aligned}
&[P_\mu, P_\nu] = 0, \\
&[P_\mu, M_{\rho\sigma}] = i\,(g_{\mu\rho}P_\sigma - g_{\mu\sigma}P_\rho), \\
&[M_{\mu\nu}, M_{\rho\sigma}] = i\,(g_{\nu\rho}M_{\mu\sigma} - g_{\nu\sigma}M_{\mu\rho} - g_{\mu\rho}M_{\nu\sigma} + g_{\mu\sigma}M_{\nu\rho}), \\
&[B_r, B_s] = i\,C^t_{rs}B_t, \\
&[B_r, P_\mu] = [B_r, M_{\mu\sigma}] = 0, \\
&[Q^i_\alpha, P_\mu] = [\bar{Q}^i_{\dot{\alpha}}, P_\mu] = 0, \\
&[Q^i_\alpha, M_{\mu\nu}] = \frac{1}{2}\,(\sigma_{\mu\nu})^\beta_\alpha Q^i_\beta, \quad [\bar{Q}^i_{\dot{\alpha}}, M_{\mu\nu}] = -\frac{1}{2}\,\bar{Q}^i_{\dot{\beta}}(\bar{\sigma}_{\mu\nu})^{\dot{\beta}}_{\dot{\alpha}}, \\
&[Q^i_\alpha, B_r] = (b_r)^i_j Q^j_\alpha, \quad [\bar{Q}^i_{\dot{\alpha}}, B_r] = -\bar{Q}^j_{\dot{\alpha}}(b_r)^i_j, \\
&\{Q^i_\alpha, \bar{Q}^j_{\dot{\beta}}\} = 2\,\delta^{ij}(\sigma^\mu)_{\alpha\dot{\beta}}P_\mu, \\
&\{Q^i_\alpha, Q^j_\beta\} = 2\,\epsilon_{\alpha\beta}Z^{ij}, \quad Z_{ij} = a^r_{ij}b_r, \quad Z^{ij} = Z^+_{ij}, \\
&\{\bar{Q}^i_{\dot{\alpha}}, \bar{Q}^j_{\dot{\beta}}\} = -2\,\epsilon_{\dot{\alpha}\dot{\beta}}Z^{ij}, \quad [Z_{ij}, anything] = 0, \\
&\alpha, \dot{\alpha} = 1, 2 \quad i, j = 1, 2, \ldots, N.
\end{aligned}
\tag{11}
$$

Here P_μ and $M_{\mu\nu}$ are the four-momentum and angular momentum operators, respectively, B_r are the internal symmetry generators, Q^i and $\bar{Q}^i$ are the spinorial SUSY generators and Z_{ij} are the so-called central charges; $\alpha, \dot{\alpha}, \beta, \dot{\beta}$ are the spinorial indices. In the simplest case one has one spinor generator Q_α (and the conjugated one $\bar{Q}_{\dot{\alpha}}$) that corresponds to the ordinary or $N = 1$ supersymmetry. When $N > 1$ one has the extended supersymmetry.

A natural question arises: how many SUSY generators are possible, i. e. what is the value of N? To answer this question, consider massless states. Let us start with the ground state labeled by the energy and the helicity, i. e. the projection of the spin on the direction of momenta, and let it be annihilated by Q_i

$$\text{Vacuum} = |E, \lambda\rangle, \qquad Q_i|E, \lambda\rangle = 0.$$

Then one- and many-particle states can be constructed with the help of creation operators as

State	Expression	# of states
vacuum	$\|E, \lambda\rangle$	1
1-particle	$\bar{Q}_i\|E, \lambda\rangle = \|E, \lambda + \frac{1}{2}\rangle_i$	N
2-particle	$\bar{Q}_i\bar{Q}_j\|E, \lambda = \|E, \lambda + 1\rangle_{ij}$	$\frac{N(N-1)}{2}$
...	...	...
N-particle	$\bar{Q}_1 \ldots \bar{Q}_N\|E, \lambda\rangle = \|E, \lambda + \frac{N}{2}\rangle$	1

The total # of states is: $\sum_{k=0}^{N} \left(\begin{array}{c} N \\ k \end{array} \right) = 2^N = 2^{N-1}$ bosons + 2^{N-1} fermions.

The energy E is not changed, since according to (11) the operators $\bar{Q}_i$ commute with the Hamiltonian.

Thus, one has a sequence of bosonic and fermionic states and the total number of the bosons equals to that of the fermions. This is a generic property of any supersymmetric theory. However, in

CPT invariant theories the number of states is doubled, since CPT transformation changes the sign of the helicity. Hence, in the CPT invariant theories, one has to add the states with the opposite helicity to the above mentioned ones.

Let us consider some examples. We take $N = 1$ and $\lambda = 0$. Then one has the following set of states:

$$\begin{array}{llcll} N=1 & \lambda=0 & & & \\ \text{helicity} & 0\ \frac{1}{2} & & \text{helicity} & 0\ -\frac{1}{2} \\ & & \overset{CPT}{\Longrightarrow} & & \\ \#\text{ of states} & 1\ 1 & & \#\text{ of states} & 1\quad 1 \end{array}$$

Hence, the complete $N = 1$ multiplet is

$$\begin{array}{llccc} N=1 & \text{helicity} & -1/2 & 0 & 1/2 \\ & \#\text{ of states} & 1 & 2 & 1 \end{array}$$

which contains one complex scalar and one spinor with two helicity states.

This is an example of the so-called self-conjugated multiplet. There are also the self-conjugated multiplets with $N > 1$ corresponding to the extended supersymmetry. Two particular examples are the $N = 4$ super Yang-Mills multiplet and the $N = 8$ supergravity multiplet

$$N = 4 \quad \text{SUSY YM} \quad \lambda = -1$$

$$\begin{array}{lccccc} \text{helicity} & -1 & -1/2 & 0 & 1/2 & 1 \\ \#\text{ of states} & 1 & 4 & 6 & 4 & 1 \end{array}$$

$$N = 8 \quad \text{SUGRA} \quad \lambda = -2$$

$$\begin{array}{ccccccccc} -2 & -3/2 & -1 & -1/2 & 0 & 1/2 & 1 & 3/2 & 2 \\ 1 & 8 & 28 & 56 & 70 & 56 & 28 & 8 & 1 \end{array}$$

One can see that the multiplets of extended supersymmetry are very rich and contain a vast number of particles.

The constraint on the number of the SUSY generators comes from the requirement of consistency of the corresponding QFT. The number of supersymmetries and the maximal spin of the particle in the multiplet are related by

$$N \leq 4S,$$

where S is the maximal spin. Since the theories with the spin greater than 1 are non-renormalizable and the theories with the spin greater than 5/2 have no consistent coupling to gravity, this imposes a constraint on the number of the SUSY generators

$$\begin{array}{ll} N \leq 4 & \text{for renormalizable theories (YM),} \\ N \leq 8 & \text{for (super)gravity.} \end{array}$$

In what follows, we shall consider the simple supersymmetry, or the $N = 1$ supersymmetry, contrary to the extended supersymmetries with $N > 1$. In this case, one has the following types of the supermultiplets which are used for the construction of the SUSY generalization of the SM

$$\begin{array}{cccc} (\phi, & \psi) & (\lambda, & A_\mu) \\ Spin = 0, & Spin = 1/2 & Spin = 1/2, & Spin = 1 \\ scalar & chiral & Majorana & vector \\ & fermion & fermion & \end{array}$$

each of them contains two physical states, one boson and one fermion. They are called chiral and vector multiplets, respectively. To construct the generalization of the SM one has to put all the particles into these multiplets. For instance, the quarks should go into the chiral multiplet and the photon into the vector multiplet.

3.2 Superspace and supermultiplets

An elegant formulation of the supersymmetry transformations and invariants can be achieved in the framework of the superspace formalism [4]. The superspace differs from the ordinary Euclidean (Minkowski) space by adding two new coordinates, θ_α and $\bar{\theta}_{\dot{\alpha}}$, which are Grassmannian, i. e. anti-commuting, variables

$$\{\theta_\alpha, \theta_\beta\} = 0, \;\; \{\bar{\theta}_{\dot{\alpha}}, \bar{\theta}_{\dot{\beta}}\} = 0, \;\; \theta_\alpha^2 = 0, \;\; \bar{\theta}_{\dot{\alpha}}^2 = 0,$$

$$\alpha, \beta, \dot{\alpha}, \dot{\beta} = 1, 2.$$

Thus, we go from the space to the superspace

$$\begin{array}{ccc} \text{Space} & \Longrightarrow & \text{Superspace} \\ x_\mu & & x_\mu, \theta_\alpha, \bar{\theta}_{\dot{\alpha}} \end{array}$$

A SUSY group element can be constructed in the superspace in the same way as the ordinary translation in the usual space

$$G(x, \theta, \bar{\theta}) = e^{\, i(-x^\mu P_\mu + \theta Q + \bar{\theta}\bar{Q})}. \tag{12}$$

It leads to a supertranslation in the superspace

$$\begin{aligned} x_\mu &\to x_\mu + i\,\theta\sigma_\mu\bar{\varepsilon} - i\,\varepsilon\sigma_\mu\bar{\theta}, \\ \theta &\to \theta + \varepsilon, \\ \bar{\theta} &\to \bar{\theta} + \bar{\varepsilon}, \end{aligned} \tag{13}$$

where ε and $\bar{\varepsilon}$ are the Grassmannian transformation parameters. From Eqn. (13) one can easily obtain the representation for the supercharges (11) acting on the superspace

$$Q_\alpha = \frac{\partial}{\partial\theta_\alpha} - i\,\sigma^\mu_{\alpha\dot{\alpha}}\bar{\theta}^{\dot{\alpha}}\partial_\mu, \quad \bar{Q}_{\dot{\alpha}} = -\frac{\partial}{\partial\bar{\theta}_{\dot{\alpha}}} + i\,\theta_\alpha\sigma^\mu_{\alpha\dot{\alpha}}\partial_\mu. \tag{14}$$

To define the fields on the superspace, consider the representations of the Super-Poincaré group (11) [3]. The simplest $N = 1$ SUSY multiplets that we discussed earlier are: the chiral one $\Phi(y, \theta)$ ($y = x + i\theta\sigma\bar{\theta}$) and the vector one $V(x, \theta, \bar{\theta})$. Being expanded in the Taylor series over the Grassmannian variables θ and $\bar{\theta}$ they give:

$$\begin{aligned} \Phi(y,\theta) =& \; A(y) + \sqrt{2}\,\theta\psi(y) + \theta\theta F(y) = \\ =& \; A(x) + i\,\theta\sigma^\mu\bar{\theta}\partial_\mu A(x) + \frac{1}{4}\,\theta\theta\bar{\theta}\bar{\theta}\,\Box A(x) \\ &+ \sqrt{2}\,\theta\psi(x) - \frac{i}{\sqrt{2}}\,\theta\theta\partial_\mu\psi(x)\sigma^\mu\bar{\theta} + \theta\theta F(x). \end{aligned} \tag{15}$$

The coefficients are the ordinary functions of x being the usual fields. They are called the *components* of the superfield. In Eq. (15) one has 2 bosonic (the complex scalar field A) and 2 fermionic (the Weyl spinor field ψ) degrees of freedom. The component fields A and ψ are called the *superpartners*. The field F is an *auxiliary* field, it has the "wrong" dimension and has no physical meaning. It is needed to close the algebra (11). One can get rid of the auxiliary fields with the help of equations of motion.

Thus, the superfield contains an equal number of the bosonic and fermionic degrees of freedom. Under the SUSY transformation they convert one into another

$$\begin{aligned} \delta_\varepsilon A &= \sqrt{2}\,\varepsilon\psi, \\ \delta_\varepsilon\psi &= i\sqrt{2}\,\sigma^\mu\bar{\varepsilon}\partial_\mu A + \sqrt{2}\,\varepsilon F, \\ \delta_\varepsilon F &= i\sqrt{2}\,\bar{\varepsilon}\sigma^\mu\partial_\mu\psi. \end{aligned} \tag{16}$$

Notice that the variation of the F-component is a total derivative, i. e. it vanishes when integrated over the space-time.

The vector superfield is real $V = V^\dagger$. It has the following Grassmannian expansion:

$$\begin{aligned} V(x,\theta,\bar\theta) = C(x) + i\,\theta\chi(x) - i\,\bar\theta\bar\chi(x) + \frac{i}{2}\,\theta\theta\,\big[M(x) + iN(x)\big] \\ - \frac{i}{2}\,\bar\theta\bar\theta\,\big[M(x) - iN(x)\big] - \theta\sigma^\mu\bar\theta\,v_\mu(x) + i\,\theta\theta\bar\theta\big[\lambda(x) + \frac{i}{2}\,\bar\sigma^\mu\partial_\mu\chi(x)\big] \\ - i\,\bar\theta\bar\theta\theta\big[\lambda + \frac{i}{2}\,\sigma^\mu\partial_\mu\bar\chi(x)\big] + \frac{1}{2}\,\theta\theta\bar\theta\bar\theta\big[D(x) + \frac{1}{2}\,\Box C(x)\big]. \end{aligned} \tag{17}$$

The physical degrees of freedom corresponding to the real vector superfield V are the vector gauge field v_μ and the Majorana spinor field λ. All other components are unphysical and can be eliminated. Indeed, one can choose a gauge (the Wess-Zumino gauge) where $C = \chi = M = N = 0$, leaving one with only physical degrees of freedom except for the auxiliary field D. In this gauge

$$\begin{aligned} V &= -\,\theta\sigma^\mu\bar\theta v_\mu(x) + i\,\theta\theta\bar\theta\bar\lambda(x) - i\,\bar\theta\bar\theta\theta\lambda(x) + \frac{1}{2}\,\theta\theta\bar\theta\bar\theta D(x), \\ V^2 &= -\frac{1}{2}\theta\theta\bar\theta\bar\theta\,v_\mu(x)v^\mu(x), \\ V^3 &= 0, \quad etc. \end{aligned} \tag{18}$$

One can define also a field strength tensor (as the analog of $F_{\mu\nu}$ in the gauge theories)

$$W_\alpha = -\frac{1}{4}\,\bar D^2 e^V D_\alpha e^{-V}, \quad \bar W_{\dot\alpha} = -\frac{1}{4}\,D^2 e^V \bar D_\alpha e^{-V}, \tag{19}$$

Here D and $\bar D$ are the supercovariant derivatives. The field strength tensor in the chosen Wess-Zumino gauge is a polynomial over the component fields:

$$W_\alpha = T^a\Big(-i\,\lambda^a_\alpha + \theta_\alpha D^a - \frac{i}{2}\,(\sigma^\mu\bar\sigma^\nu\theta)_\alpha F^a_{\mu\nu} + \theta^2(\sigma^\mu D_\mu\bar\lambda^a)_\alpha\Big), \tag{20}$$

where

$$F^a_{\mu\nu} = \partial_\mu v^a_\nu - \partial_\nu v^a_\mu + f^{abc}v^b_\mu v^c_\nu, \quad D_\mu\bar\lambda^a = \partial\bar\lambda^a + f^{abc}v^b_\mu\bar\lambda^c.$$

In the Abelian case Eqs. (19) are simplified and take the form

$$W_\alpha = -\frac{1}{4}\bar D^2 D_\alpha V, \quad \bar W_{\dot\alpha} = -\frac{1}{4}D^2\bar D_\alpha V.$$

3.2.1 Construction of SUSY Lagrangians

Let us start with the Lagrangian which has no local gauge invariance. In the superfield notation the SUSY invariant Lagrangians are the polynomials of the superfields. In the same way, as the ordinary action is the integral over the space-time of the Lagrangian density, in the supersymmetric case the action is the integral over the superspace. The space-time Lagrangian density is [3, 4]

$$\mathcal{L} = \int d^2\theta\,d^2\bar\theta\,\Phi^+_i\Phi_i + \int d^2\theta\,\big[\lambda_i\Phi_i + \frac{1}{2}\,m_{ij}\Phi_i\Phi_j + \frac{1}{3}\,y_{ijk}\Phi_i\Phi_j\Phi_k\big] + h.c. \tag{21}$$

where the first part is the kinetic term and the second one is the *superpotential* $\mathcal{W}$. We use here the integration over the superspace according to the rules of the Grassmannian integration [15]

$$\int d\theta_\alpha = 0, \quad \int \theta_\alpha\,d\theta_\beta = \delta_{\alpha\beta}.$$

Performing the explicit integration over the Grassmannian parameters, we get from Eq. (21)

$$\begin{aligned}\mathcal{L} = & \; i\,\partial_\mu\bar\psi_i\,\bar\sigma^\mu\psi_i + A_i^*\Box A_i + F_i^*F_i \\ & + \Big[\lambda_i F_i + m_{ij}\Big(A_iF_j - \frac{1}{2}\,\psi_i\psi_j\Big) + y_{ijk}\big(A_iA_jF_k - \psi_i\psi_jA_k\big) + h.c.\Big].\end{aligned} \tag{22}$$

The last two terms are the interaction ones. To obtain the familiar form of the Lagrangian, we have to solve the constraints

$$\begin{aligned}\frac{\partial\mathcal{L}}{\partial F_k^*} &= F_k + \lambda_k^* + m_{ik}^*A_i^* + y_{ijk}^*A_i^*A_j^* = 0, \\ \frac{\partial\mathcal{L}}{\partial F_k} &= F_k^* + \lambda_k + m_{ik}A_i + y_{ijk}A_iA_j = 0.\end{aligned} \tag{23}$$

Expressing the auxiliary fields F and F^* from these equations, one finally gets

$$\begin{aligned}\mathcal{L} = & \; i\,\partial_\mu\bar\psi_i\bar\sigma^\mu\psi_i + A_i^*\Box A_i - \frac{1}{2}\,m_{ij}\psi_i\psi_j - \frac{1}{2}\,m_{ij}^*\bar\psi_i\bar\psi_j \\ & - y_{ijk}\psi_i\psi_jA_k - y_{ijk}^*\bar\psi_i\bar\psi_jA_k^* - V(A_i,A_j),\end{aligned} \tag{24}$$

where the scalar potential $V = F_k^*F_k$. We will return to the discussion of the form of the scalar potential in the SUSY theories later.

Consider now the gauge invariant SUSY Lagrangians. They should contain the gauge invariant interaction of the matter fields with the gauge ones and the kinetic term and the self-interaction of the gauge fields.

Let us start with the gauge field kinetic terms. In the Wess-Zumino gauge one has

$$W^\alpha W_\alpha\big|_{\theta\theta} = \; -2\,i\lambda\sigma^\mu D_\mu\bar\lambda - \frac{1}{2}F_{\mu\nu}F^{\mu\nu} + \frac{1}{2}D^2 + \frac{i}{4}F^{\mu\nu}F^{\rho\sigma}\epsilon_{\mu\nu\rho\sigma}, \tag{25}$$

where $D_\mu\bar\lambda = \partial_\mu + ig[v_\mu,\bar\lambda]$ is the usual covariant derivative and the last, the so-called topological θ-term, is the total derivative. The gauge invariant Lagrangian now has the familiar form

$$\begin{aligned}\mathcal{L} = & \; \frac{1}{4}\int d^2\theta\,W^\alpha W_\alpha + \frac{1}{4}\int d^2\bar\theta\,\bar W^{\dot\alpha}\bar W_{\dot\alpha} \\ = & \; \frac{1}{2}D^2 - \frac{1}{4}F_{\mu\nu}F^{\mu\nu} - i\,\lambda\sigma^\mu D_\mu\bar\lambda.\end{aligned} \tag{26}$$

To obtain the gauge-invariant interaction with the matter chiral superfields, one has to modify the kinetic term by inserting the bridge operator

$$\Phi_i^+\Phi_i \;\;\Longrightarrow\;\; \Phi_i^+e^{gV}\Phi_i. \tag{27}$$

The complete SUSY and gauge invariant Lagrangian then looks like

$$\begin{aligned}\mathcal{L}_{SUSY\,YM} = & \; \frac{1}{4}\int d^2\theta\,\mathrm{Tr}(W^\alpha W_\alpha) + \frac{1}{4}\int d^2\bar\theta\,\mathrm{Tr}(\bar W^{\alpha}\bar W_\alpha) \\ & + \int d^2\theta\,d^2\bar\theta\,\bar\Phi_{ia}(e^{gV})_b^a\Phi_i^b + \int d^2\theta\,\mathcal{W}(\Phi_i) + \int d^2\bar\theta\,\bar{\mathcal{W}}(\bar\Phi_i),\end{aligned} \tag{28}$$

where $\mathcal{W}$ is the superpotential, which should be invariant under the group of symmetry of the particular model. In terms of thecomponent fields the above Lagrangian takes the form

$$\begin{aligned}\mathcal{L}_{SUSY\,YM} = & -\frac{1}{4}F_{\mu\nu}^aF^{a\mu\nu} - i\,\lambda^a\sigma^\mu D_\mu\bar\lambda^a + \frac{1}{2}D^aD^a \\ & + \big(\partial_\mu A_i - i\,gv_\mu^aT^aA_i\big)^\dagger\big(\partial_\mu A_i - i\,gv_\mu^aT^aA_i\big) - i\,\bar\psi_i\bar\sigma^\mu\big(\partial_\mu\psi_i - i\,gv_\mu^aT^a\psi_i\big) \\ & - D^aA_i^\dagger T^aA_i - i\sqrt{2}A_i^\dagger\,T^a\lambda^a\psi_i + i\sqrt{2}\,\bar\psi_iT^aA_i\bar\lambda^a + F_i^\dagger F_i \\ & + \frac{\partial\mathcal{W}}{\partial A_i}F_i + \frac{\partial\bar{\mathcal{W}}}{\partial A_i^\dagger}F_i^\dagger - \frac{1}{2}\,\frac{\partial^2\mathcal{W}}{\partial A_i\partial A_j}\,\psi_i\psi_j - \frac{1}{2}\,\frac{\partial^2\bar{\mathcal{W}}}{\partial A_i^\dagger\partial A_j^\dagger}\,\bar\psi_i\bar\psi_j.\end{aligned} \tag{29}$$

Integrating out the auxiliary fields D^a and F_i, one reproduces the usual Lagrangian.

3.2.2 The scalar potential

Contrary to the SM, where the scalar potential is arbitrary and is defined only by the requirement of the gauge invariance, in the supersymmetric theories it is completely defined by the superpotential. It consists of the contributions from the D-terms and F-terms. The kinetic energy of the gauge fields (recall Eq. (26) yields the $\frac{1}{2}D^aD^a$ term, and the matter-gauge interaction (recall Eq. (29) yields the $gD^aT^a_{ij}A^*_iA_j$ one. Together they give

$$\mathcal{L}_D = \frac{1}{2}D^aD^a + gD^aT^a_{ij}A^*_iA_j. \tag{30}$$

The equation of motion reads

$$D^a = -gT^a_{ij}A^*_iA_j. \tag{31}$$

Substituting it back into Eq. (30) yields the D-term part of the potential

$$\mathcal{L}_D = -\frac{1}{2}D^aD^a \quad \Longrightarrow \quad V_D = \frac{1}{2}D^aD^a, \tag{32}$$

where D is given by Eqn. (31).

The F-term contribution can be derived from the matter field self-interaction (22). For a general type superpotential $\mathcal{W}$ one has

$$\mathcal{L}_F = F^*_iF_i + \Big(\frac{\partial W}{\partial A_i}F_i + h.c.\Big). \tag{33}$$

Using the equations of motion for the auxiliary field F_i

$$F^*_i = -\frac{\partial W}{\partial A_i} \tag{34}$$

yields

$$\mathcal{L}_F = -F^*_iF_i \quad \Longrightarrow \quad V_F = F^*_iF_i, \tag{35}$$

where F is given by Eq. (34). The full scalar potential is the sum of the two contributions

$$V = V_D + V_F. \tag{36}$$

Thus, the form of the Lagrangian is practically fixed by the symmetry requirements. The only freedom is the field content, the value of the gauge coupling g, Yukawa couplings y_{ijk} and the masses. Because of the renormalizability constraint $V \leq A^4$ the superpotential should be limited by $\mathcal{W} \leq \Phi^3$ as in Eq. (21). All members of the supermultiplet have the same masses, i. e. the bosons and the fermions are degenerate in masses. This property of the SUSY theories contradicts to the phenomenology and requires supersymmetry breaking.

4 SUSY generalization of the Standard Model. The MSSM

As has been already mentioned, in the SUSY theories the number of the bosonic degrees of freedom equals that of fermionic. At the same time, in the SM one has 28 bosonic and 90 fermionic degrees of freedom (with the massless neutrino, otherwise 96). So the SM is to a great extent non-supersymmetric. Trying to add some new particles to supersymmetrize the SM, one should take into account the following observations:

– There are no fermions with quantum numbers of the gauge bosons;

– Higgs fields have nonzero vacuum expectation values; hence, they cannot be the superpartners of the quarks and leptons, since this would induce a spontaneous violation of the baryon and lepton numbers;
– One needs at least two complex chiral Higgs multiplets in order to give masses to the up and down quarks.

The latter is due to the form of the superpotential and the chirality of the matter superfields. Indeed, the superpotential should be invariant under the $SU(3) \times SU(2) \times U(1)$ gauge group. If one looks at the Yukawa interaction in the Standard Model, one finds that it is indeed $U(1)$ invariant since the sum of hypercharges in each vertex equals zero. For the up quarks this is achieved by taking the conjugated Higgs doublet $\tilde{H} = i\tau_2 H^\dagger$ instead of H. However, in SUSY H is the chiral superfield and hence the superpotential which is constructed out of the chiral fields, may contain only H but not $\tilde{H}$ which is the antichiral superfield.

Another reason for the second Higgs doublet is related to chiral anomalies. It is known that the chiral anomalies spoil the gauge invariance and, hence, the renormalizability of the theory. They are canceled in the SM between the quarks and leptons in each generation [16]

$$\begin{gathered}\mathrm{Tr}\, Y^3 = \; 3 \times \left(\frac{1}{27} + \frac{1}{27} - \frac{64}{27} + \frac{8}{27} \right) \; - \; 1 \; - \; 1 \; + \; 8 \; = \; 0 \\ \text{color} \quad u_L \quad d_L \quad u_R \quad d_R \qquad \nu_L \quad e_L \quad e_R\end{gathered}$$

However, if one introduces the chiral Higgs superfield, it contains higgsinos, which are the chiral fermions, and contain the anomalies. To cancel them one has to add the second Higgs doublet with the opposite hypercharge. Therefore, the Higgs sector in the SUSY models is inevitably enlarged, it contains an even number of the Higgs doublets.

Conclusion: In the SUSY models the supersymmetry associates the *known* bosons with the *new* fermions and the *known* fermions with the *new* bosons.

4.1 The field content

Consider the particle content of the Minimal Supersymmetric Standard Model [17–19]. According to the previous discussion, in the minimal version we double the number of particles (introducing the superpartner to each particle) and add another Higgs doublet (with its superpartner). Thus, the characteristic feature of any supersymmetric generalization of the SM is the presence of the superpartners (see Fig. 5) [20]. If the supersymmetry is exact, the superpartners of the ordinary particles should have the same masses and have to be observed. The absence of them at modern energies is believed to be explained by the fact that they are very heavy, that means that the supersymmetry should be broken. Hence, if the energy of accelerators is high enough, the superpartners will be created. The particle content of the MSSM then appears as shown in Table 1. Hereafter, a tilde denotes the superpartner of the ordinary particle.

The presence of the extra Higgs doublet in the SUSY model is a novel feature of the theory. In the MSSM one has two doublets with the quantum numbers (1,2,-1) and (1,2,1), respectively:

$$H_1 = \begin{pmatrix} H_1^0 \\ H_1^- \end{pmatrix} = \begin{pmatrix} v_1 + \frac{S_1 + iP_1}{\sqrt{2}} \\ H_1^- \end{pmatrix},$$

$$H_2 = \begin{pmatrix} H_2^+ \\ H_2^0 \end{pmatrix} = \begin{pmatrix} H_2^+ \\ v_2 + \frac{S_2 + iP_2}{\sqrt{2}} \end{pmatrix},$$

where v_i are the vacuum expectation values of the neutral components of the Higgs doublets.

Hence, one has $8 = 4 + 4 = 5 + 3$ degrees of freedom. As in the case of the SM, 3 degrees of freedom can be gauged away, and one is left with 5 physical states compared to 1 in the SM. Thus, in

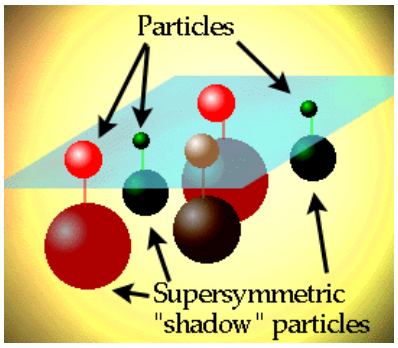

Fig. 5: The shadow world of SUSY particles

Table 1: Particle content of the MSSM

Superfield	Bosons		Fermions		$SU(3)$	$SU(2$	$U_Y(1)$
Gauge							
$\mathbf{G^a}$	gluon	g^a	gluino	$\tilde{g}^a$	8	0	0
$\mathbf{V^k}$	Weak	W^k $(W^{\pm}, Z)$	wino, zino	$\tilde{w}^k$ $(\tilde{w}^{\pm}, \tilde{z})$	1	3	0
$\mathbf{V'}$	Hypercharge	B (γ)	bino	$\tilde{b}(\tilde{\gamma})$	1	1	0
Matter							
$\mathbf{L_i}$	sleptons	$\tilde{L}_i = (\tilde{\nu}, \tilde{e})_L$	leptons	$L_i = (\nu, e)_L$	1	2	-1
$\mathbf{E_i}$		$\tilde{E}_i = \tilde{e}_R$		$E_i = e^c_R$	1	1	2
$\mathbf{Q_i}$	squarks	$\tilde{Q}_i = (\tilde{u}, \tilde{d})_L$	quarks	$Q_i = (u, d)_L$	3	2	$1/3$
$\mathbf{U_i}$		$\tilde{U}_i = \tilde{u}_R$		$U_i = u^c_R$	3^*	1	$-4/3$
$\mathbf{D_i}$		$\tilde{D}_i = \tilde{d}_R$		$D_i = d^c_R$	3^*	1	$2/3$
Higgs							
$\mathbf{H_1}$	Higgses	H_1	higgsinos	$\tilde{H}_1$	1	2	-1
$\mathbf{H_2}$		H_2		$\tilde{H}_2$	1	2	1

the MSSM, as actually in any two Higgs doublet model, one has five physical Higgs bosons: two CP-even neutral Higgs, one CP-odd neutral Higgs and two charged ones. We consider the mass eigenstates below.

4.2 Lagrangian of the MSSM

Now we can construct the Lagrangian of the MSSM. It consists of two parts; the first part is the SUSY generalization of the Standard Model, while the second one represents the SUSY breaking as mentioned above.

$$\mathcal{L}_{MSSM} = \mathcal{L}_{SUSY} + \mathcal{L}_{Breaking}, \tag{37}$$

where

$$\mathcal{L}_{SUSY} = \mathcal{L}_{Gauge} + \mathcal{L}_{Yukawa}. \tag{38}$$

We will not describe the gauge part here, since it is essentially the gauge invariant kinetic terms, but rather concentrate on Yukawa terms. They are given by the superpotential which is nothing else but the usual Yukawa terms of the SM with the fields replaced by the superfields as explained above.

$$\mathcal{L}_{Yukawa} = \epsilon_{ij}\left(y^U_{ab} Q^j_a U^c_b H^i_2 + y^D_{ab} Q^j_a D^c_b H^i_1 + y^L_{ab} L^j_a E^c_b H^i_1 + \mu H^i_1 H^j_2\right), \tag{39}$$

where $i, j = 1, 2$ are the $SU(2)$ and $a, b = 1, 2, 3$ are the generation indices; the $SU(3)$ colour indices are omitted. This part of the Lagrangian almost exactly repeats that of the SM. The only difference is the last term which describes the Higgs mixing. It is absent in the SM since there is only one Higgs field there.

However, one can write down also the different Yukawa terms

$$\mathcal{L}_{Yukawa} = \epsilon_{ij} \left(\lambda^L_{abd} L^i_a L^j_b E^c_d + \lambda^{L\prime}_{abd} L^i_a Q^j_b D^c_d + \mu'_a L^i_a H^j_2 \right) + \lambda^B_{abd} U^c_a D^c_b D^c_d. \tag{40}$$

These terms are absent in the SM. The reason is very simple: one can not replace the superfields in Eq. (40) by the ordinary fields like in Eq. (39) because of the Lorentz invariance. These terms have also another property, they violate either the lepton number L (the first 3 terms in Eq. (40)) or the baryon number B (the last term). Since both effects are not observed in Nature, these terms must be suppressed or excluded. One can avoid such terms introducing a new special symmetry called R-symmetry [21]. The global $U(1)_R$ invariance

$$U(1)_R : \;\; \theta \to e^{i\alpha}\theta, \;\; \Phi \to e^{in\alpha}\Phi, \tag{41}$$

which is reduced to the discrete group Z_2, is called R-parity. The R-parity quantum number is

$$R = (-1)^{3(B-L)+2S} \tag{42}$$

for the particles with the spin S. Thus, all the ordinary particles have the R-parity quantum number equal to $R = +1$, while all the superpartners have the R-parity quantum number equal to $R = -1$. The first part of the Yukawa Lagrangian is R-symmetric, while the second part is R-nonsymmetric. The R-parity obviously forbids the terms (40). However, it may well be that these terms are present, though experimental limits on the couplings are very severe

$$\lambda^L_{abc}, \;\; \lambda^{L\prime}_{abc} < 10^{-4}, \quad \lambda^B_{abc} < 10^{-9}.$$

Conservation of the R-parity has two important consequences

- the superpartners are created in pairs;
- the lightest superparticle (LSP) is stable. Usually it is the photino $\tilde{\gamma}$, the superpartner of the photon with some admixture of the neutral higgsino. This is the candidate for the DM particle which should be neutral and survive since the Big Bang.

4.3 Properties of interactions

If one assumes that the R-parity is preserved, then the interactions of the superpartners are essentially the same as in the SM, but two of three particles involved into the interaction at any vertex are replaced by the superpartners. The reason for it is the R-parity.

Typical vertices are shown in Fig. 6. The tilde above the letter denotes the corresponding superpartner. Note that the coupling is the same in all the vertices involving the superpartners.

4.4 Creation and decay of superpartners

The above-mentioned rule together with the Feynman rules for the SM enables one to draw diagrams describing creation of the superpartners. One of the most promising processes is the e^+e^- annihilation (see Fig. 7). The usual kinematic restriction is given by the c.m. energy $m^{max}_{sparticle} \leq \sqrt{s}/2$. Similar processes take place at hadron colliders with the electrons and the positrons being replaced by the quarks and the gluons.

Experimental signatures at the hadron colliders are similar to those at the e^+e^- machines; however, here one has wider possibilities. Besides the usual annihilation channel, one has numerous processes of gluon fusion, quark-antiquark and quark-gluon scattering (see Fig. 8).

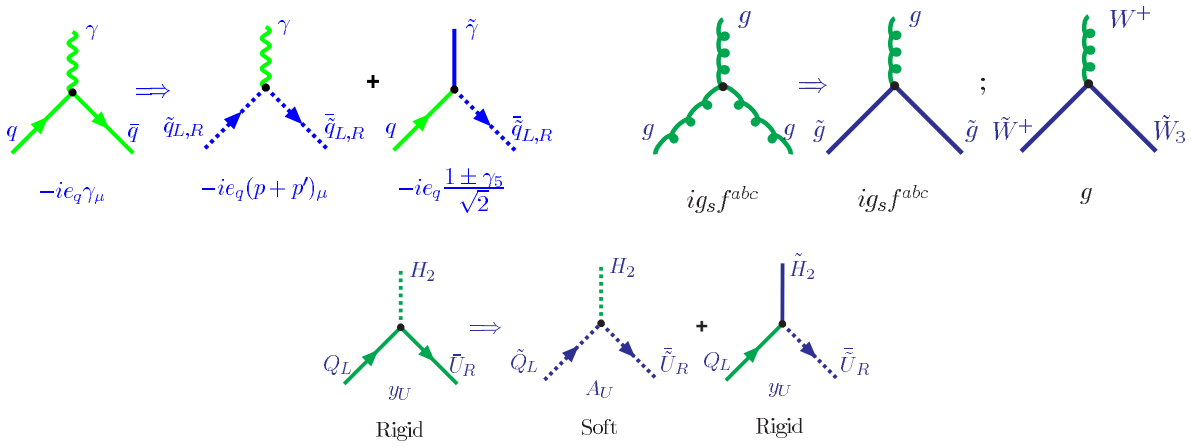

Fig. 6: The gauge-matter interaction, the gauge self-interaction and the Yukawa interaction

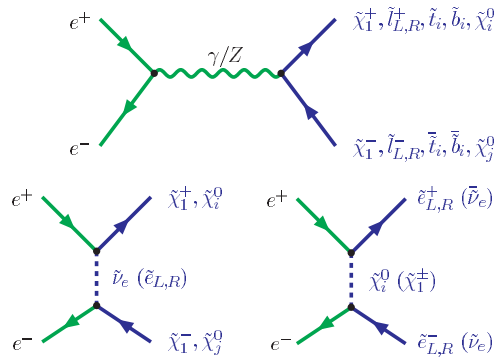

Fig. 7: Creation of the superpartners at electron-positron colliders

Creation of the superpartners can be accompanied by creation of the ordinary particles as well. We consider various experimental signatures below. They crucially depend on the SUSY breaking pattern and on the mass spectrum of the superpartners.

The decay properties of the superpartners also depend on their masses. For the quark and lepton superpartners the main processes are shown in Fig. 9.

5 Breaking of SUSY in the MSSM

Usually it is assumed that the supersymmetry is broken spontaneously via the v.e.v.s of some fields. However, in the case of supersymmetry one can not use the scalar fields like the Higgs field, but rather the auxiliary fields present in any SUSY multiplet. There are two basic mechanisms of spontaneous SUSY breaking: the Fayet-Iliopoulos (or D-type) mechanism [22] based on the D auxiliary field from the vector multiplet and the O'Raifeartaigh (or F-type) mechanism [23] based on the F auxiliary field from the chiral multiplet. Unfortunately, one can not explicitly use these mechanisms within the MSSM since none of the fields of the MSSM can develop the non-zero v.e.v. without spoiling the gauge invariance. Therefore, the spontaneous SUSY breaking should take place via some other fields.

The most common scenario for producing low-energy supersymmetry breaking is called the *hidden sector scenario* [24]. According to this scenario, there exist two sectors: the usual matter belongs to the "visible" one, while the second, "hidden" sector, contains the fields which lead to breaking of the

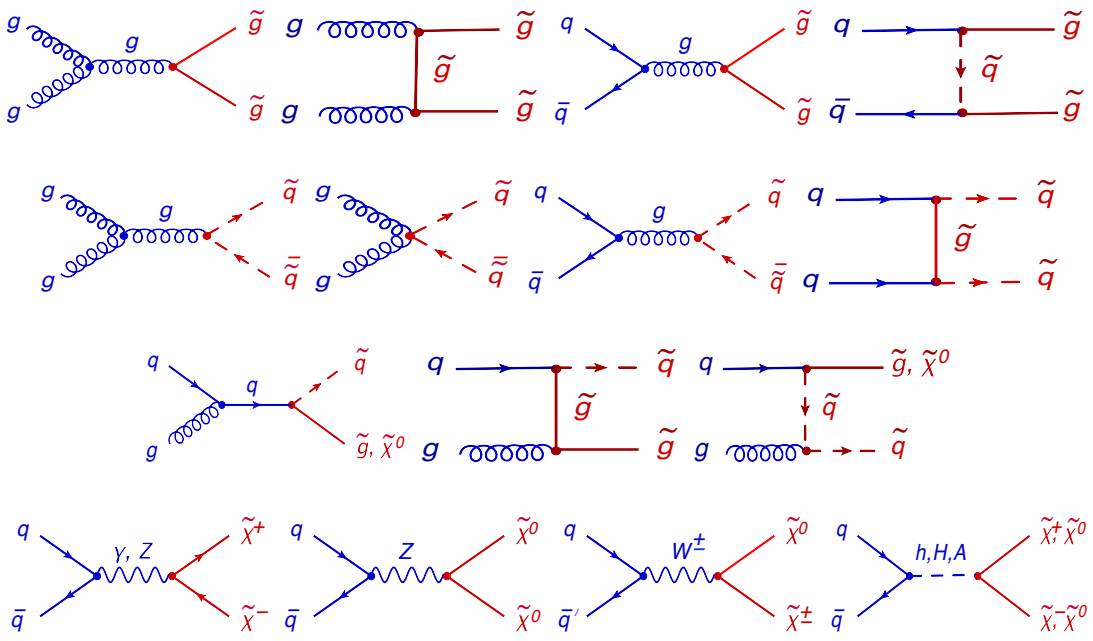

Fig. 8: Examples of diagrams for the SUSY particle production via the strong interactions (top rows for $\tilde{g}\tilde{g}$, $\tilde{q}\bar{\tilde{q}}$ and $\tilde{g}\tilde{q}$, respectively) and the electroweak interactions (the lowest row).

squarks	$\tilde{q}_{L,R} \to q + \tilde{\chi}_i^0$ $\tilde{q}_L \to q' + \tilde{\chi}_i^\pm$ $\tilde{q}_{L,R} \to q + \tilde{g}$
sleptons	$\tilde{l} \to l + \tilde{\chi}_i^0$ $\tilde{l}_L \to \nu_l + \tilde{\chi}_i^\pm$
chargino	$\tilde{\chi}_i^\pm \to e + \nu_e + \tilde{\chi}_i^0$ $\chi_i^\pm \to q + \bar{q}' + \tilde{\chi}_i^0$
gluino	$\tilde{g} \to q = \bar{q} + \tilde{\gamma}$ $\tilde{g} \to g + \tilde{\gamma}$
neutralino	$\tilde{\chi}_i^0 \to \tilde{\chi}_1^0 + l^+ + l^-$ $\tilde{\chi}_i^0 \to \tilde{\chi}_1^0 + q + \bar{q}'$ $\tilde{\chi}_i^0 \to \tilde{\chi}_1^\pm + l^\pm + \nu_l$ $\tilde{\chi}_i^0 \to \tilde{\chi}_1^0 + \nu_l + \bar{\nu}_l$

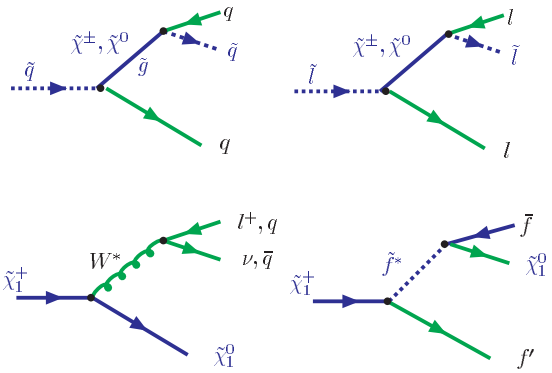

final states	$l^+l^- + \not{E}_T$
	2jets $+ \not{E}_T$
	$\gamma + \not{E}_T$
	$\not{E}_T$

Fig. 9: Decay of superpartners

supersymmetry. These two sectors interact with each other by an exchange of some fields called *messengers*, which mediate SUSY breaking from the hidden to the visible sector. There might be various types of the messenger fields: gravity, gauge, etc. The hidden sector is the weakest part of the MSSM. It contains a lot of ambiguities and leads to uncertainties of the MSSM predictions considered below.

So far there are four known main mechanisms to mediate SUSY breaking from the hidden to the visible sector:

– Gravity mediation (SUGRA) [25];

– Gauge mediation [26];

– Anomaly mediation [27];

– Gaugino mediation [28].

All the four mechanisms of soft SUSY breaking are different in details but are common in results. The predictions for the sparticle spectrum depend on the mechanism of SUSY breaking. In what follows, to calculate the mass spectrum of the superpartners, we need the explicit form of the SUSY breaking terms. For the MSSM without the R-parity violation one has in general

$$
\begin{aligned}
&-\mathcal{L}_{Breaking} = \qquad (43)\\
&= \sum_i m_{0i}^2 \left|\varphi_i\right|^2 + \left(\frac{1}{2}\sum_\alpha M_\alpha \tilde{\lambda}_\alpha \tilde{\lambda}_\alpha + B H_1 H_2 + A^U_{ab}\tilde{Q}_a \tilde{U}^c_b H_2 + A^D_{ab}\tilde{Q}_a \tilde{D}^c_b H_1 + A^L_{ab}\tilde{L}_a \tilde{E}^c_b H_1\right),
\end{aligned}
$$

where we have suppressed the $SU(2)$ indices. Here φ_i are all the scalar fields, $\tilde{\lambda}_\alpha$ are the gaugino fields, $\tilde{Q}, \tilde{U}, \tilde{D}$ and $\tilde{L}, \tilde{E}$ are the squark and slepton fields, respectively, and $H_{1,2}$ are the SU(2) doublet Higgs fields.

Eq. (43) contains a vast number of free parameters which spoils the predictiive power of the model. To reduce their number, we adopt the so-called *universality hypothesis*, i. e., we assume the universality or equality of various soft parameters at the high energy scale, namely, we put all the spin-0 particle masses to be equal to the universal value m_0, all the spin-1/2 particle (gaugino) masses to be equal to $m_{1/2}$ and all the cubic and quadratic terms, proportional to A and B, to repeat the structure of the Yukawa superpotential (39). This is the additional requirement motivated by the supergravity mechanism of SUSY breaking. The universality is not the necessary requirement and one may consider the non-universal soft terms as well. However, it will not change the qualitative picture presented below; so, for simplicity, in what follows we consider the universal boundary conditions. In this case, Eq. (43) takes the form

$$
\begin{aligned}
&-\mathcal{L}_{Breaking} = \qquad (44)\\
&= m_0^2 \sum_i \left|\varphi_i\right|^2 + \left(\frac{m_{1/2}}{2}\sum_\alpha \tilde{\lambda}_\alpha \tilde{\lambda}_\alpha + B\mu H_1 H_2 + A\left[y^U_{ab}\tilde{Q}_a \tilde{U}^c_b H_2 + y^D_{ab}\tilde{Q}_a \tilde{D}^c_b H_1 + y^L_{ab}\tilde{L}_a \tilde{E}^c_b H_1\right]\right).
\end{aligned}
$$

Thus, we are left with five free parameters, namely, $m_0, m_{1/2}, A, B$ and μ versus two parameters of the Higgs potential in the SM, m^2 and λ. In the SUSY model the Higgs potential is not arbitrary but is calculated from the Yukawa and gauge terms as we will see below.

The soft terms explicitly break the supersymmetry. As will be shown later, they lead to the mass spectrum of the superpartners different from that of the ordinary particles. Remind that the masses of the quarks and leptons remain zero until the $SU(2)$ symmetry is spontaneously broken.

5.1 The soft terms and the mass formulae

There are two main sources of the mass terms in the Lagrangian: the D-terms and the soft ones. With given values of $m_0, m_{1/2}, \mu, Y_t, Y_b, Y_\tau, A$, and B one can construct the mass matrices for all the particles.

Knowing them at the GUT scale, one can solve the corresponding RG equations, thus linking the values at the GUT and electroweak scales. Substituting these parameters into the mass matrices, one can predict the mass spectrum of the superpartners [29, 30].

5.1.1 Gaugino-higgsino mass terms

The mass matrix for the gauginos, the superpartners of the gauge bosons, and for the higgsinos, the superpartners of the Higgs bosons, is nondiagonal, thus leading to their mixing. The mass terms look like

$$\mathcal{L}_{Gaugino-Higgsino} = -\frac{1}{2}M_3\bar{\lambda}_a\lambda_a - \frac{1}{2}\bar{\chi}M^{(0)}\chi - (\bar{\psi}M^{(c)}\psi + h.c.), \tag{45}$$

where $\lambda_a, a = 1, 2, \ldots, 8$ are the Majorana gluino fields and

$$\chi = \begin{pmatrix} \tilde{B}^0 \\ \tilde{W}^3 \\ \tilde{H}_1^0 \\ \tilde{H}_2^0 \end{pmatrix}, \quad \psi = \begin{pmatrix} \tilde{W}^+ \\ \tilde{H}^+ \end{pmatrix} \tag{46}$$

are, respectively, the Majorana neutralino and the Dirac chargino fields.

The neutralino mass matrix is

$$M^{(0)} = \begin{pmatrix} M_1 & 0 & -M_Z\cos\beta\sin\theta_W & M_Z\sin\beta\sin\theta_W \\ 0 & M_2 & M_Z\cos\beta\cos\theta_W & -M_Z\sin\beta\cos\theta_W \\ -M_Z\cos\beta\sin\theta_W & M_Z\cos\beta\cos\theta_W & 0 & -\mu \\ M_Z\sin\beta\sin\theta_W & -M_Z\sin\beta\cos\theta_W & -\mu & 0 \end{pmatrix},$$

where $\tan\beta = v_2/v_1$ is the ratio of two Higgs v.e.v.s and $\sin\theta_W$ is the usual sine of the weak mixing angle. The physical neutralino masses $M_{\tilde{\chi}_i^0}$ are obtained as eigenvalues of this matrix after diagonalization.

For the chargino mass matrix one has

$$M^{(c)} = \begin{pmatrix} M_2 & \sqrt{2}M_W\sin\beta \\ \sqrt{2}M_W\cos\beta & \mu \end{pmatrix}. \tag{47}$$

This matrix has two chargino eigenstates $\tilde{\chi}_{1,2}^{\pm}$ with mass eigenvalues

$$M_{1,2}^2 = \frac{1}{2}\left[M_2^2 + \mu^2 + 2M_W^2 \mp \sqrt{(M_2^2-\mu^2)^2 + 4M_W^4\cos^2 2\beta + 4M_W^2(M_2^2+\mu^2+2M_2\mu\sin 2\beta)}\right].$$

5.1.2 Squark and slepton masses

The non-negligible Yukawa couplings cause mixing between the electroweak eigenstates and the mass eigenstates of the third generation particles. The mixing matrices for $\tilde{m}_t^2, \tilde{m}_b^2$ and $\tilde{m}_\tau^2$ are

$$\begin{pmatrix} \tilde{m}_{tL}^2 & m_t(A_t - \mu\cot\beta) \\ m_t(A_t - \mu\cot\beta) & \tilde{m}_{tR}^2 \end{pmatrix},$$

$$\begin{pmatrix} \tilde{m}_{bL}^2 & m_b(A_b - \mu\tan\beta) \\ m_b(A_b - \mu\tan\beta) & \tilde{m}_{bR}^2 \end{pmatrix},$$

$$\begin{pmatrix} \tilde{m}_{\tau L}^2 & m_\tau(A_\tau - \mu\tan\beta) \\ m_\tau(A_\tau - \mu\tan\beta) & \tilde{m}_{\tau R}^2 \end{pmatrix}$$

with

$$\tilde{m}_{tL}^2 = \tilde{m}_Q^2 + m_t^2 + \frac{1}{6}\left(4M_W^2 - M_Z^2\right)\cos 2\beta,$$
$$\tilde{m}_{tR}^2 = \tilde{m}_U^2 + m_t^2 - \frac{2}{3}(M_W^2 - M_Z^2)\cos 2\beta,$$
$$\tilde{m}_{bL}^2 = \tilde{m}_Q^2 + m_b^2 - \frac{1}{6}(2M_W^2 + M_Z^2)\cos 2\beta,$$
$$\tilde{m}_{bR}^2 = \tilde{m}_D^2 + m_b^2 + \frac{1}{3}(M_W^2 - M_Z^2)\cos 2\beta,$$
$$\tilde{m}_{\tau L}^2 = \tilde{m}_L^2 + m_\tau^2 - \frac{1}{2}(2M_W^2 - M_Z^2)\cos 2\beta,$$
$$\tilde{m}_{\tau R}^2 = \tilde{m}_E^2 + m_\tau^2 + (M_W^2 - M_Z^2)\cos 2\beta$$

and the mass eigenstates are the eigenvalues of these mass matrices. For the light generations mixing is negligible.

The first terms here ($\tilde{m}^2$) are the soft ones, which are calculated using the RG equations starting from their values at the GUT (Planck) scale. The second ones are the usual masses of the quarks and leptons and the last ones are the D-terms of the potential.

5.2 The Higgs potential

As has already been mentioned, the Higgs potential in the MSSM is totally defined by the superpotential (and the soft terms). Due to the structure of $\mathcal{L}_{Yukawa}$ the Higgs self-interaction is given by the D-terms while the F-terms contribute only to the mass matrix. The tree level potential is

$$V_{tree} = m_1^2|H_1|^2 + m_2^2|H_2|^2 - m_3^2(H_1H_2 + h.c.) + \frac{g^2 + g'^2}{8}(|H_1|^2 - |H_2|^2)^2 + \frac{g^2}{2}|H_1^* H_2|^2, \quad (48)$$

where $m_1^2 = m_{H_1}^2 + \mu^2, m_2^2 = m_{H_2}^2 + \mu^2$. At the GUT scale $m_1^2 = m_2^2 = m_0^2 + \mu_0^2$, $m_3^2 = -B\mu_0$. Notice that the Higgs self-interaction coupling in Eq. (48) is fixed and defined by the gauge interactions as opposed to the Standard Model.

The Higgs scalar potential in accordance with the supersymmetry, is positive definite and stable. It has no nontrivial minimum different from zero. Indeed, let us write the minimization condition for the potential (48)

$$\begin{aligned}\frac{1}{2}\frac{\delta V}{\delta H_1} &= m_1^2 v_1 - m_3^2 v_2 + \frac{g^2 + g'^2}{4}(v_1^2 - v_2^2)v_1 = 0,\\ \frac{1}{2}\frac{\delta V}{\delta H_2} &= m_2^2 v_2 - m_3^2 v_1 + \frac{g^2 + g'^2}{4}(v_1^2 - v_2^2)v_2 = 0,\end{aligned} \quad (49)$$

where we have introduced the notation

$$\langle H_1\rangle \equiv v_1 = v\cos\beta, \quad \langle H_2\rangle \equiv v_2 = v\sin\beta,$$
$$v^2 = v_1^2 + v_2^2, \quad \tan\beta \equiv \frac{v_2}{v_1}.$$

Solution to Eqs. (49) can be expressed in terms of v^2 and $\sin 2\beta$

$$v^2 = \frac{4(m_1^2 - m_2^2\tan^2\beta)}{(g^2 + g'^2)(\tan^2\beta - 1)}, \quad \sin 2\beta = \frac{2m_3^2}{m_1^2 + m_2^2}. \quad (50)$$

One can easily see from Eqn. (50) that if $m_1^2 = m_2^2 = m_0^2 + \mu_0^2$, v^2 happens to be negative, i. e. the minimum does not exist. In fact, real positive solutions to Eqs. (49) exist only if the following conditions are satisfied:

$$m_1^2 + m_2^2 > 2m_3^2, \quad m_1^2 m_2^2 < m_3^4, \quad (51)$$

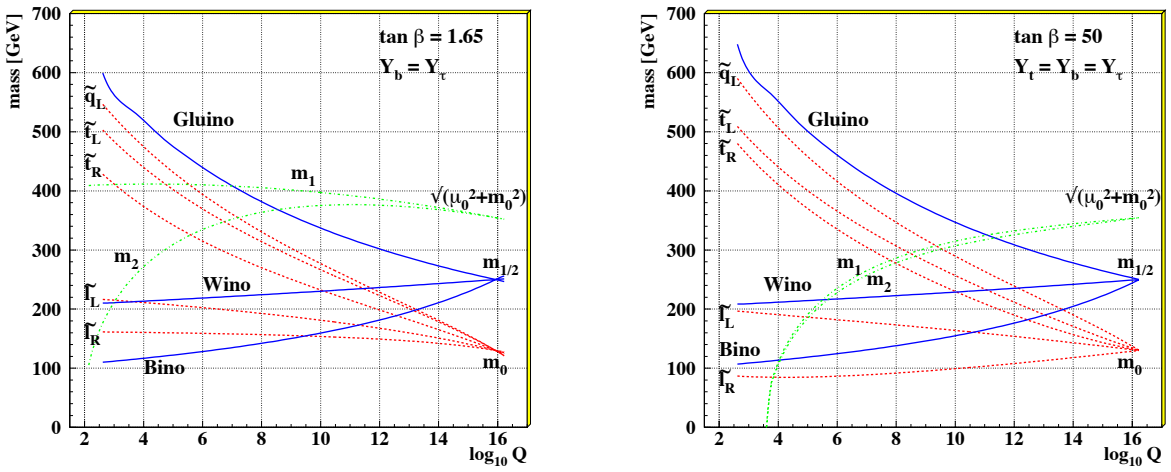

Fig. 10: An example of evolution of superparticle masses and soft supersymmetry breaking parameters $m_1^2 = m_{H_1}^2 + \mu^2$ and $m_2^2 = m_{H_2}^2 + \mu^2$ for low (left) and high (right) values of $\tan\beta$.

which is not the case at the GUT scale. This means that spontaneous breaking of the $SU(2)$ gauge invariance, which is needed in the SM to give masses for all the particles, does not take place in the MSSM.

This strong statement is valid, however, only at the GUT scale. Indeed, going down with the energy, the parameters of the potential (48) are renormalized. They become the "running" parameters with the energy scale dependence given by the RG equations.

5.3 Radiative electroweak symmetry breaking

The running of the Higgs masses leads to the remarkable phenomenon known as *radiative electroweak symmetry breaking*. Indeed, one can see in Fig. 10 that m_2^2 (or both m_1^2 and m_2^2) decreases when going down from the GUT scale to the M_Z scale and can even become negative. As a result, at some value of Q^2 the conditions (51) are satisfied, so that the nontrivial minimum appears. This triggers spontaneous breaking of the $SU(2)$ gauge invariance. The vacuum expectations of the Higgs fields acquire nonzero values and provide masses to the quarks, leptons and $SU(2)$ gauge bosons, and additional contributions to the masses of their superpartners.

In this way one also obtains the explanation of why the two scales are so much different. Due to the logarithmic running of the parameters, one needs a long "running time" to get m_2^2 (or both m_1^2 and m_2^2) to be negative when starting from a positive value of the order of $M_{SUSY} \sim 10^2 \div 10^3$ GeV at the GUT scale.

5.4 The superpartners mass spectrum

The mass spectrum is defined by the low energy parameters. To calculate the low energy values of the soft terms, we use the corresponding RG equations [31]. Having all the RG equations, one can now find the RG flow for the soft terms. Taking the initial values of the soft masses at the GUT scale in the interval between $10^2 \div 10^3$ GeV consistent with the SUSY scale suggested by the unification of the gauge couplings (8) leads to the RG flow of the soft terms shown in Fig. 10. [29, 30]

One should mention the following general features common to any choice of initial conditions:

– The gaugino masses follow the running of the gauge couplings and split at low energies. The gluino mass is running faster than the other ones and is usually the heaviest due to the strong interaction.

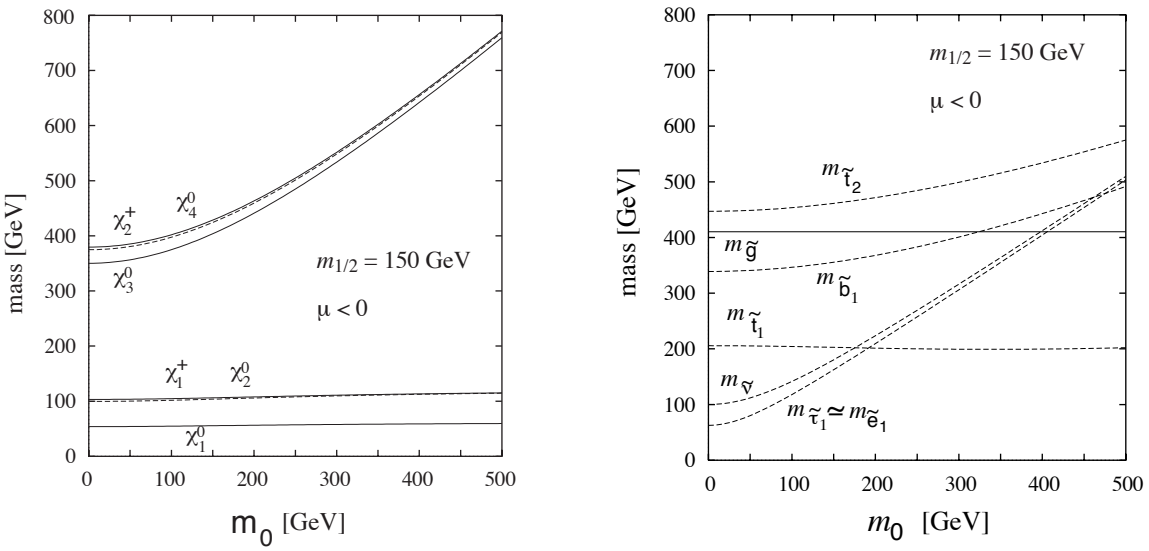

Fig. 11: The masses of sparticles as functions of the initial value m_0

– The squark and slepton masses also split at low energies, the stops (and sbottoms) being the lightest due to the relatively big Yukawa couplings of the third generation.
– The Higgs masses (or at least one of them) are running down very quickly and may even become negative.

The typical dependence of the mass spectra on the initial conditions at the GUT scale (m_0) is also shown in Fig. 11 [32, 33]. For a given value of $m_{1/2}$ the masses of the lightest particles are practically independent of m_0, while the masses of the heavier ones increase with it monotonically. One can see that the lightest neutralinos and charginos as well as the top-squark may be rather light.

5.5 The Higgs boson masses

Provided conditions (51) are satisfied, one can also calculate the masses of the Higgs bosons taking the second derivatives of the potential (48) with respect to the real and imaginary parts of the Higgs fields ($H_i = S_i + iP_i$) in the minimum. The mass matrices at the tree level are

CP-odd components P_1 and P_2:

$$\mathcal{M}^{odd} = \left.\frac{\partial^2 V}{\partial P_i \partial P_j}\right|_{H_i=v_i} = \begin{pmatrix} \tan\beta & 1 \\ 1 & \cot\beta \end{pmatrix} m_3^2, \tag{52}$$

CP-even neutral components S_1 and S_2:

$$\mathcal{M}^{even} = \left.\frac{\partial^2 V}{\partial S_i \partial S_j}\right|_{H_i=v_i} = \begin{pmatrix} \tan\beta & -1 \\ -1 & \cot\beta \end{pmatrix} m_3^2 + \begin{pmatrix} \cot\beta & -1 \\ -1 & \tan\beta \end{pmatrix} M_Z^2 \frac{\sin 2\beta}{2}, \tag{53}$$

Charged components H^- and H^+:

$$\mathcal{M}^{ch} = \left.\frac{\partial^2 V}{\partial H_i^+ \partial H_j^-}\right|_{H_i=v_i} = \begin{pmatrix} \tan\beta & 1 \\ 1 & \cot\beta \end{pmatrix} (m_3^2 + M_W^2 \frac{\sin 2\beta}{2}). \tag{54}$$

Diagonalizing the mass matrices, one gets the mass eigenstates:

$$\begin{cases} G^0 = -\cos\beta P_1 + \sin\beta P_2, \text{ Goldstone boson} \to Z_0, \\ A = \sin\beta P_1 + \cos\beta P_2, \text{ Neutral CP} - \text{odd Higgs}, \end{cases}$$

$$\begin{cases} G^+ = -\cos\beta (H_1^-)^* + \sin\beta H_2^+, \text{ Goldstone boson} \to W^+, \\ H^+ = \sin\beta (H_1^-)^* + \cos\beta H_2^+, \text{ Charged Higgs}, \end{cases}$$

$$\begin{cases} h = -\sin\alpha S_1 + \cos\alpha S_2, \text{ SM CP} - \text{even Higgs}, \\ H = \cos\alpha S_1 + \sin\alpha S_2, \text{ Extra heavy Higgs}, \end{cases}$$

where the mixing angle α is given by

$$\tan 2\alpha = \tan 2\beta \left(\frac{m_A^2 + M_Z^2}{m_A^2 - M_Z^2} \right).$$

The physical Higgs bosons acquire the following masses [18]:

CP-odd neutral Higgs A:

$$m_A^2 = m_1^2 + m_2^2, \tag{55}$$

Charged Higgses $H^\pm$:

$$m_{H^\pm}^2 = m_A^2 + M_W^2, \tag{56}$$

CP-even neutral Higgses H, h:

$$m_{H,h}^2 = \frac{1}{2} \left[m_A^2 + M_Z^2 \pm \sqrt{(m_A^2 + M_Z^2)^2 - 4 m_A^2 M_Z^2 \cos^2 2\beta} \right], \tag{57}$$

where, as usual,

$$M_W^2 = \frac{g^2}{2} v^2, \quad M_Z^2 = \frac{g^2 + g'^2}{2} v^2.$$

This leads to the once celebrated SUSY mass relations

$$\begin{gathered} m_{H^\pm} \geq M_W, \;\; m_h \leq m_A \leq M_H, \\ m_h \leq M_Z |\cos 2\beta| \leq M_Z, \\ m_h^2 + m_H^2 = m_A^2 + M_Z^2. \end{gathered} \tag{58}$$

Thus, the lightest neutral Higgs boson happens to be lighter than the Z-boson, which clearly distinguishes it from the SM one. Though we do not know the mass of the Higgs boson in the SM, there are several indirect constraints leading to the lower boundary of $m_h^{SM} \geq 135$ GeV. After including the leading one-loop radiative corrections, the mass of the lightest Higgs boson in the MSSM, m_h, reads

$$m_h^2 = M_Z^2 \cos^2 2\beta + \frac{3 g^2 m_t^4}{16 \pi^2 M_W^2} \log \frac{\tilde{m}_{t_1}^2 \tilde{m}_{t_2}^2}{m_t^4} + \ldots \tag{59}$$

which leads to about 40 GeV increase [34]. The second loop correction is negative but small [35].

It is interesting, that the Higgs mass upper bound depends crucially on some parameters of the model, and is almost independent on the choice of the other parameters. For example, the 1 GeV change in the mass of the top quark leads to the $\sim$1 GeV change in the Higgs mass upper bound. The dependence of the maximal Higgs mass on the supersymmetry breaking scale M_S is shown in the left panel of Fig. 12 [36] for different scenarios of SUSY breaking. The widths of bands corresponds to the variation of the top mass in the range 170–176 GeV.

The right panel of Fig. 12 shows the dependence of the maximal Higgs mass on $\tan\beta$ for the fixed value of $m_t = 173$ GeV while other parameters of the model vary within the ranges [37]:

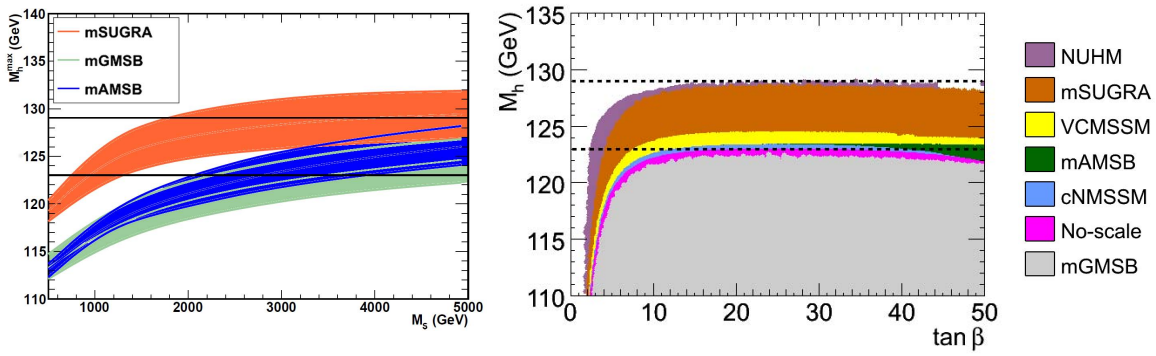

Fig. 12: The maximal Higgs mass in the constrained MSSM scenarios mSUGRA, mAMSB and mGMSB, as a function of the scale M_S when the top quark mass is varied in the range m_t = 170–176 GeV (left) and as a function of $\tan\beta$ (right).

$$\begin{aligned}
\text{mSUGRA:} \quad & 50\ \text{GeV} \le m_0 \le 3\ \text{TeV}, \quad 50\ \text{GeV} \le m_{1/2} \le 3\ \text{TeV}, \quad |A_0| \le 9\ \text{TeV};\\
\text{GMSB:} \quad & 10\ \text{TeV} \le \Lambda \le 1000\ \text{TeV}, \quad 1 \le M_{\text{mess}}/\Lambda \le 10^{11}, \quad N_{\text{mess}} = 1;\\
\text{AMSB:} \quad & 1\ \text{TeV} \le m_{3/2} \le 100\ \text{TeV}, \quad 50\ \text{GeV} \le m_0 \le 3\ \text{TeV}.
\end{aligned}$$

5.6 The lightest superparticle

One of the crucial questions is the properties of the lightest superparticle. Different SUSY breaking scenarios lead to different experimental signatures and different LSP.

- Gravity mediation
  In this case, the LSP is the lightest neutralino $\tilde{\chi}_1^0$, which is almost 90% photino for the low $\tan\beta$ solution and contains more higgsino admixture for high $\tan\beta$. The usual signature for LSP is the missing energy; $\tilde{\chi}_1^0$ is stable and is the best candidate for the cold dark matter particle in the Universe. Typical processes, where the LSP is created, end up with jets + $\not{E}_T$, or leptons + $\not{E}_T$, or both jets + leptons + $\not{E}_T$.
- Gauge mediation
  In this case the LSP is the gravitino $\tilde{G}$, which also leads to the missing energy. The actual question here is what is the NLSP, the next-to-lightest particle, is. There are two possibilities:
  i) $\tilde{\chi}_1^0$ is the NLSP. Then the decay modes are: $\tilde{\chi}_1^0 \to \gamma\tilde{G},\ h\tilde{G},\ Z\tilde{G}$. As a result, one has two hard photons + $\not{E}_T$, or jets + $\not{E}_T$.
  ii) $\tilde{l}_R$ is the NLSP. Then the decay mode is $\tilde{l}_R \to \tau\tilde{G}$ and the signature is a charged lepton and the missing energy.
- Anomaly mediation
  In this case, one also has two possibilities:
  i) $\tilde{\chi}_1^0$ is the LSP and wino-like. It is almost degenerate with the NLSP.
  ii) $\tilde{\nu}_L$ is the LSP. Then it appears in the decay of the chargino $\tilde{\chi}^+ \to \tilde{\nu}l$ and the signature is the charged lepton and the missing energy.
- R-parity violation
  In this case, the LSP is no longer stable and decays into the SM particles. It may be charged (or even colored) and may lead to rare decays like the neutrinoless double β-decay, etc.

Experimental limits on the LSP mass follow from the non-observation of the corresponding events. The modern lower limit is around 40 GeV .

6 Constrained MSSM

6.1 Parameter space of the MSSM

The Standard Model has the following set of free parameters:

i) three gauge couplings α_i;
ii) three (or four if the Dirac neutrino mass term is included) matrices of the Yukawa couplings y^i_{ab}, where $i = U, D, L(N)$;
iii) two parameters of the Higgs potential (λ and m^2).

The parameters of the Yukawa sector are usually traded for the masses, mixing angles and phases of the mixing matrices.

In the MSSM one has the same set of parameters except for the parameters of the Higgs potential which is fixed by supersymmetry, but in addition one has

iv) the Higgs fields mixing parameter μ;
v) the soft supersymmetry breaking terms.

The main uncertainty comes from the unknown soft terms. With the universality hypothesis one is left with the following set of 5 free parameters defining the mass scales

$$\mu,\ m_0,\ m_{1/2},\ A \text{ and } B \leftrightarrow \tan\beta = \frac{v_2}{v_1}.$$

When choosing the set of parameters and making predictions, one has two possible ways to proceed:

i) take the low-energy parameters like the superparticle masses $\tilde{m}_{q1}, \tilde{m}_{q2}, m_A$, $\tan\beta$, mixings X_{stop}, μ, etc. as input and calculate the cross-sections as functions of these parameters. The disadvantage of this approach is the large number of free parameters.
ii) take the high-energy parameters like the above mentioned 5 parameters as input, run the RG equations and find the low-energy values. Now the calculations can be carried out in terms of the initial parameters. The advantage is that their number is relatively small. A typical range of these parameters is

$$100 \text{ GeV} \leq m_0, m_{1/2}, \mu \leq 3 \text{ TeV},$$
$$-3m_0 \leq A_0 \leq 3m_0, \quad 1 \leq \tan\beta \leq 70.$$

The experimental constraints are sufficient to determine these parameters, albeit with large uncertainties.

6.2 The choice of constraints

When subjecting constraints on the MSSM, perhaps, the most remarkable fact is that all of them can be fulfilled simultaneously. In our analysis we impose the following constraints on the parameter space of the MSSM:

– LEP II experimental lower limits on the SUSY masses;
– Limits from the Higgs searches;
– Limits from precision measurement of rare decay rates ($B_s \to s\gamma, B_s \to \mu^+\mu^-, B_s \to \tau\nu$);
– Relic abundance of the Dark Matter in the Universe;
– Direct Dark Matter searches;
– Anomalous magnetic moment of the muon;

– Radiative electroweak symmetry breaking;
– Gauge coupling constant unification;
– Neutrality of the LSP;
– Tevatron and LHC limits on the superpartner masses.

In what follows we use the set of experimental data shown in Table 2.

Table 2: List of all constraints used in the fit to determine the excluded region of the CMSSM parameter space.

Constraint	Data	Ref.
Ωh^2	0.113 ± 0.004	[38]
$b \to s\gamma$	$(3.55 \pm 0.24) \cdot 10^{-4}$	[39]
$b \to \tau\nu$	$(1.68 \pm 0.31) \cdot 10^{-4}$	[39]
Δa_μ	$(290 \pm 63(exp) \pm 61(theo)) \cdot 10^{-11}$	[40]
$B_s \to \mu\mu$	$B_s \to \mu\mu < 4.5 \cdot 10^{-9}$	[41]
m_h	$m_h > 114.4$ GeV	[42]
m_A	$m_A > 510$ GeV for $\tan\beta \approx 50$	[43]
ATLAS	$\sigma_{had}^{SUSY} < 0.001 - 0.03$ pb	[44]
CMS	$\sigma_{had}^{SUSY} < 0.003 - 0.03$ pb	[45]
XENON100	$\sigma_{\chi N} < 1.8 \cdot 10^{-45} - 6 \cdot 10^{-45} cm^2$	[46]

Having in mind the above mentioned constraints one can find the most probable region of the parameter space by minimizing the χ^2 function [30]. Since the parameter space is 5 dimensional one can not plot it explicitly and is bounded to use various projections. We will accept the following strategy: we first choose the value of the Higgs mixing parameter μ from the requirement of radiative EW symmetry breaking and then take the plane of parameters $m_0 - m_{1/2}$ adjusting the remained parameters A_0 and $\tan\beta$ at each point minimizing the χ^2. We present the restrictions coming from various constraints in the $m_0 - m_{1/2}$ plane.

The most probable region of the parameter space is determined by the minimum χ^2_{min} value. The 95% C.L. (90% C.L.) limit is reached for the values of χ^2 of 5.99 (4.61), respectively. The χ^2 function is defined as

$$\begin{aligned}\chi^2 = &\frac{\left(\Omega h^2 - 0.1131\right)^2}{\sigma^2_{\Omega h^2}} + \frac{\left(b \to s\gamma - 3.55 \cdot 10^{-4}\right)^2}{\sigma^2_{b\to s\gamma}} \\ &+ \frac{\left(b \to \tau\nu - 1.68 \cdot 10^{-4}\right)^2}{\sigma^2_b \to \tau\nu} + \frac{\left(\Delta a_\mu - 302 \cdot 10^{-11}\right)^2}{\sigma^2_{\Delta a_\mu}} \\ &+ \chi^2_{B_s\to\mu\mu} + \chi^2_{m_h} + \chi^2_{CMS} + \chi^2_{ATLAS} + \chi^2_{m_A} + \chi^2_{DDMS}\end{aligned} \tag{60}$$

In what follows we show the influence of various constraints and determine the allowed region of the parameter space with 95% C.L.

7 Electroweak constraints

7.1 Region excluded by the $B_s \to s\gamma$ decay rate

The next two constraints are related to the rare decays where SUSY may contribute. The first one is the $b \to s\gamma$ decay which in the SM given by the first two diagrams shown in Fig. 13 and leads to [47]

$$BR^{SM}(b \to s\gamma) = (3.15 \pm 0.23) \cdot 10^{-4}$$

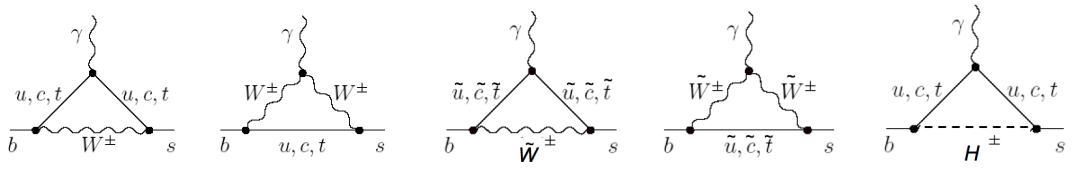

Fig. 13: The diagrams contributing to $b \to s\gamma$ decay in the SM and in the MSSM

while experiment gives [39]

$$BR^{exp}(b \to s\gamma) = (3.55 \pm 0.24) \cdot 10^{-4}.$$

These two values almost coincide but still leave some room for SUSY.

SUSY contribution comes from the last three diagrams shown in Fig. 13 The $\tan\beta$-enhanced corrections to the chargino and charged Higgs contributions can be summarized as follows: the $\tan\beta$-enhanced chargino contributions to $BR(b \to s\gamma)$ is [48]

$$BR^{SUSY}(b \to s\gamma)\Big|_{\chi^\pm} \propto \mu A_t \tan\beta f(\tilde{m}^2_{t_1}, \tilde{m}^2_{t_1}, m_{\chi^\pm}) \frac{m_b}{v(1+\delta m_b)}, \tag{61}$$

where all dominant higher-order contributions are included through δm_b, and f is the integral appearing in the one-loop diagram. The relevant charged-Higgs contributions to $BR(b \to s\gamma)$ in the large $\tan\beta$ regime is [48]

$$BR^{SUSY}(b \to s\gamma)\Big|_{H^\pm} \propto \frac{m_b(h_t \cos\beta - \delta h_t \sin\beta)}{v \cos\beta(1+\delta m_b)} g(m_H^\pm, m_t), \tag{62}$$

where g is the loop integral appearing in the diagram.

The influence of this constraint is shown below together with the $B_s \to \mu^+\mu^-$ one.

7.2 Region excluded by the $B_s \to \mu^+\mu^-$ decay rate

The second example is the $B_s \to \mu^+\mu^-$ decay. In the SM it is given by the first two diagrams shown in Fig. 14. The branching ratio is [49]

$$BR^{SM}(B_s \to \mu^+\mu^-) = (3.23 \pm 0.27) \cdot 10^{-9},$$

while the recent experiment gives only the lower bound [50] [1]

$$BR^{exp}(B_s \to \mu^+\mu^-) < 4.5 \cdot 10^{-9}.$$

In the MSSM one has several additional diagrams but the main contribution enhanced by $\tan^6\beta$ (!) comes from the one shown on the right of Fig. 14.

The branching ratio for $B_s \to \mu^+\mu^-$ is given in [52, 53] which we write in the form

$$BR(B_s \to \mu^+\mu^-) = \frac{2\tau_B M_B^5}{64\pi} f_{B_s}^2 \sqrt{1 - \frac{4m_l^2}{M_B^2}} \times \left[\left(1 - \frac{4m_l^2}{M_B^2}\right) \left| \frac{(C_S - C'_S)}{(m_b + m_s)} \right|^2 + \left| \frac{(C_P - C'_P)}{(m_b + m_s)} + 2\frac{m_\mu}{M_{B_s}^2}(C_A - C'_A) \right|^2 \right] \tag{63}$$

[1] While the Lectures have been prepared the first evidence for the decay $B_s \to \mu^+\mu^-$ based on 1.1 fb^{-1} of data recorded in 2012 at $\sqrt{s} = 8$ TeV has been reported [51]. The data show an excess of events with respect to the background-only prediction with a statistical significance of 3.5σ. A fit to the data gives $BR(B_s \to \mu^+\mu^-) = (3.2^{+1.5}_{-1.2}) \cdot 10^{-9}$ which is in agreement with the SM prediction, thus leaving less room for SUSY.

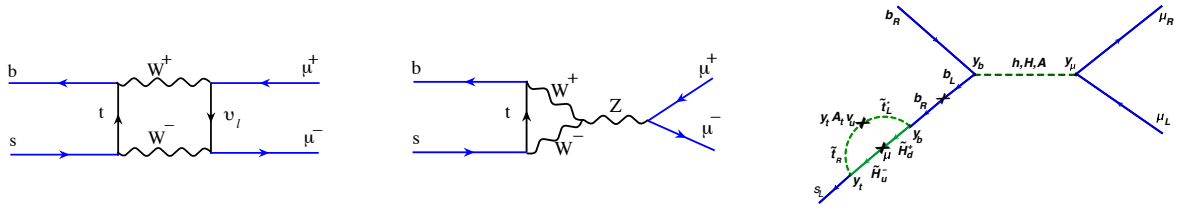

Fig. 14: The diagrams contributing to $B_s \to \mu^+\mu^-$ decay in the SM and in the MSSM

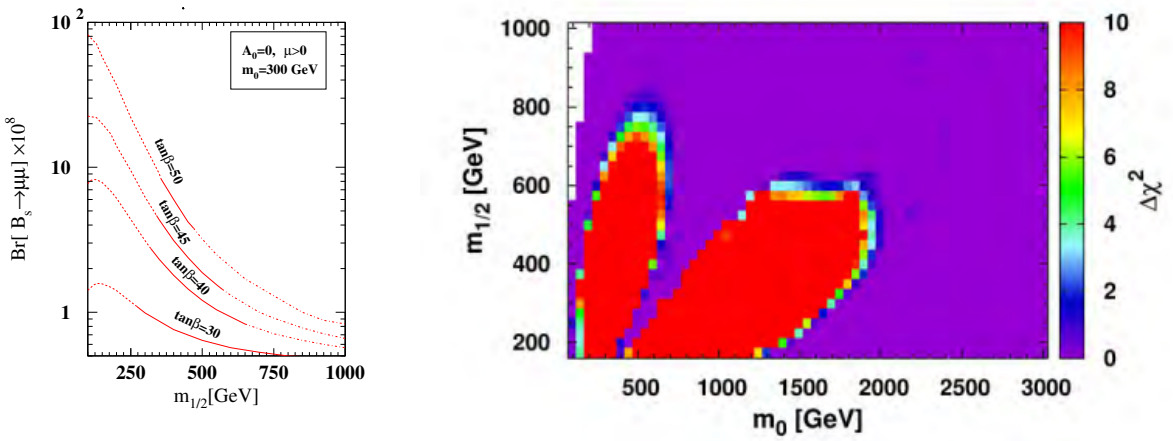

Fig. 15: The values of the branching ratio of the $B_s \to \mu^+\mu^-$ decay in the MSSM (left) and constraints on parameters space of the MSSM from electroweak observables (right).

where f_{B_s} is the B_s decay constant, M_B is the B-meson mass, τ_B is the mean life time and m_l is the mass of the lepton. C_S, C'_S, C_P, C'_P include the SUSY loop contributions due to the diagrams involving the particles such as stop, chargino, sneutrino, Higgs etc. For large $\tan\beta$, the dominant contribution to C_S is given approximately by

$$C_S \simeq \frac{G_F\alpha}{\sqrt{2}\pi} V_{tb}V_{ts}^* \left(\frac{\tan^3\beta}{4\sin^2\theta_W}\right)\left(\frac{m_b m_\mu m_t \mu}{M_W^2 M_A^2}\right)\frac{\sin 2\theta_{\tilde{t}}}{2}\left(\frac{m^2_{\tilde{t}_1}\log\left(m^2_{\tilde{t}_1}/\mu^2\right)}{\mu^2 - m^2_{\tilde{t}_1}} - \frac{m^2_{\tilde{t}_2}\log\left(m^2_{\tilde{t}_2}/\mu^2\right)}{\mu^2 - m^2_{\tilde{t}_2}}\right) \tag{64}$$

where $m_{\tilde{t}_{1,2}}$ are the two stop masses, and $\theta_{\tilde{t}}$ is the rotation angle to diagonalize the stop mass matrix. We need to multiply the above expression by the factor $1/(1+\epsilon_b)^2$ to include the SUSY QCD corrections. ϵ_b is proportional to $\mu\tan\beta$ [54]. Thus, for large $\tan\beta$ the amplitude grows like $\tan^6\beta$ and might come in contradiction with experiment [55]. One observes, however, that the $\tan\beta$ dependence can be compensated by the strong suppression in the last term if the stop masses become equal. This means that in order to get not too large branching ratio the stop masses have to be degenerate.

The values of the branching ratio for various parameters are shown on the left part of Fig. 15 [53] and the restrictions on the parameter space – on the right of Fig. 15.

7.3 Region excluded by the anomalous magnetic moment of muon

The theoretical value of $g-2$ has been reviewed in Ref. [56] which is in agreement with the latest values from [57]. Recent measurement of the anomalous magnetic moment of the muon indicates small

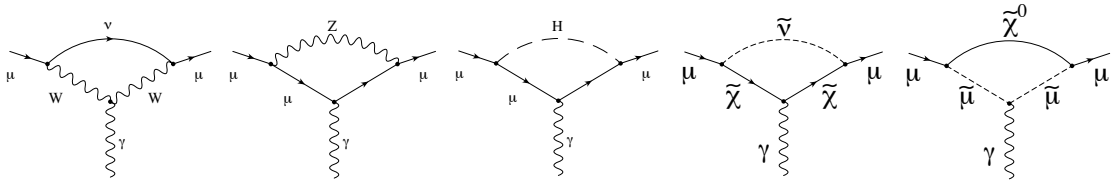

Fig. 16: The diagrams contributing to a_μ in the SM and in the MSSM

deviation from the SM of the order of 3 σ [40]:

$$\begin{aligned} a_\mu^{exp} &= 11\,659\,2080(63)\cdot 10^{-11} \\ a_\mu^{SM} &= 11\,659\,1790(64)\cdot 10^{-11} \\ \Delta a_\mu &= a_\mu^{exp} - a_\mu^{theor} = (290 \pm 90)\cdot 10^{-11}, \end{aligned}$$

where the SM contribution comes from

$$\begin{aligned} a_\mu^{QED} &= 11\,658\,4718.1\ (0.2)\cdot 10^{-11} \\ a_\mu^{weak} &= 153.2\ (1.8)\cdot 10^{-11} \\ a_\mu^{hadron} &= 6918.7\ (65)\cdot 10^{-11}, \end{aligned}$$

so that the accuracy of the experiment finally reaches the order of the weak contribution. The corresponding diagrams are shown in Fig. 16.

The deficiency may be easily filled with the SUSY contribution coming from the last two diagrams of Fig. 16. They are similar to that of the weak interactions after replacing the vector bosons by the charginos and neutralinos.

The total contribution to a_μ from these diagrams is [58]

$$\begin{aligned} a_\mu^{SUSY} = -\frac{g_2^2}{8\pi^2}\Bigg\{ & \sum_{\chi_i^0,\tilde{\mu}_j} \frac{m_\mu}{m_{\chi_i^0}}\Big[(-1)^{j+1}\sin 2\theta B_1(\eta_{ij})\tan\theta_W N_{i1}\big[\tan\theta_W N_{i1} + N_{i2}\big] \\ & + \frac{m_\mu}{2M_W\cos\beta} B_1(\eta_{ij}) N_{i3}[3\tan\theta_W N_{i1} + N_{i2}] \\ & + \left(\frac{m_\mu}{m_{\chi_i^0}}\right)^2 A_1(\eta_{ij})\left\{\frac{1}{4}[\tan\theta_W N_{i1} + N_{i2}]^2 + [\tan\theta_W N_{i1}]^2\right\}\Big] \\ & - \sum_{\chi_j^\pm}\left[\frac{m_\mu m_{\chi_j^\pm}}{m_{\tilde{\nu}}^2}\frac{m_\mu}{\sqrt{2}M_W\cos\beta} B_2(\kappa_j) V_{j1}U_{j2} + \left(\frac{m_\mu}{m_{\tilde{\nu}}}\right)^2 \frac{A_1(\kappa_j)}{2} V_{j1}^2\right]\Bigg\}. \end{aligned} \tag{65}$$

where N_{ij} are elements of the matrix diagonalizing the neutralino mass matrix, and U_{ij}, V_{ij} are the corresponding ones for the chargino mass matrix, the functions A and B are the one-loop triangle integrals.

For large $\tan\beta$ it can be approximated as [59]

$$\left|a_\mu^{SUSY}\right| \simeq \frac{\alpha(M_Z)}{8\pi\sin^2\theta_W}\frac{m_\mu^2\tan\beta}{m_{SUSY}^2}\left(1 - \frac{4\alpha}{\pi}\log\frac{m_{SUSY}}{m_\mu}\right) \simeq 14.0\cdot 10^{-10}\left(\frac{100\ \text{GeV}}{m_{SUSY}}\right)^2\tan\beta,$$

where m_μ is the muon mass, m_{SUSY} is an average mass of the supersymmetric particles in the loop (essentially the chargino mass). It is proportional to μ and $\tan\beta$ and requires the positive sign of μ that kills a half of the parameter space of the MSSM [60].

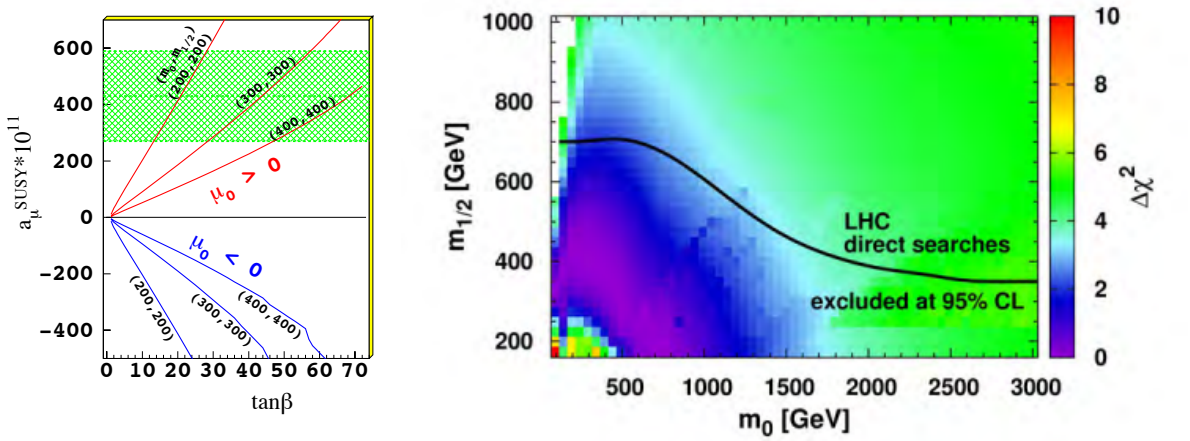

Fig. 17: The dependence of a_μ^{SUSY} versus $\tan\beta$ for various values of the SUSY breaking parameters m_0 and $m_{1/2}$ (left). The horizontal band shows the discrepancy between the experimental data and the SM estimate. The allowed regions of the parameters space (right). The black contour shows the constraint from the LHC searches.

If the SUSY particles are light enough they give the desired contribution to the anomalous magnetic moment. However, if they are too light the contribution exceeds the gap between the experiment and the SM. For too heavy particles the contribution is too small. The values of a_μ^{SUSY} versus $\tan\beta$ for various values of the SUSY breaking parameters m_0 and $m_{1/2}$ are shown on the left of Fig. 17 and the restrictions on the parameter space are presented on the right panel of Fig. 17. However, the allowed region is almost excluded by the direct SUSY searches at the LHC as can be seen in Fig. 17 on the right panel. So the observed deviation from the SM might be caused by the other reasons.

7.4 Region excluded by the pseudo-scalar Higgs mass m_A

The pseudo-scalar Higgs boson production is enhanced by $\tan\beta$. The main diagrams for for the gluon fusion and associated Higgs production with a b-quark are shown in Fig. 18 together with the corresponding cross-sections. Since the b-quark production is mostly in the forward direction, the scale on the right-hand side indicates if at least one b-quark is required to be in the acceptance, defined by $\eta < 2.5$, and have a transverse momentum above 20 GeV/c.

The pseudo-scalar Higgs boson mass is determined by the relic density constraint, because the dominant neutralino annihilation contribution comes from the A-boson exchange in the region outside the small co-annihilation regions. One expects $m_A \propto m_{1/2}$ from the relic density constraint, which can be fulfilled with $\tan\beta$ values around 50 in the whole $(m_0 - m_{1/2})$ plane [61]. Since the A production cross section at the LHC is proportional to $\tan^2\beta$ the pseudo-scalar mass limit increases up to 496 GeV for the large values of $\tan\beta$ preferred by the relic density (see Fig. 18 right panel). The corresponding m_A-values are displayed in the left panel of Fig. 19 and the m_A values excluded by the LHC searches lead to the excluded region, shown by the contour line in Fig. 19.

The rather strong limits on the pseudo-scalar Higgs boson mass from LHC [43, 65], especially at large values of $\tan\beta$, lead then to constraints on $m_{1/2}$ of about 400 GeV for intermediate values of m_0, as shown in the left panel of Fig. 19 [66].

7.5 Effect of a SM Higgs mass m_h around 125 GeV

The 95% C.L. LEP limit of 114.4 GeV contributes for the small and intermediate SUSY masses to the χ^2 function. In recent publications CMS [67] and ATLAS [68] collaborations show evidence for the

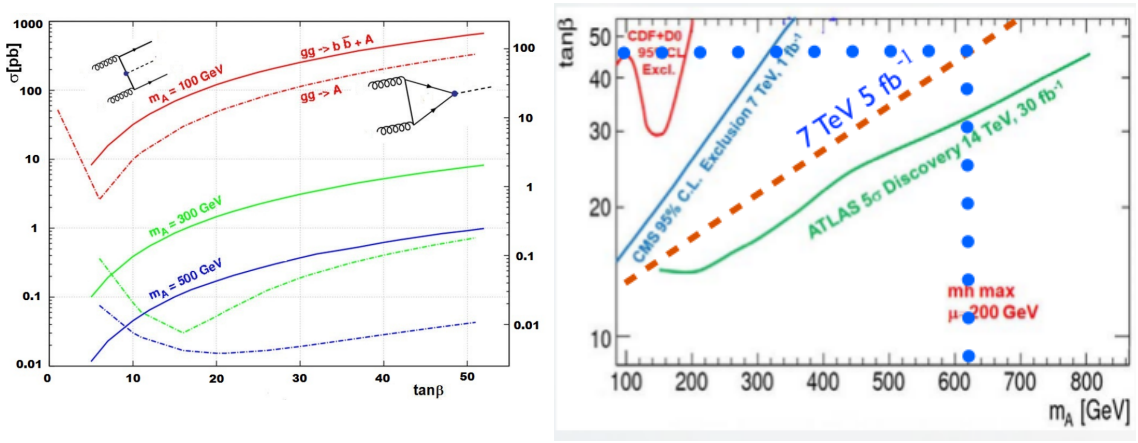

Fig. 18: Left: The pseudoscalar Higgs production cross section as function of $\tan\beta$, both for the gluon fusion diagram and associated Higgs production with a b-quark for the different Higgs mass values indicated. Right: expected discovery reach for the ATLAS detector at 14 TeV and a luminosity of 30 fb^{-1} [62]. The region already excluded at the Tevatron [63] and the expected exclusion reach after the initial 7 TeV run at the LHC [64] have been indicated as well (assuming a luminosity of 1 fb^{-1}). These sensitivity projections for future LHC running of the ATLAS and CMS detectors are preliminary.

Higgs with a mass around 125 GeV. If we assume this to be the evidence for the SM Higgs boson, which has similar properties as the lightest SUSY Higgs boson in the decoupling regime, we can check the consequences for the CMSSM. If the Higgs mass of 125 GeV is included to the fit, the best-fit point moves to higher SUSY masses, but there is rather strong tension between the relic density constraint, $B_s \to \mu^+\mu^-$ and the Higgs mass, so the best-fit point depends strongly on the error assigned to the Higgs mass, as shown in Fig. 19 (right panel). The experimental error on the Higgs mass is about 2 GeV, but the theoretical error can be easily 3 GeV. Therefore, we have plotted the best-fit point for Higgs uncertainties between 2 and 5 GeV. One sees that the best-fit points wanders by several TeV. Clearly this needs a more detailed investigation in the future. It should be noted that the fit does not provide the maximum mixing scenario. If we exclude all other constraints, the maximum value of the Higgs mass can reach 125 GeV, albeit also at similarly large values of $m_{1/2}$. A negative sign of the mixing parameter μ shows similar results [66].

8 The problem of the dark matter in the Universe

As has been already mentioned the shining matter does not compose all the matter in the Universe. According to the latest precise data [69] the matter content of the Universe is the following:

$$\Omega_{total} = 1.02 \pm 0.02,$$
$$\Omega_{vacuum} = 0.73 \pm 0.04,$$
$$\Omega_{matter} = 0.23 \pm 0.04,$$
$$\Omega_{baryon} = 0.044 \pm 0.004,$$

so that the dark matter prevails the usual baryonic matter by factor of 6.

Besides the rotation curves of spiral galaxies the dark matter manifests itself in the observation of gravitational lensing effects [11] and the large structure formation. It is believed that the dark matter played the crucial role in the formation of large structures like clusters of galaxies and the usual matter just fell down in a potential well attracted by the gravitational interaction afterwards. The dark matter can not make compact objects like the usual matter since it does not take part in the strong interaction

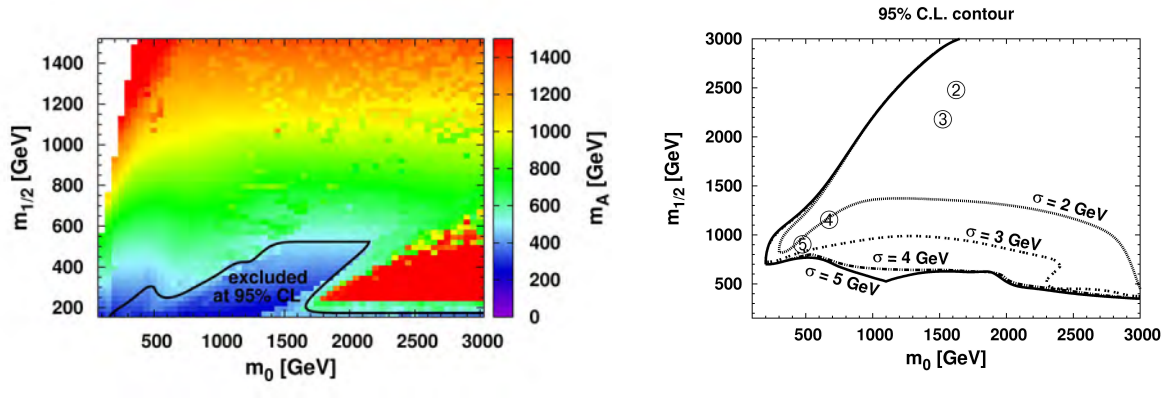

Fig. 19: Left: values of m_A in the $(m_0 - m_{1/2})$ plane after optimizing $\tan\beta$ and A_0. The region below the solid line is excluded at 95% C.L. Right: The influence of a Higgs mass of 125 GeV. If it is imposed in the fit, the best-fit point moves to higher SUSY masses, but the location is strongly dependent on the assumed error for the calculated Higgs mass. This error is indicated by the number inside the circle for the best-fit point: $\Delta\chi^2 = 5.99(2\sigma)$ contour.

and can not lose energy by the photon emission since it is neutral. For this reason the dark matter can be trapped in much larger scale structures like galaxies.

In general one may assume two possibilities: either the dark matter interacts only gravitationally, or it participates also in the weak interaction. The latter case is preferable since then one may hope to detect it via the methods of the particle physics. What makes us to believe that the dark matter is probably the Weakly Interacting Massive Particle (WIMP)? This is because the cross-section of the DM annihilation which can be figured out of the amount of the DM in the Universe is close to a typical weak interaction cross-section. Indeed, let us assume that all the DM is made of particles of a single type. Then the amount of the DM can be calculated from the Boltzman equation [70, 71]

$$\frac{dn_\chi}{dt} + 3Hn_\chi = -\langle\sigma v\rangle(n_\chi^2 - n_{\chi,eq}^2), \tag{66}$$

where $H = \dot{R}/R$ is the Hubble constant and $n_{\chi,eq}$ is the equilibrium concentration. The relic abundance is expressed in terms of n_χ as

$$\Omega_\chi h^2 = \frac{m_\chi n_\chi}{\rho_c} \approx \frac{2\cdot 10^{-27}\ \text{cm}^3\ \text{sec}^{-1}}{\langle\sigma v\rangle}. \tag{67}$$

Having in mind that $\Omega_\chi h^2 \approx 0.113 \pm 0.009$ and $v \sim 300$ km/sec one gets

$$\sigma \approx 10^{-34}\ \text{cm}^2 = 100\ \text{pb}, \tag{68}$$

which is a typical electroweak cross-section.

8.1 Supersymmetric interpretation of the Dark Matter

Supersymmetry offers several candidates for the role of the cold dark matter particle. If one looks at the particle content of the MSSM from the point of view of a heavy neutral particle, one finds several such particles, namely: the superpartner of the photon (the photino $\tilde{\gamma}$), the superpartner of the Z-boson (the particle called zino $\tilde{z}$), the superpartner of the neutrino (the sneutrino $\tilde{\nu}$) and the superpartners of the Higgs bosons (the higgsinos $\tilde{H}$). The DM particle can be the lightest of them, the LSP. The others decay

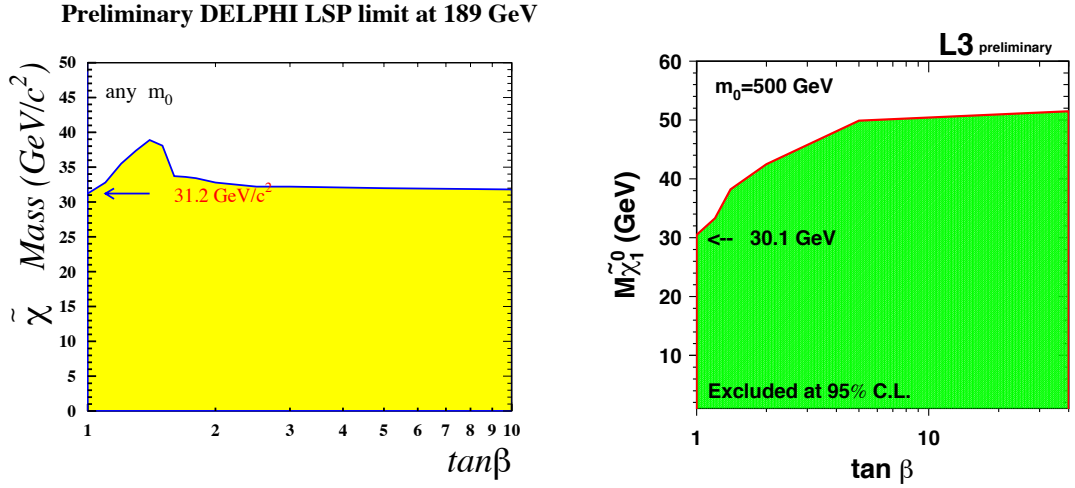

Fig. 20: Exclusion limits on the LSP mass from Delphi and L3 Collaboration (LEP) [72]

to the LSP and the SM particles, while the LSP is stable and can survive since the Big Bang. As a rule the lightest supersymmetric particle is the neutralino, the spin 1/2 particle which is the combination of the photino, zino and two neutral higgsinos and is the eigenstate of the mass matrix

$$|\tilde{\chi}_1^0\rangle = N_1|B_0\rangle + N_2|W_0^3\rangle + N_3|H_1\rangle + N_4|H_2\rangle.$$

Thus, supersymmetry actually predicts the existence of the dark matter. Moreover, one can choose the parameters of soft supersymmetry breaking in such a way that one gets the right amount of the DM. This requirement serves as a constraint for these parameters and is consistent with the requirements coming from the particle physics.

The search for the LSP was one of the tasks of LEP. They were supposed to be produced as a result of the chargino decays and be detected via the missing transverse energy and momentum. Negative results defined the limit on the LSP mass as shown in Fig. 20.

The DM particles which form the halo of the galaxy annihilate to produce the ordinary particles in the cosmic rays. Identifying them with the LSP from a supersymmetric model one can calculate the annihilation rate and study the secondary particle spectrum. The dominant annihilation diagrams of the neutralino LSP are shown in Fig. 21. The usual final states are either the quark-antiquark pairs or the W and Z bosons. Since the cross sections are proportional to the final state fermion mass, the heavy fermion final states, i. e. the third generation quarks and leptons, are expected to be dominant. The W and Z final states from the t-channel chargino and neutralino exchange have usually a smaller cross section.

The dominant contribution comes from the A-boson exchange: $\chi + \chi \to A \to b\bar{b}$. The sum of the diagrams should yield $\langle \sigma v \rangle = 2 \cdot 10^{-26}$ cm^3/sec to get the correct relic density.

The spectral shape of the secondary particles the from DM annihilation is well known from the fragmentation of the mono-energetic quarks studied at the electron-positron colliders, like LEP at CERN, which has been operating up to the centre-of-mass energy of about 200 GeV, i. e. it corresponds to the neutralino mass up to 100 GeV. The different quark flavours all yield similar gamma spectra at high energies. Hence, the specrta of the positrons, photons and antiprotons is known. The relative amount of γ, p^- and e^+ is also known. One expects around 37 photons per collision.

The gamma rays from the DM annihilation can be distinguished from the background by their completely different spectral shape: the background originates mainly from cosmic rays hitting the gas of the disc and producing abundantly π^0-mesons, which decay into two photons. The initial cosmic ray spectrum is a steep power law spectrum, which yields a much softer gamma ray spectrum than the

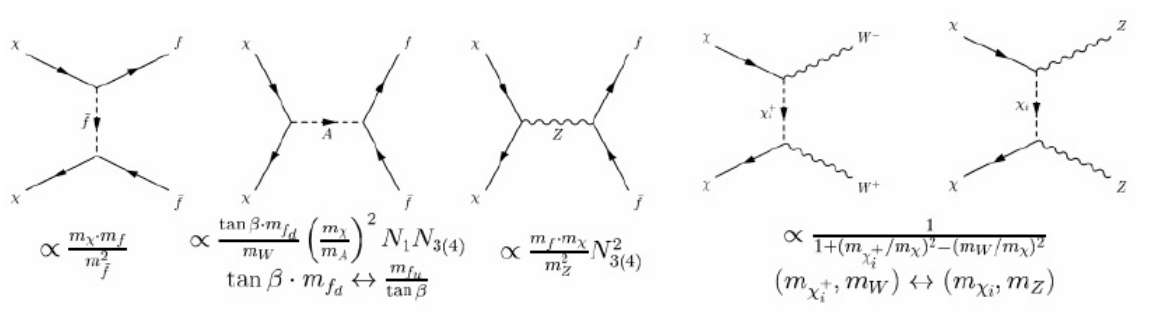

Fig. 21: The dominant annihilation diagrams for the lightest neutralino in the MSSM

fragmentation of the hard mono-energetic quarks from the DM annihilation. The spectral shape of the gamma rays from the background is well known from fixed target experiments given the known cosmic ray spectrum.

Unfortunately, modern data on diffuse galactic gamma rays, do not indicate statistically significant departure from the background. Local excess observed in some experiments like EGRET space telescope [73] and FERMI [74] is well inside the uncertainties of the background.

8.2 Region excluded by the relic density

The observed relic density of the dark matter corresponds to $\Omega h^2 = 0.113 \pm 0.004$ [38]. This number is inversely proportional to the annihilation cross section. The dominant annihilation contribution comes from A-boson exchange in most of the parameter space. The cross section for $\chi + \chi \to A \to b\bar{b}$ can be written as:

$$\langle \sigma v \rangle \sim \frac{M_\chi^4 m_b^2 \tan^2\beta}{\sin^4 2\theta_W \, M_Z^2} \frac{\left(N_{31}\sin\beta - N_{41}\cos\beta\right)^2 \left(N_{21}\cos\theta_W - N_{11}\sin\theta_W\right)^2}{\left(4M_\chi^2 - M_A^2\right)^2 + M_A^2\Gamma_A^2}. \tag{69}$$

As have been mentioned, the correct relic density requires $\langle \sigma v \rangle = 2 \cdot 10^{-26}$ cm^3/s, which implies that the annihilation cross section σ is of the order of a 100 pb. Such a high cross section can be obtained only close to the resonance. Actually on the resonance the cross section is too high, so one needs to be in the tail of the resonance, i .e. $m_A \approx 2.2\, m_\chi$ or $m_A \approx 1.8\, m_\chi$. So one expects $m_A \propto m_{1/2}$ from the relic density constraint. This constraint can be fulfilled with $\tan\beta$ values around 50 in the whole $(m_0 - m_{1/2})$ plane, except for the narrow co-annihilation regions [61]. The results can be extended to larger values of m_0, as shown in the left panel of Fig. 22 [75].

8.3 Region excluded by direct DM searches

There are two methods of the dark matter detection: direct and indirect. In the direct detection one assumes that the particles of the dark matter to the Earth and interact with the nuclei of a target. In the underground experiments one can hope to observe such events measuring the recoil energy. There are several experiments of this type: DAMA, Zeplin, CDMS and Edelweiss. Among them only the DAMA collaboration claims to observe a positive outcome in the annual modulation of the signal with the fitted dark matter particle mass around 50 GeV [76].

All the other experiments do not see it though CDMS collaboration recently announced about a few events of a desired type [77]. The reason of this disagreement might be in the different methodology and the targets used since the cross-section depends on the spin of the target nucleus. The collected statistics is also essentially different. DAMA has accumulated by far more data and this is the only experiment which studies the modulation of the signal that may be crucial for reducing the background.

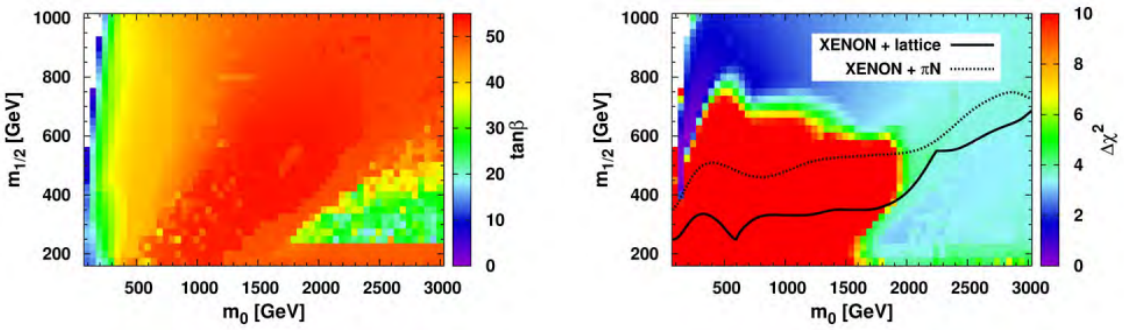

Fig. 22: Left: Fitted values of $\tan\beta$ in the $(m_0 - m_{1/2})$ plane after optimizing A_0 to fulfil the relic density and EWSB constraints at every point. The relic density requires $\tan\beta \approx 50$ in most of the parameter space, where pseudo-scalar Higgs exchange dominates. In the (non-red) edges where $\tan\beta$ is lower, the co-annihilation contributes. Right: $\Delta\chi^2 = \chi^2 - \chi^2_{min}$ distribution in the $(m_0 - m_{1/2})$ plane after imposing the electroweak constraints in comparison with the XENON100 limits [46] on the direct WIMP-nucleon cross-section for the two values of the form factors (dotted line: πN scattering, dashed dotted line: lattice gauge theories).

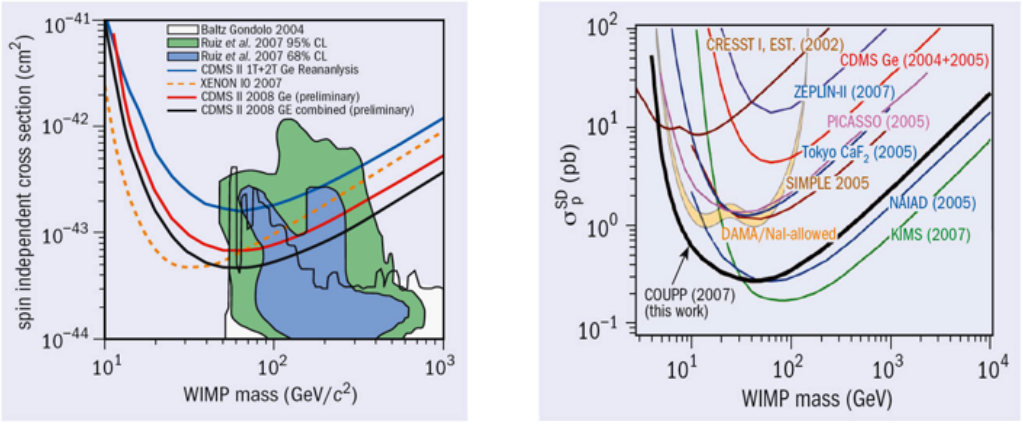

Fig. 23: The exclusion plots from the direct dark matter detection experiments. The spin-independent case (left) from Chicagoland Observatory for Underground Particle Physics (COUPP) and the spin-dependent case (right) from Cryogenic Dark Matter Search (CDMS).

The cross section for direct scattering of WIMPS on nuclei has an experimental upper limit of about 10^{-8} pb, i. e. many orders of magnitude below the annihilation cross section. This cross section is related to the annihilation cross section by similar Feynman diagrams. The many orders of magnitude are naturally explained in Supersymmetry by the fact that both cross sections are dominated by Higgs exchange and the fact that the Yukawa couplings to the valence quarks in the proton or neutron are negligible. Most of the scattering cross section comes from the heavier sea-quarks. However, the density of these virtual quarks inside the nuclei is small, which is one of the reasons for the small elastic scattering cross section. In addition, the momentum transfer in elastic scattering is small, so the propagator leads to a cross section inversely proportional to the fourth power of the Higgs mass.

The typical exclusion plots for the spin-independent and spin-dependent cross-sections are shown in Fig. 23 where one can see DAMA allowed region overlapping with the other exclusion curves. Still today we have no convincing evidence for direct dark matter detection or exclusion. Scattering of the

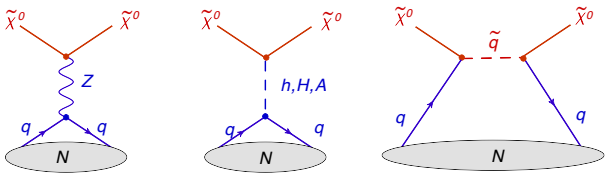

Fig. 24: Examples of diagrams for elastic neutralino-nucleon scattering

LSP on nuclei can only happen via elastic scattering, provided R-parity is conserved [13, 70]. The corresponding diagrams are shown in Fig. 24.

The big blob indicates that one enters a low energy regime, in which case the protons and neutrons inside the nucleus cannot be resolved. In this case the spin-independent scattering becomes coherent on all nuclei and the cross section becomes proportional to the number of nuclei:

$$\sigma = \frac{4}{\pi} \frac{m_{\rm DM}^2 m_N^2}{(m_{\rm DM} + m_N)^2} \left(Z f_p + (A - Z) f_n\right)^2 \tag{70}$$

where A and Z are the atomic mass and atomic number of the target nuclei and the form factors are [78]

$$f_{p,n} = \sum_{q=u,d,s} G_q f_{Tq}^{(p,n)} \frac{m_{p,n}}{m_q} + \frac{2}{27} f_{TG}^{(p,n)} \sum_{q=c,b,t} G_q \frac{m_{p,n}}{m_q}, \tag{71}$$

where $G_q = \lambda_{\rm DM} \lambda_q / M_M^2$. Here M denotes the mediator, and $\lambda_{\rm DM}$, λ_f denote the mediator's couplings to DM and quark. The parameters $f_{Tq}^{(p)}$ are defined by

$$m_p f_{Tq}^{(p)} \equiv \langle p | m_q \bar{q} q | p \rangle \tag{72}$$

and similar for $f_{Tq}^{(n)}$, whilst $f_{TG}^{(p,n)} = 1 - \sum_{q=u,d,s} f_{Tq}^{(p,n)}$.

Since the particle which mediates the scattering is typically much heavier than the momentum transfer, the scattering can be written in terms of an effective coupling, which can be determined phenomenologically from πN scattering or from lattice QCD calculations.

The default values of the effective couplings in micrOMEGAs [79] are: $f_{Tu}^{(p)} = 0.033$, $f_{Td}^{(p)} = 0.023$, $f_{Ts}^{(p)} = 0.26$, $f_{Tu}^{(n)} = 0.042$, $f_{Td}^{(n)} = 0.018$, $f_{Ts}^{(n)} = 0.26$. The lower values from the lattice calculations [80] are: $f_{Tu}^{(p)} = 0.020$, $f_{Td}^{(p)} = 0.026$, $f_{Ts}^{(p)} = 0.02$, $f_{Tu}^{(n)} = 0.014$, $f_{Td}^{(n)} = 0.036$, $f_{Ts}^{(n)} = 0.02$. Hence the most important coupling to the strange quarks vary from 0.26 to 0.02 [81], which implies an order of magnitude uncertainty in the elastic neutralino-nucleon scattering cross section.

Another normalization uncertainty in direct dark matter experiments arises from the uncertainty in the local DM density, which can take values between 0.3 and 1.3 GeV/cm^3, as determined from the rotation curve of the Milky Way, see Ref. [82–85].

The excluded region from the XENON100 cross section limit [46] for two choices of form factors is shown in Fig. 22. At large values of m_0 EWSB forces the higgsino component of the WIMP to increase and consequently the exchange via the Higgs, which has an amplitude proportional to the bino-higgsino mixing, starts to increase. This leads to an increase in the excluded region at large m_0 and has here a similar sensitivity as the LHC. If we would take the less conservative effective couplings from the default values of micrOMEGAs the XENON100 limit would be 50% higher than the LHC limit [66].

9 Search for SUSY at colliders

9.1 Experimental signatures at e^+e^- colliders

Experiments are finally beginning to push into a significant region of supersymmetry parameter space. We know the sparticles and their couplings, but we do not know their masses and mixings. Given the mass spectrum one can calculate the cross-sections and consider the possibilities of observing the new particles at modern accelerators. Otherwise, one can get restrictions on the unknown parameters.

We start with the e^+e^- colliders. In the leading order the processes of creation of the superpartners are given by the diagrams shown in Fig. 7 above. For a given center of mass energy the cross-sections depend on the masses of the created particles and vanish at the kinematic boundary. Experimental signatures are defined by the decay modes which vary with the mass spectrum. The main ones are summarized below, see, e. g. [19, 86]

Production	Decay Modes	Signatures
• $\tilde{l}_{L,R}\tilde{l}_{L,R}$	$\tilde{l}^{\pm}_R \to l^{\pm}\tilde{\chi}^0_i$	acompl pair of
	$\tilde{l}^{\pm}_L \to l^{\pm}\tilde{\chi}^0_i$	charged lept + $\not{E}_T$
• $\tilde{\nu}\tilde{\nu}$	$\tilde{\nu} \to l^{\pm}\tilde{\chi}^0_1$	$\not{E}_T$
• $\tilde{\chi}^{\pm}_1\tilde{\chi}^{\pm}_1$	$\tilde{\chi}^{\pm}_1 \to \tilde{\chi}^0_1 l^{\pm}\nu$	isol lept + 2 jets + $\not{E}_T$
	$\tilde{\chi}^{\pm}_1 \to \tilde{\chi}^0_2 f\bar{f}'$	pair of acompl
	$\tilde{\chi}^{\pm}_1 \to l\tilde{\nu}_l$	leptons + $\not{E}_T$
	$\to l\nu_l\tilde{\chi}^0_1$	
	$\tilde{\chi}^{\pm}_1 \to \nu_l\tilde{l}$	4 jets + $\not{E}_T$
	$\to \nu_l l\tilde{\chi}^0_1$	
• $\tilde{\chi}^0_i\tilde{\chi}^0_j$	$\tilde{\chi}^0_i \to \tilde{\chi}^0_1 X$	$X = \nu_l\bar{\nu}_l$ invisible
		$= \gamma, 2l$, 2 jets
		$2l + \not{E}_T, l + 2j + \not{E}_T$
• $\tilde{t}_i\tilde{t}_j$	$\tilde{t}_1 \to c\tilde{\chi}^0_1$	2 jets + $\not{E}_T$
	$\tilde{t}_1 \to b\tilde{\chi}^{\pm}_1$	2 b-jets + 2 lept + $\not{E}_T$
	$\to bf\bar{f}'\tilde{\chi}^0_1$	
• $\tilde{b}_i\tilde{b}_j$	$\tilde{b}_i \to b\tilde{\chi}^0_1$	2 b-jets + $\not{E}_T$
	$\tilde{b}_i \to b\tilde{\chi}^0_2$	2 b-jets + 2 lept+$\not{E}_T$
	$\to bf\bar{f}'\tilde{\chi}^0_1$	2 b-jets + 2 jets + $\not{E}_T$

The characteristic feature of all the possible signatures is the missing energy and transverse momentum, which is a trade mark of the new physics.

Numerous attempts to find the superpartners at LEP II gave no positive result thus imposing the lower bounds on their masses [87]. Typical LEP II limits on the superpartner masses are

$$m_{\chi^0_1} > 40 \text{ GeV},\ m_{\tilde{e}} > 105 \text{ GeV},\ m_{\tilde{t}} > 90 \text{ GeV}$$
$$m_{\chi^{\pm}_1} > 100 \text{ GeV},\ m_{\tilde{\mu}} > 100 \text{ GeV},\ m_{\tilde{b}} > 80 \text{ GeV},\ m_{\tilde{\tau}} > 80 \text{ GeV}$$

9.2 Experimental signatures at hadron colliders

Experimental SUSY signatures at the Tevatron and LHC are similar. The strategy of the SUSY searches is based on the assumption that the masses of the superpartners indeed are in the region of 1 TeV so that they might be created on the mass shell with the cross-section big enough to distinguish them from the background of the ordinary particles. Calculation of the background in the framework of the Standard Model thus becomes essential since the secondary particles in all the cases are the same.

There are many possibilities to create the superpartners at the hadron colliders. Besides the usual annihilation channel there are numerous processes of the gluon fusion, quark-antiquark and quark-gluon scattering. The maximal cross-sections of the order of a few picobarn can be achieved in the process of gluon fusion.

As a rule all the superpartners are short lived and decay into the ordinary particles and the lightest superparticle. The main decay modes of the superpartners which serve as the manifestation of SUSY are

Production	Decay Modes	Signatures
• $\tilde{g}\tilde{g}, \tilde{q}\tilde{q}, \tilde{g}\tilde{q}$	$\tilde{g} \to q\bar{q}\tilde{\chi}_1^0$ $q\bar{q}'\tilde{\chi}_1^\pm$ $g\tilde{\chi}_1^0$ $\tilde{q} \to q\tilde{\chi}_i^0$ $\tilde{q} \to q'\tilde{\chi}_i^\pm$	$\not{E}_T$ + multijets (+leptons)
• $\tilde{\chi}_1^\pm\tilde{\chi}_2^0$	$\tilde{\chi}_1^\pm \to \tilde{\chi}_1^0 l^\pm\nu$ $\tilde{\chi}_2^0 \to \tilde{\chi}_1^0 ll$	Trilepton + $\not{E}_T$
	$\tilde{\chi}_1^\pm \to \tilde{\chi}_1^0 q\bar{q}'$ $\tilde{\chi}_2^0 \to \tilde{\chi}_1^0 ll$	Dilept + jet + $\not{E}_T$
• $\tilde{\chi}_1^+\tilde{\chi}_1^-$	$\tilde{\chi}_1^+ \to l\tilde{\chi}_1^0 l^\pm\nu$	Dilepton + $\not{E}_T$
• $\tilde{\chi}_i^0\tilde{\chi}_i^0$	$\tilde{\chi}_i^0 \to \tilde{\chi}_1^0 X$	$\not{E}_T$ + Dilept+jets
• $\tilde{t}_1\tilde{t}_1$	$\tilde{t}_1 \to c\tilde{\chi}_1^0$	2 acollin jets + $\not{E}_T$
	$\tilde{t}_1 \to b\tilde{\chi}_1^\pm$ $\tilde{\chi}_1^\pm \to \tilde{\chi}_1^0 q\bar{q}'$	sing lept + $\not{E}_T + b's$
	$\tilde{t}_1 \to b\tilde{\chi}_1^\pm$ $\tilde{\chi}_1^\pm \to \tilde{\chi}_1^0 l^\pm\nu$	Dilept + $\not{E}_T + b's$
• $\tilde{l}\tilde{l}, \tilde{l}\tilde{\nu}, \tilde{\nu}\tilde{\nu}$	$\tilde{l}^\pm \to l \pm \tilde{\chi}_i^0$	Dilepton + $\not{E}_T$
	$\tilde{l}^\pm \to \nu_l\tilde{\chi}_i^\pm$	Single lept + $\not{E}_T$
	$\tilde{\nu} \to \nu\tilde{\chi}_1^0$	$\not{E}_T$

Note again the typical events with the missing energy and transverse momentum that is the main difference from the background processes of the Standard Model. Contrary to the e^+e^- colliders, at hadron machines the background is extremely rich and essential. The missing energy is carried away by the heavy particle with the mass of the order of 100 GeV that is essentially different from the processes with the neutrino in the final state. In hadron collisions the superpartners are always created in pairs and then further quickly decay creating a cascade with the ordinary quarks (i. e. hadron jets) or leptons in the final state plus the missing energy. For the case of the gluon fusion with the creation of gluino it is presented in Table 3 (right panel).

The chargino and neutralino can also be produced in pairs through the Drell-Yang mechanism $pp \to \tilde{\chi}_1^\pm\tilde{\chi}_2^0$ and can be detected via their lepton decays $\tilde{\chi}_1^\pm\tilde{\chi}_2^0 \to \ell\ell\ell + \not{E}_T$. Hence the main signal

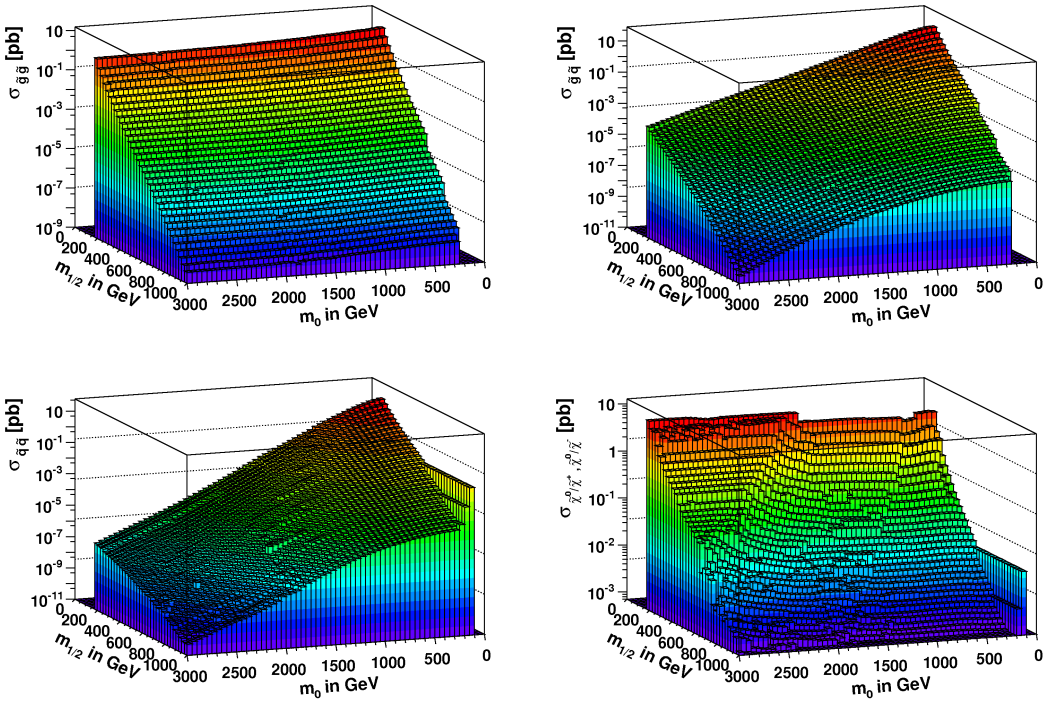

Fig. 25: The cross-sections for the SUSY particles production for the diagrams shown in Fig. 8: clockwise via the strong interactions ($\tilde{g}\tilde{g}$, $\tilde{g}\tilde{q}$ and $\tilde{q}\bar{\tilde{q}}$, respectively) and the electroweak interactions.

of their creation is the isolated leptons and the missing energy, see Table 3 (left panel). The main background in the trilepton channel comes from the creation of the standard particles $WZ/ZZ, t\bar{t}, Zb\bar{b}$ ï£¡ $b\bar{b}$. There might be also the supersymmetric background from the cascade decays of the squarks and gluinos in multilepton modes.

9.3 Excluded region by direct searches for SUSY at the LHC

The background from the SM processes results in the same final states although with different kinematics. The missing energy in this case is taken away by the light neutrinos. The corresponding processes are shown in Table 4.

Numerous SUSY searches have been already performed at the Tevatron. The pair-produced squarks and gluinos have at least two large-E_T jets associated with the large missing energy. The final state with the lepton(s) is possible due to the leptonic decays of the $\tilde{\chi}_1^{\pm}$ and/or $\tilde{\chi}_2^0$.

In the trilepton channel the Tevatron is sensitive up to $m_{1/2} \leq 250$ GeV if $m_0 \leq 200$ GeV and up to $m_{1/2} \leq 200$ GeV if $m_0 \geq 500$ GeV. The existing limits on the squark and gluino masses at the Tevatron are [88]: $m_{\tilde{q}} \geq 300$ GeV, $m_{\tilde{g}} \geq 195$ GeV.

In the proton-proton collisions at the LHC the supersymmetric particles can be produced according to the main diagrams shown in the first three rows of Fig. 8, while the main diagrams for the electroweak production are shown in the last row. The corresponding cross-sections are shown in Fig. 25 for the centre-of-mass energy of 7 TeV [75]. One observes that the cross-section for the "strong" production of $\tilde{q}\bar{\tilde{q}}$ and $\tilde{g}\tilde{q}$ are large for the low values of m_0 and $m_{1/2}$, the gluino production $\tilde{g}\tilde{g}$ is the strongest at the small values of $m_{1/2}$ and the electroweak production of gauginos starts to increase at the large values of m_0. The reason for the increase of the electroweak production at large m_0 is the decrease of the Higgs mixing parameter μ, as determined from the EWSB, which leads to stronger mixing of the Higgsino

Table 3: Creation of the lightest chargino and the second neutralino with further cascade decay (left). Creation of the pair of gluinos with further cascade decay (right).

Process	Final states
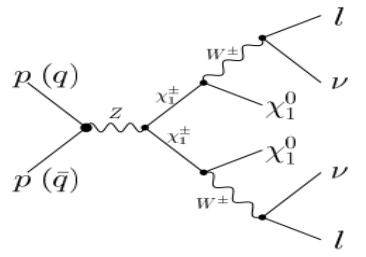	2ℓ 2ν $\not{E}_T$
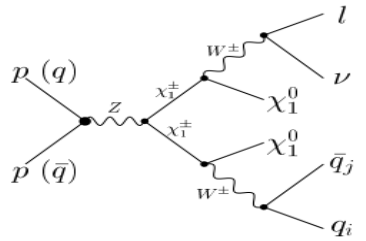	ℓ ν $2j$ $\not{E}_T$
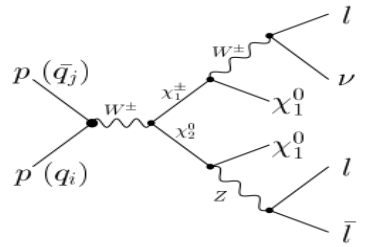	3ℓ ν $\not{E}_T$
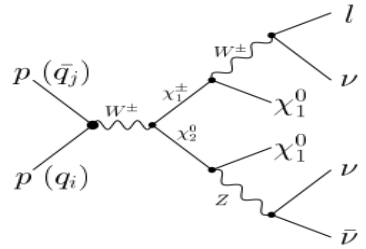	ℓ 3ν $\not{E}_T$
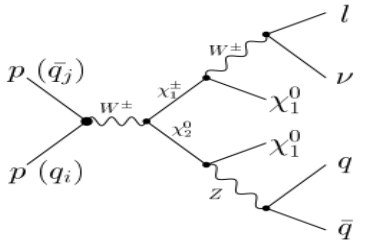	ℓ ν $2j$ $\not{E}_T$

Process	Final states
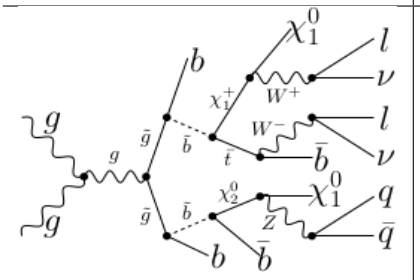	2ℓ 2ν $6j$ $\not{E}_T$
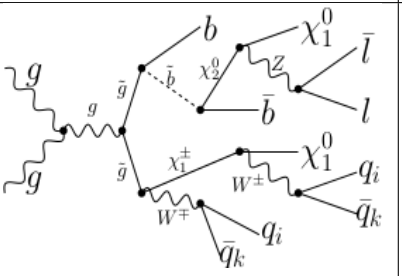	2ℓ $6j$ $\not{E}_T$
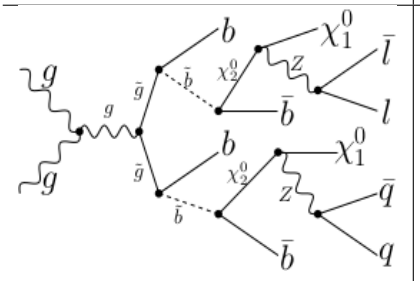	2ℓ $6j$ $\not{E}_T$
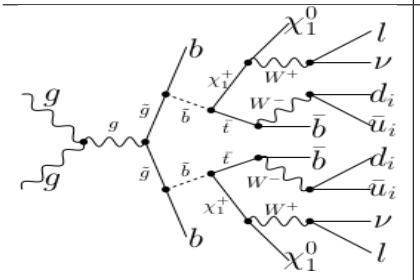	2ℓ 2ν $8j$ $\not{E}_T$
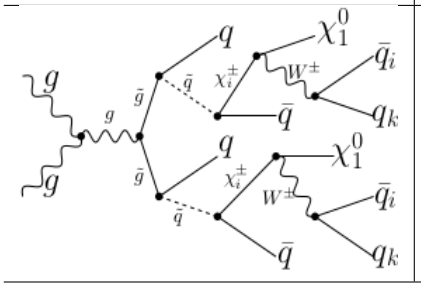	$8j$ $\not{E}_T$

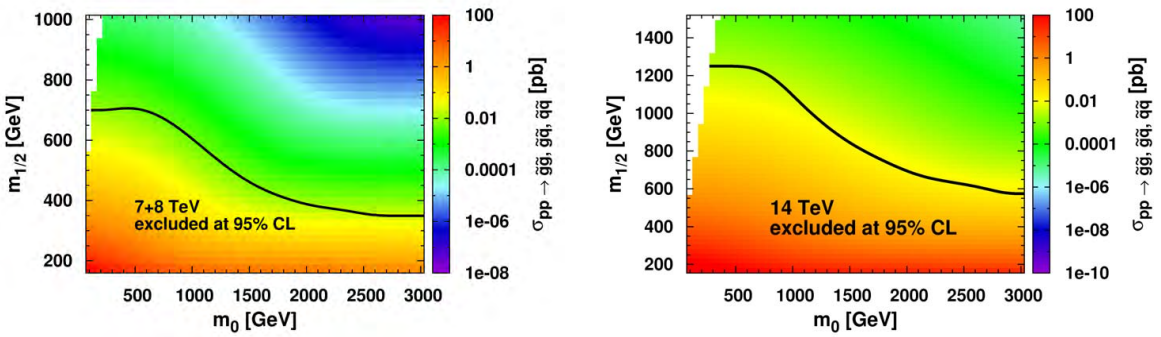

Fig. 26: Left: The total production cross-section of the strongly interacting particles in comparison with the LHC excluded limits for 7+8 TeV. Here the data from ATLAS and CMS were combined and correspond to the integrated luminosity of 1.3 and 1.1 fb^{-1}, respectively. One observes that the cross-section of 0.1 to 0.2 pb is excluded at 95% CL. Right: the cross sections at 14 TeV and expected exclusion for the same limit on the cross-section as at 7 TeV.

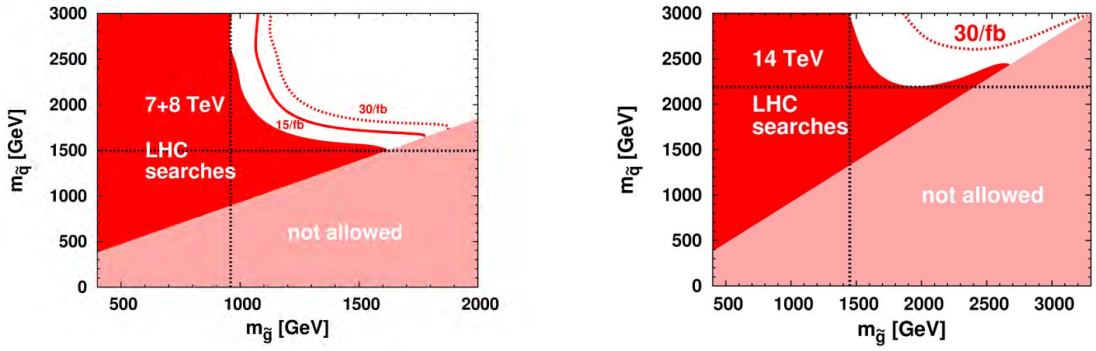

Fig. 27: As in Fig. 26, but the excluded region is translated into the $m_{\tilde{q}}, m_{\tilde{g}}$ plane. The red area corresponds to the excluded regions for the integrated luminosity slightly above 1 fb^{-1}; the expectations for the higher luminosities have been indicated as well.

component in the gauginos and so the coupling to the weak gauge bosons and Higgs bosons increases, thus increasing the amplitudes for the diagrams in the last row of Fig. 8.

The "strong" production cross sections are characterized by a large number of jets from the long decay chains and the missing energy from the escaping neutralino. These characteristics can be used to efficiently suppress the background. For the electroweak production, both the number of jets and the missing transverse energy is low, since the LSP is not boosted so strongly as in the decay of the heavier strongly interacting particles. Hence, the electroweak gaugino production needs the leptonic decays to reduce the background, so these signatures need more luminosity and cannot compete at present with the sensitivity of the "strong" production of the squarks and gluinos.

The total cross-section for the strongly interacting particles are shown in Fig. 26 together with the excluded region from the direct searches for SUSY particles at the LHC. One observes that the excluded region (below the solid line) follows rather closely the total cross-section, indicated by the colour shading. From the colour coding one observes that the excluded region corresponds to the cross-section limit of about $0.1 - 0.2$ pb.

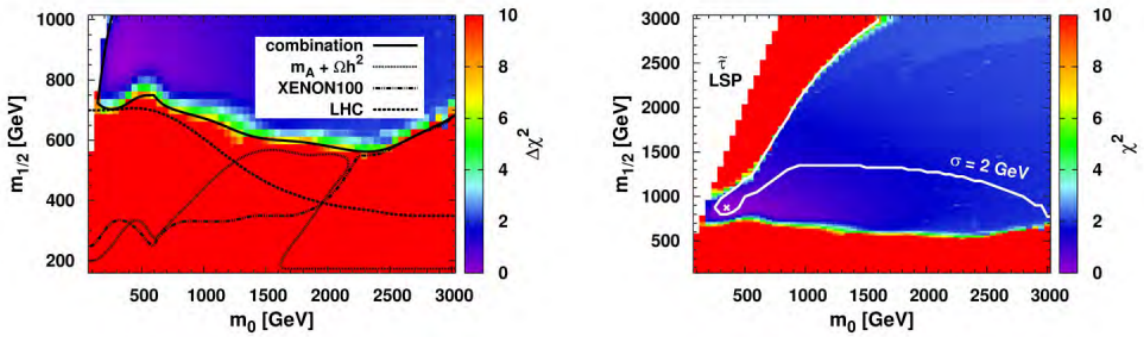

Fig. 28: Left: Combined constraints from the LHC searches, the relic density from WMAP, the direct DM searches from XENON100, limits on the pseudo-scalar Higgs mass and $g-2$ of muon (without the 125 GeV Higgs boson mass constraint). Right: The account of the 125 GeV Higgs boson mass constraint with 2 GeV mass uncertainty. The region below the white line is excluded at 95% C.L.

The drop of the excluded region at large values of m_0 is due to the fact that in this region the squarks become heavy, which means that the contributions from the diagrams in the second and third rows of Fig. 8 start to diminish. Here only the higher energies will help and doubling the LHC energy from 7 to 14 TeV, as planned in the coming years, quickly increases the cross-section for the gluino production by orders of magnitude, as shown in the right panel of Fig. 26. The expected sensitivity at 14 TeV, plotted as the exclusion contour in case nothing is found, assumes the same efficiency and luminosity (slightly above one fb^{-1} per experiment) as at 7 TeV.

These limits can be translated to the squark and gluino masses as follows. The squark masses have a starting value at the GUT scale equal to m_0, but have important contributions from the gluinos in the colour field, so the squark masses are given by $m_{\tilde{q}}^2 \approx m_0^2 + 6.6 m_{1/2}^2$, as was determined from the renormalization group equations [30]. Similarly the gluino mass is given by $2.7 m_{1/2}$. The term proportional to $m_{1/2}$ in the squark mass corresponds to the self-energy diagrams, which imply that if the "gluino-cloud" is heavy, the squarks cannot be light. This leads to the regions indicated as not allowed ones in Fig. 27. Note that these regions are forbidden in any model with the coupling between the squarks and gluinos, so they are not specific to the CMSSM. The squark masses below 1.1 TeV and the gluino masses below 0.62 TeV are excluded for the LHC data at 7 TeV, as shown in the left panel of Fig. 27. Expected sensitivities for the higher integrated luminosities at 7 and 14 TeV have been indicated as well. One observes that increasing the energy is much more effective than increasing the luminosity. At 14 TeV the squarks with masses of 1.7 TeV and gluinos with masses of 1.02 TeV are within reach with 1 fb^{-1} per experiment, as shown in the right panel of Fig. 27.

9.4 Excluded region for combination of constraints

If one combines the excluded regions from the direct searches at the LHC, the relic density from the WMAP, the already stringent limits on the pseudo-scalar Higgs mass with the XENON100 limits one obtains the excluded region shown in the left panel of Fig. 28. Here the $g-2$ limit is included with the conservative linear addition of theoretical and experimental errors. One observes that the combination excludes $m_{1/2}$ below 525 GeV in the CMSSM for $m_0 < 1500$ GeV, which implies the lower limit on the WIMP mass of 230 GeV and a gluino mass of 1370 GeV, respectively.

As discussed earlier, the LHC becomes rather insensitive to the large m_0 region because of the decreasing cross-section for the production of strongly interaction particles and the large background for the production of gauginos. However, in this region one obtains the increased sensitivity above the LHC limits from the relic density and the direct DM searches.

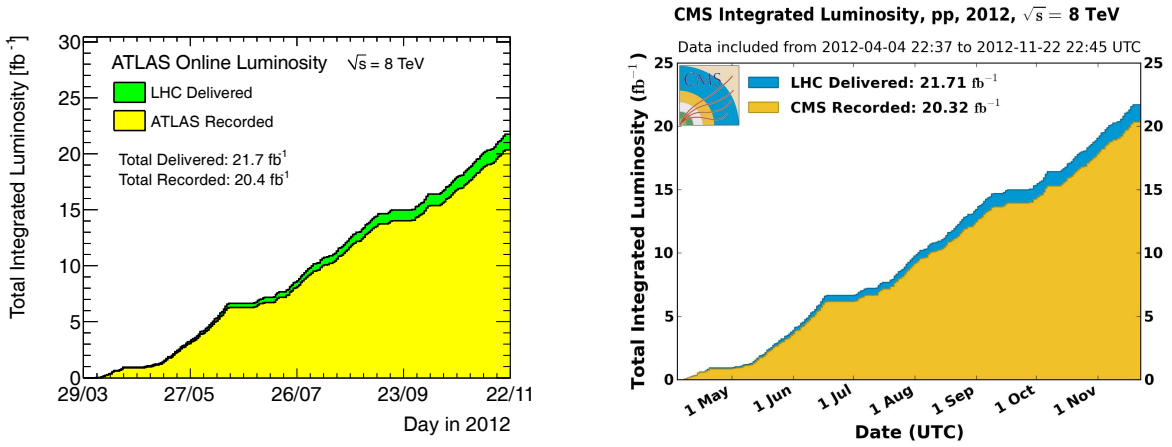

Fig. 29: Cumulative luminosity versus day delivered by LHC, and recorded by ATLAS (left) and CMS (right) experiments for pp collisions at $\sqrt{s}$ = 8 TeV in 2012 from counting rates measured by the luminosity detectors.

If a Higgs mass of the lightest Higgs boson of 125 GeV is imposed, the preferred region is well above this excluded region, but the size of the preferred region is strongly dependent on the size of the assumed theoretical uncertainty as was shown in Fig. 19. Accepting the 2 GeV uncertainty we get the excluded region shown in Fig. 28 (right panel), which is far above the existing LHC limits and leads to strongly interacting superpartners above 2 TeV. However, in models with an extended Higgs sector, like NMSSM [89], a Higgs mass of 125 GeV can be obtained for lower values of $m_{1/2}$, in which case the regions excluded in the MSSM become viable.

10 The reach of the LHC

10.1 LHC luminosity

The Large Hadron Collider is the unique machine for the new physics searches at the TeV scale. Its c.m. energy is planned to be 14 TeV with very high luminosity up to a few hundred fb^{-1}. At the moment the total integrated luminosity in 2012 is already more than 20 fb^{-1}. Fig. 29 shows the luminosity delivered in 2012 in pp collisions at the center-of mass energy of 8 TeV and recorded by ATLAS [90] and CMS [91] experiments.

10.2 Expected LHC reach for SUSY

The LHC is supposed to cover a wide range of parameters of the MSSM (see Figs. below) and discover the superpartners with the masses below 2 TeV. This will be a crucial test for the MSSM and the low energy supersymmetry. The LHC potential to discover supersymmetry is widely discussed in the literature [92, 93].

To present the region of reach for the LHC in different channels of sparticle production it is useful to take the same plane of soft SUSY breaking parameters m_0 and $m_{1/2}$. In this case one usually assumes certain luminosity which will be presumably achieved during the accelerator operation. Thus, for instance, in Fig. 30 the regions of reach in different channels are shown. The lines of the constant squark mass form the arch curves, and those for the gluino are almost horizontal. The curved lines show the reach bounds in different channel of creation of the secondary particles. The theoretical curves are obtained within the MSSM for a certain choice of the other soft SUSY breaking parameters. As one can see, for the fortunate circumstances the wide range of the parameter space up to the masses of the order of 2 TeV will be examined. The LHC will be able to discover SUSY with the squark and gluino masses up to $2 \div 2.5$ TeV for the luminosity $L_{tot} = 100$ fb^{-1}. The most powerful signature for the squark and

Table 4: The background at the hadron colliders: the weak interaction processes (left), and the strong interaction processes (right).

Process	Final states
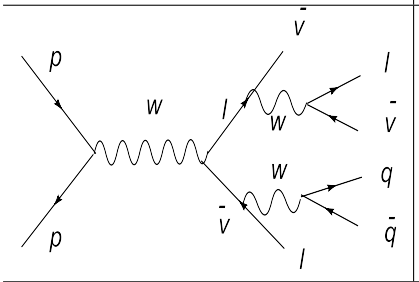	2ℓ $2j$ $\not{E}_T$
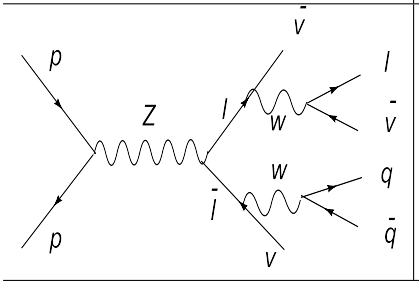	ℓ $2j$ $\not{E}_T$

Process	Final states
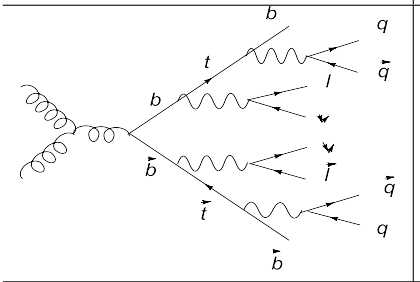	2ℓ $6j$ $\not{E}_T$
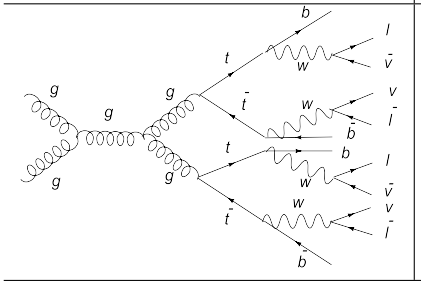	4ℓ $4j$ $\not{E}_T$

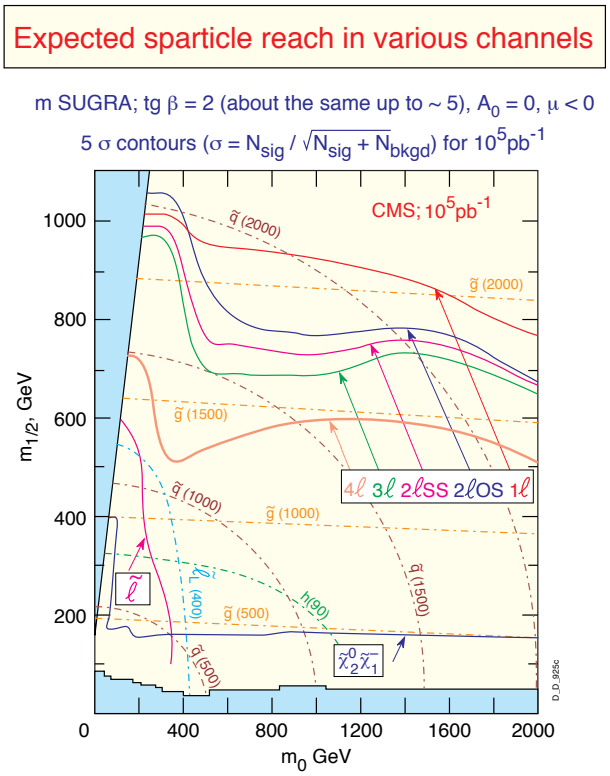

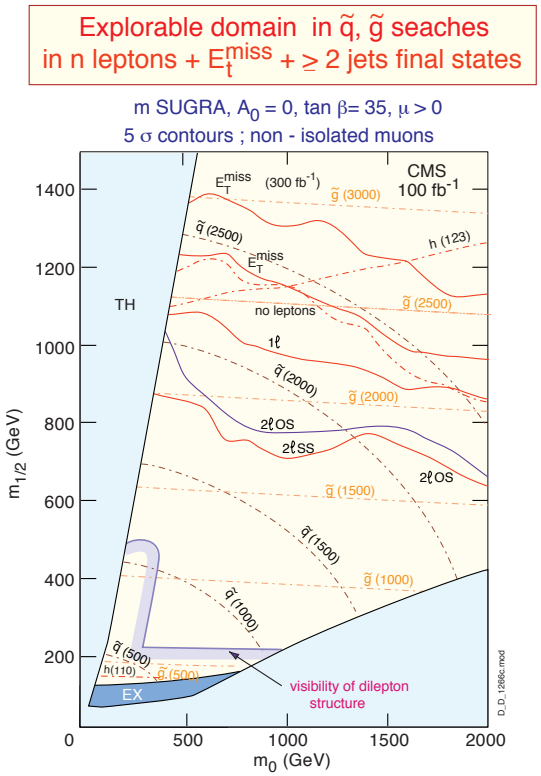

Fig. 30: The expected range of reach for the superpartners in various channels at the LHC(left) and the expected domain of searches for the squarks and gluions at the (right) [94].

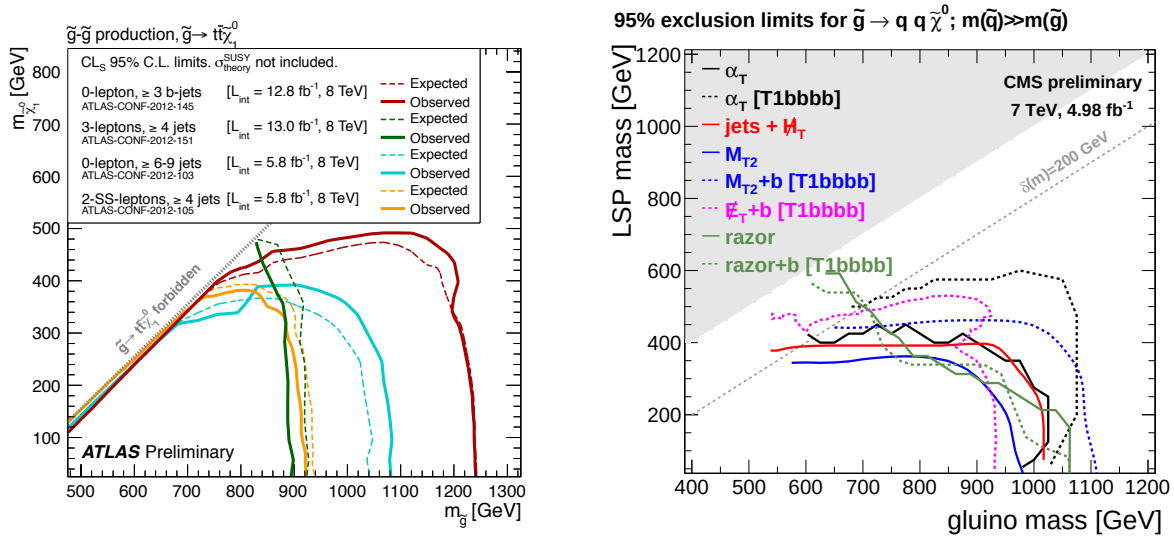

Fig. 31: Left: ATLAS exclusion limits at 95% CL for 8 TeV analyses in the $m_{\tilde{g}} - m_{\tilde{\chi}_1^0}$ plane for the *Gtt* simplified model where a pair of gluinos decays via off-shell stop to four top quarks and two neutralinos (LSP). Right: CMS exclusion limits at 95% CL for 7 TeV analyses of gluino decay $\tilde{g} \to qq\tilde{\chi}_1^0$, assuming $m_{\tilde{q}} >> m_{\tilde{g}}$.

gluino detection are the multijet events; however, the discovery potential depends on the relation between the LSP, squark, and gluino masses, and decreases with the increase of the LSP mass. The same is true for the sleptons. The typical signal used for the slepton detection is the dilepton pair with the missing energy without hadron jets. For the luminosity of $L_{tot} = 100$ fb^{-1} the LHC will be able to discover sleptons with the masses up to 400 GeV [92, 93].

10.3 Recent results on SUSY searches

Direct searches of the superpartners at the LHC in different channels have pushed the lower limits on their masses, mainly of the gluinos and the squarks of the light two generations, upwards to the TeV range. On the other hand, for the third generation the limits are rather weak and the masses around a few hundred GeV are still allowed. The light third generation squarks are also consistent with the recent observation of the Higgs-like boson with the mass around 125 GeV.

We present here examples on the superparticle searches in various scenarios depicted as exclusion plots. Everywhere in these plots the excluded region is the one below the corresponding curve (lower masses, lower values of parameters).

The fisrt example is the gluino pair production $pp \to \tilde{g}\tilde{g}$ and $\tilde{g} \to t\bar{t}\tilde{\chi}_1^0$ decay in the so-called *Gtt* simplified model. Four different final states (0 leptons with ≥ 3 b-jets [95]; 3 leptons with ≥ 4 jets [96]; 0 leptons with $\geq$ 6-9 jets [97]; and a pair of the same-sign leptons with more than 4 jets [98]) are considered. The first two analysis performed using 12.8 fb^{-1} and 13.0 fb^{-1} data and the last two ones using 5.8 fb^{-1} data. The results slightly differ quantitatively, however, the conclusion is the non-observation of the gluino lighter than 900 GeV (conservative limit) or even 1200 GeV for the lightest neutralino mass less than around 300 GeV.

Another example is the result of searches of the top-squark pair production by ATLAS collaboration based on 4.7 fb^{-1} of pp collision data taken at $\sqrt{S}$ = 7 TeV. The exclusion limits at 95% CL are shown in the $\tilde{t}_1 - \tilde{\chi}_1^0$ mass plane. The dashed and solid lines show the expected and observed limits, respectively, including all uncertainties except the theoretical signal cross-section uncertainty (PDF and scale). The dotted lines represent the results obtained when reducing the nominal signal cross-section by

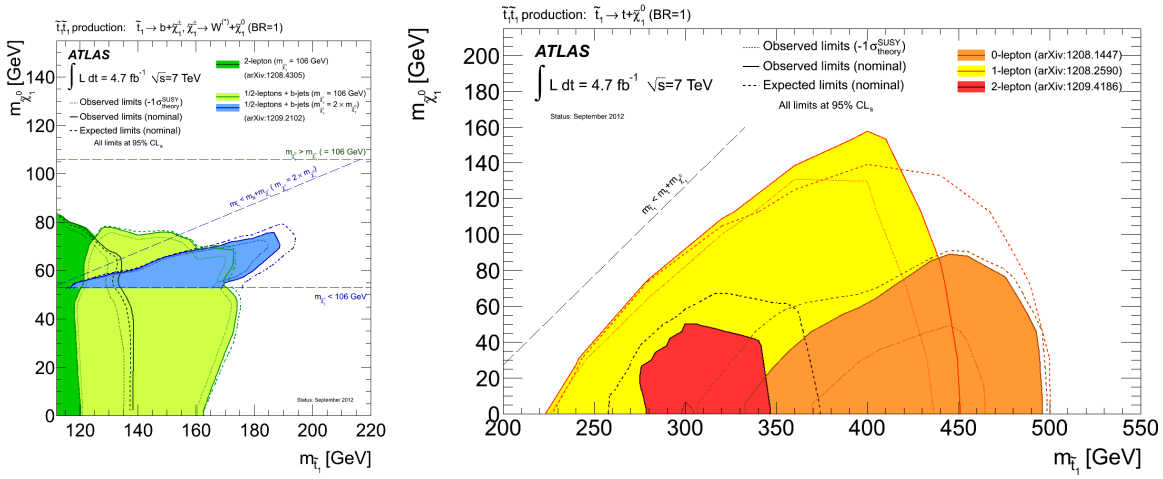

Fig. 32: Summary of the five dedicated ATLAS searches for the top-squark pair production based on 4.7 fb^{-1} of the pp collision data taken at $\sqrt{s}$ = 7 TeV.

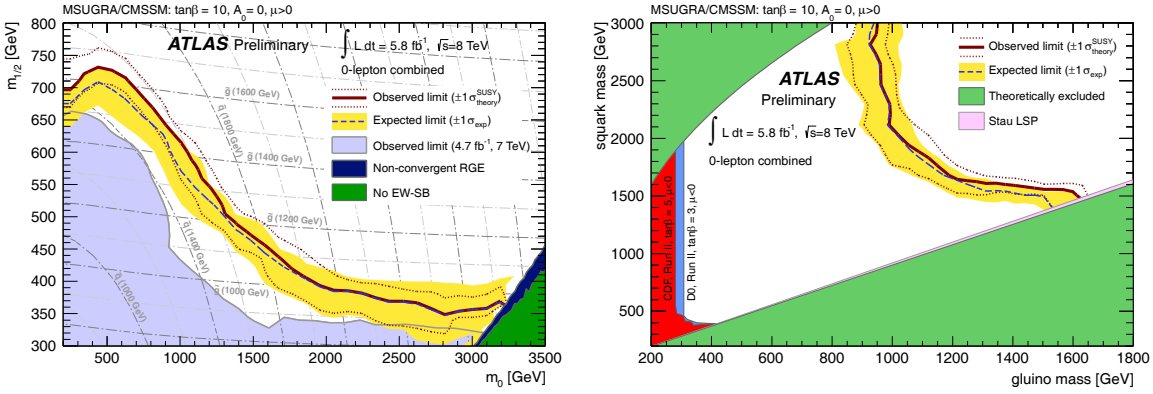

Fig. 33: 95% CL exclusion limits for MSUGRA/CMSSM models with $\tan\beta = 10$, $A_0 = 0$ and $mu > 0$ presented in the $m_0 - m_{1/2}$ plane (left) and in the $m_{gluino} - m_{squark}$ plane (right). The blue dashed lines show the expected limits at 95% CL, with the light (yellow) bands indicating the 1σ excursions due to experimental uncertainties. The observed limits are indicated by medium (maroon) curves. Previous results from ATLAS [104] are represented by the shaded (light blue) area. The theoretically excluded regions (green and blue) are described in Ref. [105].

1σ of its theoretical uncertainty. Depending on the stop mass there can be two different decay channels. For relatively light stops with masses below 200 GeV, the decay $\tilde{t}_1 \to b + \tilde{\chi}_1^{\pm}$, $\tilde{\chi}_1^{\pm} \to W^* + \tilde{\chi}_1^0$ is assumed in all the cases, with two hypotheses on the $\tilde{\chi}_1^{\pm}$, $\tilde{\chi}_1^0$ mass hierarchy, $m(\tilde{\chi}_1^{\pm}) = 106$ GeV and $m(\tilde{\chi}_1^{\pm}) = 2m(\tilde{\chi}_1^0)$ [99, 100], see the left panel of Fig. 32. For the heavy stop masses above 200 GeV, the decay $\tilde{t}_1 \to t + \tilde{\chi}_1^0$ is assumed to dominate, the excluded regions are shown in the right panel of Fig. 32 [99–101].

All the exclusion plots discussed above can give direct limits on the masses of supersymmetric particles under certain assumptions (mass relations, dominant decay channels, modified or/and simplified models, etc.). The latest mass limits for the different models and final state channels obtained by ATLAS are shown in Fig. 34 [106]. Fig. 35 [107, 108] shows the best exclusion limits of the CMS collaboration for 4.98 fb^{-1} data and $\sqrt{s} = 7$ TeV as well as observed limits plotted in the CMSSM $(m_0 - m_{1/2})$ plane.

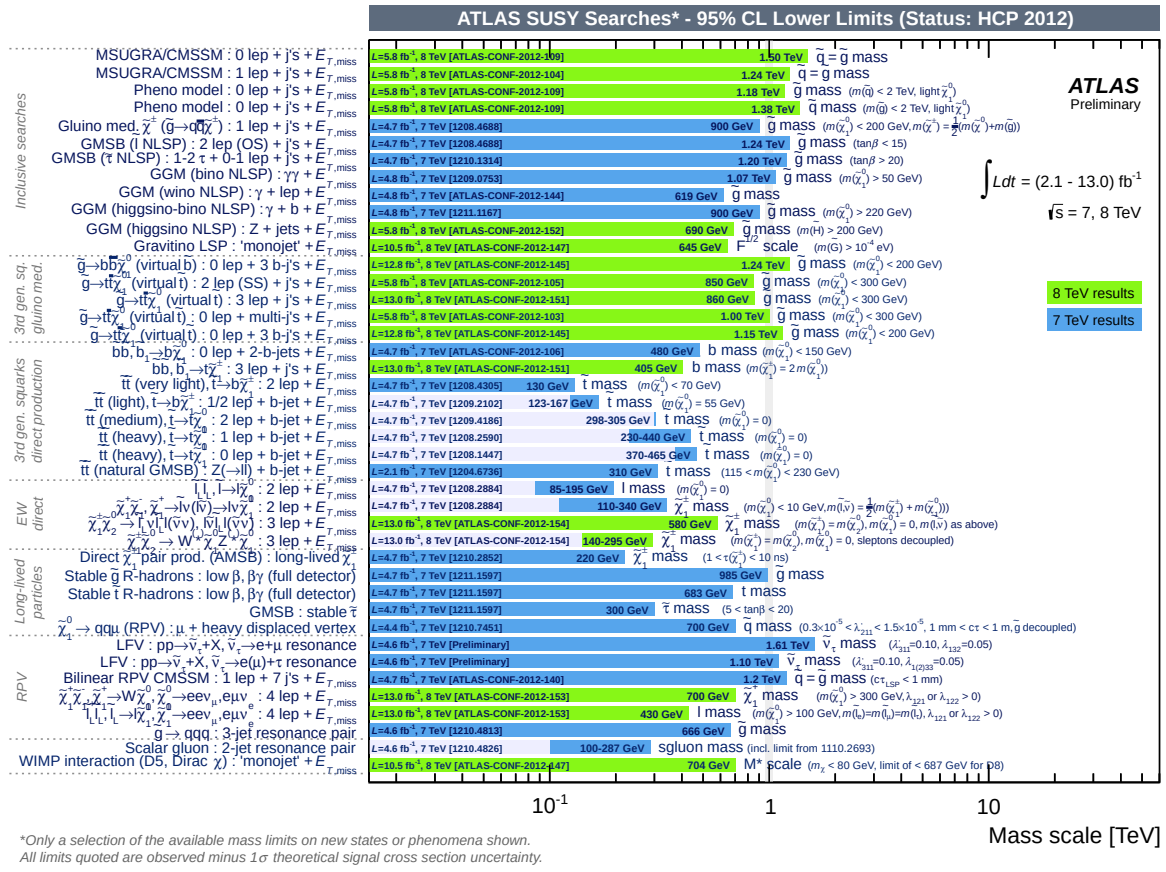

Fig. 34: Mass reach of ATLAS searches for supersymmetry (representative selection)

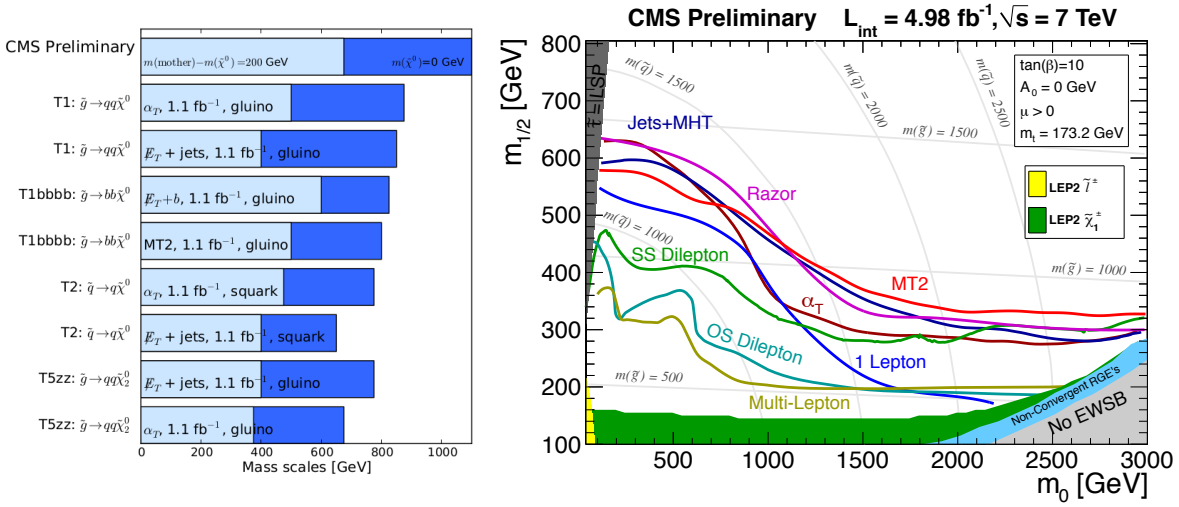

Fig. 35: Left: Best exclusion limits for the gluino and squark masses, for m_{χ^0} = 0 GeV (dark blue) and $m(mother) - m_{\chi^0}$ = 200 GeV (light blue), for each topology, for the hadronic results. Right: Observed limits from several 2011 CMS SUSY searches plotted in the CMSSM $(m_0 - m_{1/2})$ plane.

11 Conclusion

Supersymmetry remains the most popular extension of the Standard Model. Comparison of the MSSM with precision experimental data is as good as for the SM. At the same time, supersymmetry stabilizes the SM due to the cancellation of quadratic divergences to the Higgs boson mass. The prediction of the Higgs boson mass in the MSSM in the region indicated by experimental data can be also considered as an argument if favour of supersymmetry. Besides, the relic density of the DM is not described in the SM but is naturally explained in the MSSM. What is remarkable, the cross section of neutralino annihilation happens to be precisely equal to what is needed for a correct relic density.

Constrained MSSM with a few free parameters seems to satisfy all experimental and theoretical requirements, though recently some tension with the light Higgs boson mass has appeared. The natural way out would be either to release some constraints thus introducing more free parameters or to extend the minimal model, for instance, enlarging the Higgs sector like in the NMSSM. Since it is not clear which model might be correct, all possibilities are open. Unfortunately, there is no "model independent" way of describing SUSY searches, as well as a "smoking gun" process for SUSY except for the discovery of superpartners in the events with missing transverse energy.

Today after 40 years since the invention of supersymmetry we have no single convincing evidence that supersymmetry is realized in particle physics. Still it remains very popular in quantum field theory and in string theory due to its exceptional properties but needs experimental justification.

Let us remind the main *pros* and *contras* for supersymmetry in particle physics

Pro:

- Provides natural framework for unification with gravity
- Leads to gauge coupling unification (GUT)
- Solves the hierarchy problem
- Is a solid quantum field theory
- Provides natural candidate for the WIMP cold DM
- Predicts new particles and thus generates new job positions

Contra:

- Does not shed new light on the problem of
  - Quark and lepton mass spectrum
  - Quark and lepton mixing angles
  - the origin of CP violation
  - Number of flavours
  - Baryon asymmetry of the Universe
- Doubles the number of particles

Low energy supersymmetry promises us that new physics is round the corner at the TeV scale to be exploited at colliders and astroparticle experiments of this decade. If our expectations are correct, very soon we will face new discoveries, the whole world of supersymmetric particles will show up and the table of fundamental particles will be enlarged in increasing rate. This would be a great step in understanding the microworld.

Coming back to the question in the title of these lectures, whether SUSY is alive or not, we can say that so far the parameter space of SUSY models is large enough to incorporate all data. Slight tension that appears in particular models can be removed by extension of a model. However, there exist some broad prediction of low energy SUSY that is falsifiable. This is the presence of superpartners at TeV scale. At least some of them should be light enough to be discovered at the LHC at full energy run at 14 TeV. Otherwise, if the scale of SUSY exceeds several TeV, we loose the main arguments in favour of low

energy supersymetry, namely, the unification of the gauge couplings and the solution of the hierarchy problem. Then the need for a low energy supersymmetry becomes questionable and the possibilities to test it become hardly feasible. The future will show whether we are right in our expectations or not.

Acknowledgements

The authors would like to express their gratitude to the organizers of the School for their effort in creating a pleasant atmosphere and support. This work was partly supported by RFBR grant # 11-02-01177 and Russian Ministry of Education and Science grant # 3802.2012.2.

References

[1] Y. A. Golfand and E. P. Likhtman, *JETP Letters* **13** (1971) 452;
D. V. Volkov and V. P. Akulov, *JETP Letters* **16** (1972) 621;
J. Wess and B. Zumino, *Phys. Lett.* **B49** (1974) 52.

[2] P. Fayet and S. Ferrara, *Phys. Rep.* **32** (1977) 249;
M. F. Sohnius, *Phys. Rep.* **128** (1985) 41;
H. P. Nilles, *Phys. Rep.* **110** (1984) 1;
H. E. Haber and G. L. Kane, *Phys. Rep.* **117** (1985) 75;
A. B. Lahanas and D. V. Nanopoulos, *Phys. Rep.* **145** (1987) 1.

[3] J. Wess and J. Bagger, *Supersymmetry and Supergravity*, Princeton Univ. Press, 1983.

[4] A. Salam, J. Strathdee, *Nucl. Phys.* **B76** (1974) 477;
S. Ferrara, J. Wess, B. Zumino, *Phys. Lett.* **BS1** (1974) 239.

[5] S. J. Gates, M. Grisaru, M. Roček and W. Siegel, *Superspace or One Thousand and One Lessons in Supersymmetry*, Benjamin & Cummings, 1983;
P. West, *Introduction to supersymmetry and supergravity*, World Scientific, 1990;
S. Weinberg,*The quantum theory of fields*, Vol. 3, Cambridge, UK: Univ. Press, 2000.

[6] S. Coleman and J .Mandula, *Phys. Rev.* **159** (1967) 1251.

[7] G. G. Ross, *Grand Unified Theories*, Benjamin & Cummings, 1985.

[8] C. Amsler et al. (Particle Data Group), *Phys. Lett.* **B667** (2008) 1.

[9] U. Amaldi, W. de Boer and H. Fürstenau, *Phys. Lett.* **B260** (1991) 447.

[10] Y. Sofue, V. Rubin, *Ann. Rev. Astron. Astrophys.* **39** (2001) 137, and refs therein.

[11] C.S. Kochanek, *Astrophys. J.* **453** (1995) 545;
N.Kaiser, G.Squires, *Astrophys. J.* **404** (1993) 441.

[12] V.A. Ryabov, V.A. Tsarev and A.M. Tskhovrebov, *Phys. Usp.* **51** (2008) 1091, and refs therein.

[13] G. Jungman, M. Kamionkowski and K. Griest, *Phys. Rep.* **267** (1996) 195;
H. Goldberg, *Phys. Rev. Lett.* **50** (1983) 1419;
J.R. Ellis, et al., *Nucl. Phys.* **B238** (1984) 453.

[14] M.B. Green, J.H. Schwarz and E. Witten, *Superstring Theory*, Cambridge, UK: Univ. Press, 1987.

[15] F.A. Berezin, *The Method of Second Quantization*, Moscow, Nauka, 1965.

[16] M. Peskin and D. Schröder, *An Introduction to Quantum Field Theory*, Addison-Wesley, 1995.

[17] H. Baer and X. Tata, *Weak Scale Supersymmetry*, Cambridge University Press, 2006.

[18] H.E. Haber, *Introductory Low-Energy Supersymmetry*, Lectures given at TASI 1992, (SCIPP 92/33, 1993), `hep-ph/9306207`;
D.I. Kazakov, *Beyond the Standard Model (In search of supersymmetry)*, Lectures at the ESHEP 2000, CERN-2001-003, `hep-ph/0012288`;
D. I. Kazakov, *Beyond the Standard Model*, Lectures at the ESHEP 2004, `hep-ph/0411064`;
D.I. Kazakov, *Nucl. Phys. Proc. Suppl.* **203-204** (2010) 118.

[19] A.V. Gladyshev, D.I. Kazakov, *Supersymmetry and LHC*, Phys. Atom. Nucl. **70** (2007) 1553, hep-ph/0606288.

[20] http://atlasinfo.cern.ch/Atlas/documentation/EDUC/physics14.html

[21] P. Fayet, *Nucl. Phys.* **B90** (1975) 104;
A. Salam and J. Srathdee, *Nucl. Phys.* **B87** (1975) 85.

[22] P. Fayet and J. Illiopoulos, *Phys. Lett.* **B51** (1974) 461.

[23] L. O'Raifeartaigh, *Nucl.Phys.* **B96** (1975) 331

[24] L. Hall, J. Lykken and S. Weinberg, *Phys. Rev.* **D27** (1983) 2359;
S.K. Soni and H.A. Weldon, *Phys. Lett.* **B126** (1983) 215;
I. Affleck, M. Dine and N. Seiberg, *Nucl. Phys.* **B256** (1985) 557.

[25] H. P. Nilles, *Phys. Lett.* **B115** (1982) 193;
A.H. Chamseddine, R. Arnowitt and P. Nath, *Phys. Rev. Lett.* **49** (1982) 970;
A.H. Chamseddine, R. Arnowitt and P. Nath, *Nucl. Phys.* **B227** (1983) 121;
R. Barbieri, S. Ferrara and C. A. Savoy, *Phys. Lett.* **B119** (1982) 343;
N. Ohta, *Prog. Theor. Phys.* **70** (1983) 542.

[26] M. Dine, W. Fischler and M. Srednicki, *Nucl. Phys.* **B189** (1981) 575;
S. Dimopoulos and S. Raby, *Nucl. Phys.* **B192** (1982) 353;
M. Dine and W. Fischler, *Phys. Lett.* **B110** (1982) 227;
M. Dine and W. Fischler, *Nucl. Phys.* **B204** (1982) 346;
M. Dine and A.E. Nelson, *Phys. Rev.* **D48** (1993) 1277;
M. Dine, A.E. Nelson and Y. Shirman, *Phys. Rev.* **D51** (1995) 1362.

[27] L. Randall and R. Sundrum, *Nucl. Phys*. **B557** (1999) 79;
G.F. Giudice, M.A. Luty, H. Murayama and R. Rattazzi, *JHEP*, **9812** (1998) 027.

[28] D.E. Kaplan, G.D. Kribs and M. Schmaltz, *Phys. Rev.* **D62** (2000) 035010;
Z. Chacko, M.A. Luty, A.E. Nelson and E. Ponton, *JHEP*, **0001** (2000) 003.

[29] G.G. Ross and R.G. Roberts, *Nucl. Phys.* **B377** (1992) 571;
V. Barger, M.S. Berger and P. Ohmann, *Phys. Rev.* **D47** (1993) 1093.

[30] W. de Boer, R. Ehret and D. Kazakov, *Z. Phys.* **C67** (1995) 647;
W. de Boer et al., *Z. Phys.* **C71** (1996) 415.

[31] L.E. Ibáñez, C. Lopéz and C. Muñoz, *Nucl. Phys.* **B256** (1985) 218.

[32] V. Barger, M.S. Berger and P. Ohman, *Phys. Rev.* **D49** (1994) 4908.

[33] V. Barger, M.S. Berger, P. Ohmann and R. Phillips, *Phys. Lett.* **B314** (1993) 351;
P. Langacker and N. Polonsky, *Phys. Rev.* **D49** (1994) 1454;
S. Kelley, J.L. Lopez and D.V. Nanopoulos, *Phys. Lett.* **B274** (1992) 387.

[34] M. Carena, M. Quiros and C.E.M. Wagner, *Nucl. Phys.* **B461** (1996) 407;
A.V. Gladyshev, D.I. Kazakov, W. de Boer, G. Burkart, R. Ehret, *Nucl. Phys.* **B498** (1997) 3;
A.V. Gladyshev, D.I. Kazakov, *Mod. Phys. Lett.* **A10** (1995) 3129.

[35] S. Heinemeyer, W. Hollik and G. Weiglein, *Phys. Lett.* **B455** (1999) 179;
S. Heinemeyer, W. Hollik and G. Weiglein, *Eur. Phys. J.* **C9** (1999) 343.

[36] A. Arbey, M. Battaglia, A. Djouadi, F. Mahmoudi, *JHEP* **1209** (2012) 107.

[37] A. Arbey, M. Battaglia, A. Djouadi, F. Mahmoudi, J. Quevillon, *Phys. Lett.* **B708** (2012) 162.

[38] E. Komatsu et al., *Astrophys. J. Suppl.* **192** (2011) 18.

[39] http://www.slac.stanford.edu/xorg/hfag/rare/ichep10/radll/OUTPUT/TABLES/radll.pdf

[40] Muon G-2 Collaboration, *Phys. Rev.* **D73** (2006) 072003.

[41] LHCb collaboration, *Phys. Rev. Lett.* **108** (2012) 231801

[42] ALEPH Collaboration, DELPHI Collaboration, L3 Collaboration, OPAL Collaborations, LEP

WG for Higgs Boson Searches Collaboration, *Eur. Phys. J.* **C47** (2006) 547.

[43] CMS Collaboration, *Phys. Lett.* **B713** (2012) 68.
ATLAS Collaboration, *Phys. Lett.* **B705** (2011) 174.

[44] ATLAS Collaboration, *Search for squarks and gluinos using final states with jets and missing transverse momentum with the ATLAS detector in $\sqrt{s}$ = 7 TeV proton-proton collisions*, ATLAS-CONF-2012-033.

[45] ATLAS Collaboration, *Search for supersymmetry with the razor variables at CMS*, CMS-PAS-SUS-12-005.

[46] E. Aprile, et al., *Phys. Rev. Lett.* **107** (2011) 131302.

[47] M. Misiak and M. Steinhauser, *Nucl. Phys.* **B764** (2007) 62; *Nucl. Phys.* **B840** (2010) 271.

[48] W. de Boer, H.J. Grimm, A. Gladyshev, D. Kazakov, *Phys. Lett.* **B438** (1998) 281;
W. de Boer, M. Huber, A. Gladyshev, D. Kazakov, *Eur. Phys. J.* **C20** (2001) 689;
W. de Boer, M. Huber, A. Gladyshev, D. Kazakov, *The $b \to X(s)\gamma$ decay rate in NLO, Higgs boson limits, and LSP masses in the Constrained Minimal Supersymmetric Model*, `hep-ph/0007078`, and refs therein

[49] A. J. Buras, J. Girrbach, D. Guadagnoli, and G. Isidori, *Eur. Phys. J.* **C72** (2012) 2172.

[50] F. Abe, et al. [CDF Collaboration], *Phys. Rev.* **D57** (1998) 3811.

[51] R. Aaij, et al. *Phys. Rev. Lett.* **110** (2013) 021801.

[52] C. Bobeth, T. Ewerth, F. Kruger and J. Urban, *Phys. Rev*. **D 64** (2001) 074014.

[53] R.L. Arnowitt, B. Dutta, T. Kamon, and M. Tanaka, *Phys. Lett.* **B538** (2002) 121.

[54] M.S. Carena, D. Garcia, U. Nierste et al., *Nucl. Phys.* **B577** (2000) 88.

[55] C. Beskidt, et al., *Phys. Lett.* **B705** (2011) 493.

[56] F. Jegerlehner, A. Nyffeler, *Phys.Rep.* **477** (2009) 1.

[57] M. Davier, A. Hecker, B. Malaescu, Z. Zhang, *Eut. Phys. J.* **C71** (2011) 1515.

[58] J.L. Lopez, D.V. Nanopoulos, Xu Wang, *Phys.Rev.* **D49** (1994) 366.

[59] A. Czarnecki and W. Marciano, *Phys. Rev.* **D64** (2001) 013014.

[60] W. de Boer, M. Huber, C. Sander, D.I. Kazakov, *Phys. Lett.* **B515** (2001) 283.

[61] C. Beskidt, et al., *Phys. Lett.* **B695** (2011) 143.

[62] ATLAS Collaboration, Note ATL-PHYS-PUB-2010-011,
`http://cdsweb.cern.ch/record/1279115/files/ATL-PHYS-PUB-2010-011.pdf`.

[63] D. Benjamin, et al. [Tevatron New Phenomena & Higgs Working Group],
`arXiv:1003.3363 [hep-ex]`.

[64] G.L. Bayatian, et al. [CMS Collaboration], *J. Phys.* **G34** (2007) 995.

[65] CMS Collaboration, *Phys. Rev. Lett.* **106** (2011) 231801.

[66] C. Beskidt, W. de Boer, D.I. Kazakov, F. Ratnikov, *Eur. Phys. J.* **C72** (2012) 2166.

[67] CMS Collaboration, *Phys. Lett.* **B710** (2012) 26.

[68] ATLAS Collaboration, *Phys. Rev.* **D86** (2012) 032003.

[69] C.L. Bennett, et al., *Astrophys. J. Suppl.* **148** (2003) 1;
D.N. Spergel et al., *Astrophys. J. Suppl.* **148** (2003) 175.

[70] E. Kolb and M.S. Turner, *The Early Universe*, Frontiers in Physics, Addison Wesley, 1990.

[71] D.S. Gorbunov, V.A. Rubakov, *Introduction to the theory of the early Universe*, Moscow, URSS, 2008 (in Russian).

[72] Delphi Collab., *Eur. Phys. J.* **C1** (1998) 1;
L3 Collab., *Phys. Lett.* **B472** (2000) 420.

[73] `http://heasarc.gsfc.nasa.gov/docs/cgro/egret/`

[74] http://fermi.gsfc.nasa.gov/

[75] C. Beskidt, W. de Boer, D.I. Kazakov, F. Ratnikov, *JHEP* **1205** (2012) 094.

[76] R. Bernabei, et al. [DAMA Collaboration], *Eur. Phys. J.* **C56** (2008) 333.

[77] Z. Ahmed, et al. [CDMS Collaboration], *Science* **327** (2010) 1619;
Z. Ahmed, et al. [CDMS Collaboration], *Phys. Rev.* **D81** (2010) 042002.

[78] J. R. Ellis, K. A. Olive, and C. Savage, *Phys. Rev.* **D77** (2008) 065026.

[79] G. Belanger, F. Boudjema, A. Pukhov, et al., *Comput. Phys. Commun.* **180** (2009) 747.

[80] J. Cao, K.-i. Hikasa, W. Wang et al., *Phys. Rev.* **D82** (2010) 051701.

[81] J. M. Alarcon, J. Martin Camalich and J. A. Oller, *Phys. Rev.* **D85** (2012) 051503.

[82] M. Weber and W. de Boer, *Astron. Astrophys.* **509** (2010) A25.

[83] W. de Boer and M. Weber, *JCAP* **1104** (2011) 002.

[84] P. Salucci, F. Nesti, G. Gentile and C. F. Martins, *Astron. Astrophys.* **523** (2010) A83.

[85] R. Catena and P. Ullio, *JCAP* **1008** (2010) 004.

[86] D.Yu. Bogachev, A.V. Gladyshev, D.I. Kazakov, A.S. Nechaev, *Int. J. Mod. Phys.* **A21** (2006) 5221.

[87] ALEPH Collaboration, *Phys. Lett.* **B499** (2001) 67.

[88] D. Acosta, et al. [CDF Collaboration], *Phys. Rev. Lett.* **90** (2003) 251801;
T. Affolder et al. [CDF Collaboration], *Phys. Rev. Lett.* **87** (2003) 251803;
T.Kamon, Proc. of IX Int. Conf. "SUSY-01", WS 2001, p.196, hep-ex/0301019.

[89] U. Ellwanger, C. Hugonie, A.M. Teixeira, *Phys. Rept.* **496** (2010) 1, and refs therein;
M. Maniatis, *Int. J. Mod. Phys.* **A25** (2010) 3505, and refs therein.

[90] https://twiki.cern.ch/twiki/bin/view/AtlasPublic/LuminosityPublicResults

[91] https://twiki.cern.ch/twiki/bin/view/CMSPublic/LumiPublicResults

[92] F.E. Paige, *SUSY Signatures in ATLAS at LHC*, hep-ph/0307342;
D.P. Roy, *Acta Phys. Polon.* **B34** (2003) 3417;
D.R. Tovey, *Phys. Lett* **B498** (2001) 1;
H. Baer, C.Balaz, A. Belyaev, T. Krupovnickas and X. Tata, *JHEP* **0306** (2003) 054;
G. Belanger, F. Boudjema, F. Donato, R. Godbole and S. Rosier-Lees, *Nucl. Phys.* **B581** (2000) 3.

[93] O. Buchmueller et al., *Eur. Phys. J.* **C72** (2012) 1878;
S. Sekmen et al., *JHEP* **1202** (2012) 075;
S.S. AbdusSalam et al, *Eur. Phys. J.* **C71** (2011) 1835;
H. Baer, V. Barger, P. Huang, A. Mustafayev, *Phys. Rev.* **D84** (2011) 091701;
S. Heinemeyer, *SUSY Predictions for and from the LHC*, arXiv:1103.0952 [hep-ph];
B. Altunkaynak, M. Holmes, P. Nath, B.D. Nelson, G. Peim, *Phys. Rev.* **D82** (2010) 115001;
N.V. Krasnikov, V.A. Matveev, *Phys. Atom. Nucl.* **73** (2010) 191;
M. Spiropulu, *Eur. Phys. J.* **C59** (2009) 445;
D.P. Roy, *Acta Phys. Polon.* **B34** (2003) 3417;
F.E. Paige,*Czech. J. Phys.* **55** (2005) B185;
M. Dittmar, *SUSY discovery strategies at the LHC*, hep-ex/9901004;
MSSM Working Group, A. Djouadi et al., hep-ph/9901246.

[94] http://CMSinfo.cern.ch/Welcome.html- /CMSdocuments/CMSplots

[95] ATLAS collaboration, *Search for gluino pair production in events with missing transverse momentum and at least three b-jets using 13.0 fb*$^{-}1$ *of pp Collisions at* $\sqrt{s} = 8$ *TeV with the ATLAS Detector*, ATLAS-CONF-2012-145.

[96] ATLAS collaboration, *Search for supersymmetry in events with three leptons, multiple jets, and missing transverse momentum in 13.0 fb*$^{-}1$ *of pp collisions with the ATLAS detector at* $\sqrt{s} =$ 8 *TeV*, ATLAS-CONF-2012-151.

[97] ATLAS collaboration, *Search for new phenomena using large jet multiplicities and missing transverse momentum with ATLAS in 5.8 fb^{-1} of $\sqrt{s}$=8 TeV proton-proton collisions*, ATLAS-CONF-2012-103.

[98] ATLAS collaboration, *Search for Supersymmetry in final states with two same-sign leptons, jets and missing transverse momentum with the ATLAS detector in pp collisions at $\sqrt{s}$=8 TeV*, ATLAS-CONF-2012-105.

[99] ATLAS collaboration, *Eur. Phys. J.* **C72** (2012) 2237.

[100] ATLAS collaboration, *Search for light top squark pair production in final states with leptons and b-jets with the ATLAS detector in $\sqrt{s}$ = 7 TeV proton-proton collisions*, `arxiv:1209.2102`

[101] ATLAS collaboration, *Phys. Rev. Lett.* **109** (2012) 211802.

[102] ATLAS collaboration, *Phys. Rev. Lett.* **109** (2012) 211803.

[103] ATLAS collaboration, *JHEP* **1211** (2012) 094 .

[104] ATLAS Collaboration, *Search for squarks and gluinos with the ATLAS detector in final states with jets and missing transverse momentum using 4 .7 fb^{-1} of $\sqrt{s} = 7$ TeV proton-proton collision data*, `arXiv:1208.0949`.

[105] K. Matchev and R. Remington, *Updated templates for the interpretation of LHC results on supersymmetry in the context of mSUGRA*, `arXiv:1202.6580`.

[106] `https://twiki.cern.ch/twiki/bin/view/AtlasPublic/CombinedSummaryplots`

[107] CMS Collaboration, *Interpretation of Searches for Supersymmetry with Simplified Models*, CMS-PAS-SUS-11-016.

[108] `https://twiki.cern.ch/twiki/bin/view/CMSPublic/SUSYSMSSummaryplots`